Fuel Cell Transport All-Terrain Transport (FCATT) Proton Exchange Membrane (PEM) Fuel Cell Degradation Mechanism Analysis

Prepared by:

Dr. Theodore Burye
Chemical Engineer
theodore.e.burye2.civ@mail.mil
Fuel Cell Technologies
Ground Vehicle Power and Mobility (GVPM)
Tank Automotive Research Development and Engineering Center (TARDEC)

Acknowledgements

The Gas Chromatography (GC), Mass Spectroscopy (MS), Optical Microscopy, and Stack Cell Voltage data were acquired from the Fuel Cell laboratory located at TARDEC in building 212B. Theodore Burye, from the Fuel Cell Technologies group, collected the GC, MS, and optical microscopy data. Benjamin Paczkowski, from the Fuel Cell Technologies group, collected the Stack Cell Voltage data.

The Scanning Electron Microscopy (SEM), Energy Dispersive Spectroscopy (EDS), and X-ray Diffraction (XRD) data were acquired from the Metallurgy laboratory located at TARDEC in building 200C. Demetrios Tzelepis, from the Characterization & Failure Analysis group, helped collect XRD data.

The Fourier-Transform Infrared (FTIR) Spectroscopy data collected from the Proton Exchange Membrane (PEM) material samples, at room temperature, were acquired from the Elastomer, Isomer, Polymer laboratory located at TARDEC in building 215. William Roland and William Bradford, from the Characterization & Failure Analysis group, collected the TGA data.

The Thermo-Gravimetric Analysis (TGA) and Fourier-Transform Infrared (FTIR) Spectroscopy data collected from the analysis of PEM material off-gas analysis were acquired from the Southwest Research Institute in San Antonio, TX per, project number 23374.02.001. Michael Rubal, Ph.D, collected and analyzed the data.

Table of Contents

1. Abbreviations List 14
2. Introduction 15
3. Experimental Operating Conditions 16
3.1. Introduction 16
3.2. Platinum Degradation Experimental Setup 18
3.2.1. Acetic Acid Concentration Effects 18
3.2.2. Temperature Effects 19
3.2.1. Electrical Bias Effects 20
3.2.2. Solution Conductivity Effects 22
3.3. Characterization Techniques 23
3.3.1. Gas Chromatography and Mass Spectroscopy 23
3.3.2. Scanning Electron Microscopy (SEM) and Electron Dispersive Spectroscopy (EDS) 26
3.3.3. X-Ray Diffraction (XRD) 26
3.3.4. Fourier-Transform Infrared Spectroscopy (FTIR) 26
3.3.5. Thermo-Gravimetric Analysis – Fourier Transform Infrared Spectroscopy (TGA-FTIR) 26
3.3.6. Conductivity Measurements 27
4. Fuel Cell All-Terrain Transport (FCATT) Proton Exchange Membrane (PEM) Material Acetic Acid Production Mechanism Characterization 28
4.1. Introduction 28
4.2. FCATT Exhaust Water Characterization and Discussion 28
4.3. FCATT PEM Material FTIR and TGA-FTIR Characterization 31
4.4. Industrial Acetic Acid Production Reactions 36
4.4.1. Methanol Carbonylation 36
4.4.2. Acetaldehyde Oxidation 37
4.4.3. Ethylene Oxidation 37
4.4.4. Oxidative Fermentation 37
4.5. FCATT Stack MEA Acetic Acid Reaction Mechanisms 37
4.6. FCATT Stack PEM Material Acetic Acid Reaction Mechanisms 38
4.7. Fuel Cell All-Terrain Transport (FCATT) Proton Exchange Membrane (PEM) Material Acetic Acid Production Mechanism Summary 39

5. Platinum Electrocatalyst Loss Degradation Investigation 40
5.1. Introduction 40
5.2. Solvent Purity Characterization 40
5.3. Impact of Temperature and Acetic Acid Concentration 44
5.4. Impact of Electrical Bias and Acetic Acid Concentration 51
5.4.1. Resistivity Comparison between Samples and Literature Results 51
5.4.2. Sample Strain Induced by Platinum Sputtering Process 53
5.4.3. Current Density Comparison between Samples and FCATT Cells 54
5.4.4. Impact of 15.5V Electrical Bias Effects and Acetic Acid Concentration 56
5.4.1. Impact of 0.8V Electrical Bias Effects using 5 vol% Acetic Acid 67
5.5. Platinum Electrocatalyst Loss Degradation Investigation Summary 73
6. Platinum Electrocatalyst Loss Degradation Mechanism Determination 75
6.1. Conductivity or Reduction of Platinum/Acetic Acid Reaction Barrier Effects 75
6.2. Particle Size and Strain Effects 82
6.3. Platinum Electrocatalyst Loss Degradation Mechanism Determination Summary 87
7. Stack Operating Techniques and Cell Fabrication Approaches to Minimize or Prevent Electrocatalyst Loss 89
7.1. Continuous vs. Cycling Voltage Application Characterization 89
7.2. Substrate Material Characterization 95
7.3. Electrocatalyst/Coating Material Characterization 99
7.4. Electrocatalyst/Coating Deposition Thickness Characterization 101
7.5. Combined Electrocatalyst/Coating Deposit Material Thickness Characterization 104
7.6. Operating Techniques and Cell Fabrication Approaches Summary 106
8. Overall Project Conclusions 107
8.1. PEM Material Acetic Acid Production Mechanism Characterization Summary 107
8.2. Platinum Electrocatalyst Loss Degradation Mechanism Characterization Summary 107
8.3. Operating Techniques and Cell Fabrication Approaches 107

8.4. Overall Recommendations to Reduce and/or Prevent Electrocatalyst/Coating Loss in FCATT PEM Fuel Cell 108
9. References 110
10. Appendix A: Supplementary Information 114
11. Appendix B: Platinum and Copper in Glacial Acetic Acid 116
11.1. Copper in Glacial Acetic Acid 116
11.2. Platinum in Glacial Acetic Acid 119

List of Tables

Table 1: Deionized Water, 99.7 vol% Acetic Acid, 99vol% Propionic Acid and 99vol% Butyric Acid Compounds in Figure 26 44
Table 2: Common Gas Chromatograph/Mass Spectrometer Carrier Gas Mass Numbers 44
Table 3: Platinum Sputter Coating Resistivity Calculation Parameters 51
Table 4: FCATT PEM Stack Operating Voltage, Current and Current Density Values.. 55
Table 5: PEM Material Sputter Coated with Platinum Operating Voltage, Current and Current Density Values 55
Table 6: Weak Organic Acid Solvent Properties 76
Table 7: Solvent Properties for Sputter Coated Platinum Loss Conductivity Experiments 78
Table 8: Copper Mass Loss in Glacial Acetic Acid 116
Table 9: Platinum Mass Loss in Glacial Acetic Acid 119

List of Figures

Figure 1: Gen 2 Membrane Electrode Assembly Sheet. 16
Figure 2: Platinum Sputtering Target..... 17
Figure 3: Non-sputtered (left) and Platinum Sputtered (right) FCATT Fuel Cell PEM Materials..... 18
Figure 4: Beaker used to Hold PEM Material Sample for Temperature Experiments.... 19
Figure 5: Heating Equipment Setup. 20
Figure 6: Diagram of Platinum Layer for Electrical Bias Experiments 21
Figure 7: Diagram of Ceramic Spacer and Electrical Leads for Electrical Bias Experiments 21
Figure 8: Electrical Bias at Room Temperature Experimental Setup..... 22
Figure 9: Deionized Water and Acetic Acid GC Oven Temperature Profile..... 23
Figure 10: Propionic Acid GC Oven Temperature Profile..... 24
Figure 11: Butyric Acid GC Oven Temperature Profile..... 25
Figure 12: FCATT PEM Stack Cathode Exhaust Water (top) and Anode Exhaust Water (bottom)..... 28
Figure 13: Chromatographs of PEM Stack Membrane Electrode Assembly's (MEA) for Cell 1 (top), Cell 20 (middle) and Cell 31 (bottom) Heated to 65°C..... 29
Figure 14: Chromatographs of Proton Exchange Membrane (PEM) for Cell 1 (top), Cell 20 (middle) and Cell 31 (bottom) Heated to 65°C. 30
Figure 15: Fourier-Transform Infrared Spectroscopy Scan Results for PEM Material within Cell 1 and Cell 31..... 31
Figure 16: Cell 1 TGA Mass Loss and Derivative Raw Data Plots 32
Figure 17: Cell 1 FTIR Scan Raw Data and Database Results at 5.33min (188°C)..... 33
Figure 18: Cell 1 FTIR Scan Raw Data and Database Results at 15.82min (502°C).... 33
Figure 19: Cell 1 FTIR Scan Raw Data and Database Results at 15.82min (502°C).... 33
Figure 20: Cell 31 TGA Mass Loss and Derivative Raw Data Plots 34
Figure 21: Cell 31 FTIR Scan Raw Data and Database Results at 8.00min (267°C).... 35
Figure 22: Cell 31 FTIR Scan Raw Data and Database Results at 14.76min (407°C).. 35
Figure 23: Cell 31 FTIR Scan Raw Data and Database Results at 16.18min (513°C).. 35
Figure 24: Cell 31 FTIR Scan Raw Data and Database Results at 16.71min (529°C).. 36
Figure 25: Cell 1 Cathode (top left)/Anode (bottom left) and Cell 31 Cathode (top right)/Anode (bottom right) Energy Dispersive Spectroscopy Platinum Electrocatalyst Elemental Map 41
Figure 26: Deionized Water (bottom), 99.7 vol% Acetic Acid, 99 vol% Propionic Acid and 99 vol% Butyric Acid (top) Chromatograms Comparison Plot 42

Figure 27: Deionized Water (bottom), 99.7 vol% Acetic Acid, 99 vol% Propionic Acid and 99 vol% Butyric Acid (top) Mass Spectrogram Comparison Plot 43
Figure 28: PEM Material Typical Scanning Electron Microscopy Image of EDS Sample Location 45
Figure 29: Typical Initial Energy Dispersive Spectroscopy Scan of PEM Material Sputter Coated with Platinum 46
Figure 30: Enlarged Section of Typical Initial Energy Dispersive Spectroscopy Scan from PEM Material Sputter Coated with Platinum 47
Figure 31: Before (blue bars, top row) and After (orange bars, top row) Platinum Peak Height Comparison for Heating Effects in 0 vol% Acetic Acid (left column), 5 vol% Acetic Acid (middle column) and 99.7 vol% Acetic Acid (right column). Bottom Row Shows Delta Values between Before and After. 48
Figure 32: Before (blue bars, top row) and After (orange bars, top row) Silicon Peak Height Comparison for Heating Effects in 0 vol% Acetic Acid (left column), 5 vol% Acetic Acid (middle column) and 99.7 vol% Acetic Acid (right column). Bottom Row Shows Delta Values between Before and After. 49
Figure 33: Before (blue bars, top row) and After (orange bars, top row) Platinum/Silicon Peak Height Ratio Comparisons for Heating Effects in 0 vol% Acetic Acid (left column), 5 vol% Acetic Acid (middle column) and 99.7 vol% Acetic Acid (right column) Calculated from Figure 31 and Figure 32. Bottom Row Shows Delta Values between Before and After 50
Figure 34: Platinum Sputter Coating Resistivity Calculations (blue dots) using Parameters in Table 3 Compared to Reported Intrinsic Platinum Resistivity from Literature (green dots). 52
Figure 35: Optical Microscopy Images of Platinum Sputter Coated PEM Material Samples Before (left column) and After (right column) 15.5V Electrical Bias for 100 (top row), 200 (middle row) and 400 (bottom row) Cycles in Contact with 0 vol% Acetic Acid Solvent at Room Temperature. 57
Figure 36: EDS Data for Platinum Sputter Coated PEM Material Samples with a 15.5V Electrical Bias for 100 (top row), 200 (middle row) and 400 (bottom row) Cycles in Contact with 0 vol% Acetic Acid Solvent at Room Temperature. Platinum (left column) and Silicon (right column) EDS Data Before (yellow) and After (red and purple) Cycling is Reported too. 59
Figure 37: Optical Microscopy Images of Platinum Sputter Coated PEM Material Samples Before Cycling (left column), After Cycling (middle column) and Solution Interaction Area Cutout After Cycling (right column) on Samples with a 15.5V Electrical

Bias Applied for 50 (top row), 100 (middle row) and 200 (bottom row) Cycles in Contact with 5 vol% Acetic Acid Solvent at Room Temperature..... 60
Figure 38: EDS Data for Platinum Sputter Coated PEM Material Samples with a 15.5V Electrical Bias for 50 (top row), 100 (middle row) and 200 (bottom row) Cycles in Contact with 5 vol% Acetic Acid Solvent at Room Temperature. Platinum Levels are Reported in the Platinum Rich (left column) and No Platinum (2nd from left column) Regions and Silicon Levels in the Platinum Rich (2nd from right column) and No Platinum (right column) are as well. EDS Data Before (yellow) and After (red and purple) Cycling is Reported too. 61
Figure 39: Optical Microscopy Images of Platinum Sputter Coated PEM Material Samples Before (left column) and After (right column) on Samples with a 15.5V Electrical Bias Applied for 100 (top row), 200 (middle row) and 400 (bottom row) Cycles in Contact with 99.7 vol% Acetic Acid Solvent at Room Temperature. 62
Figure 40: EDS Data for Platinum Sputter Coated PEM Material Samples with a 15.5V Electrical Bias Applied for 100 (top row), 200 (middle row) and 400 (bottom row) Cycles in Contact with 99.7 vol% Acetic Acid Solvent at Room Temperature. Platinum (left column) and Silicon (right column) EDS Data is Reported Before (yellow) and After (red and purple) Cycling. 63
Figure 41: Before Cycling (blue bars, top row) and After Cycling (orange bars, top row) Comparison for 15.5V Electrical Bias Effects Outside Solvent Interaction Area for 100, 200 and 400 Cycles. Changes in Platinum (left column) and Silicon (right column) Values are Shown from EDS Data in Figure 36. Bottom Row Shows Delta Values between Before and After..... 64
Figure 42: Before Cycling (blue bars, top row) and After Cycling (orange bars, top row) Platinum Peak Comparison for Electrical Bias Effects using 15.5V in 0 vol% Acetic Acid (left column), 5 vol% Acetic Acid Platinum Rich (2nd from left column), 5 vol% Acetic Acid no Platinum (2nd from right column) and 99.7 vol% Acetic Acid (right column) which was Extracted from Figure 36, Figure 38 and Figure 40, Respectively. Bottom Row Shows Delta Values between Before and After..... 65
Figure 43: Before Cycling and After Cycling Silicon Peak Comparison for Electrical Bias Effects using 15.5V in 0 vol% Acetic Acid (left column), 5 vol% Acetic Acid Platinum Rich (2nd from left column), 5 vol% Acetic Acid no Platinum (2nd from right column) and 99.7 vol% Acetic Acid (right column) which was Extracted from Figure 38. Bottom Row Shows Delta Values between Before and After..... 66
Figure 44: Before Cycling (blue bars, top row) and After Cycling (orange bars, top row) Platinum/Silicon Peak Ratio Comparison for Electrical Bias Effects using 15.5V in 0

vol% Acetic Acid (left column), 5 vol% Acetic Acid Platinum Rich (2nd from left column), 5 vol% Acetic Acid no Platinum (2nd from right column) and 99.7 vol% Acetic Acid (right column) which was Calculated from Figure 42 and Figure 43. Bottom Row Shows Delta Value between Before and After. 67
Figure 45: Optical Microscopy Images of Platinum Sputter Coated on PEM Material Samples Before (left column) and After (right column) on Samples with a 0.8V Electrical Bias Applied for 100 (top row), 200 (middle row) and 400 (bottom row) Cycles in Contact with 5 vol% Acetic Acid Solvent at Room Temperature. 68
Figure 46: EDS Data for Platinum Sputter Coated on PEM Material Samples with a 0.8V Electrical Bias Applied for 100 (top row), 200 (middle row) and 400 (bottom row) Cycles in Contact with 5 vol% Acetic Acid Solvent at Room Temperature. Platinum (left column) and Silicon (right column) EDS Data are Shown Before (yellow) and After (red and purple) Cycling. 69
Figure 47: Before (blue bars, top row) and After (orange bars, top row) Platinum (top left plot) and Silicon (top right plot) Comparison for Electrical Bias Effects using a 0.8V in 5 vol% Acetic Acid which was Extracted from Figure 46. Bottom Row Shows Delta Value between Before and After..... 70
Figure 48: Before (blue bars, top row) and After (orange bars, top row) Platinum/Silicon Peak Ratio Comparison for Electrical Bias Effects using a 0.8V in 5 vol% Acetic Acid which was Calculated from Figure 47. Bottom Row Shows Delta Value between Before and After..... 71
Figure 49: Acetic Acid (blue triangles), Propionic Acid (orange squares) and Butyric Acid (black circles) Conductivity Values across Entire Solution Molarity Range 77
Figure 50: Acetic Acid (blue triangles), Propionic Acid (orange squares) and Butyric Acid (black circles) Conductivity Values across Entire Solution Solvent Fraction Range..... 78
Figure 51: Platinum Sputter Coated PEM Material Samples in Contact with 5 vol% Acetic Acid (top row), 5 vol% Propionic Acid (middle row) and 5 vol% Butyric Acid (bottom row) for 100 Cycles with a 15.5V Electrical Bias Applied. Optical Microscopy Images are Shown Before Cycles were Applied (left column), After Cycles were Applied (middle column) and an Interior Image After Cycles were Applied (right column). 79
Figure 52: Deionized Water (0 vol% Acetic Acid) Conductivity Values over Time. Horizontal Dashed Lines Represent an Equivalent Amount of Time to Complete 100 (blue line), 200 (green line) and 400 (red line) Cycles and the Times those Measurements Occur on the Plot in Relation to the Reported Conductivity Values. 80

Figure 53: XRD Scan of Platinum Sputter Coated PEM Material Samples Before (blue data) and After Applying a 15.5V Electrical Bias for 100 (red data), 200 (green data) and 400 (yellow data) Cycles using 0 vol% Acetic Acid. 82
Figure 54: XRD Scan of Platinum Sputter Coated PEM Material Samples After Applying a 15.5V Electrical Bias for 50 (top, blue), 100 (top, red) and 200 (top, green) Cycles and a 0.8V Electrical Bias for 100 (bottom, orange), 200 (bottom, purple) and 400 (bottom, red) Cycles using 5 vol% Acetic Acid. 83
Figure 55: Particle Size Distribution (top) and Strain Distribution (bottom) Value Calculated from XRD Results for Platinum Sputter Coated PEM Material Samples with 15.5V Applied Bias in Contact with Different Solvent Acetic Acid Volume Fraction Values. Results are Shown before Experimentation (purple bar), with 0 vol% Acetic Acid (blue bars), with 5 vol% Acetic Acid (red bars) and 99.7 vol% Acetic Acid (green bars). 85
Figure 56: Particle Size Distribution (top) and Strain Distribution (bottom) Values Calculated from XRD Results for Platinum Sputter Coated PEM Material Samples with 15.5V (blue bars) and 0.8V (red bars) Applied Bias in contact with 5 vol% Acetic Acid. Starting values Before Experimentation are Shown in Purple. 86
Figure 57: Electrical Bias Cycling Optical Microscopy Results (left column) and Continuous Bias Optical Microscopy Results (right column) Applied using 15.5V and 20 mA. 50 Cycles/8 Minutes (top row), 100 Cycles/17 Minutes (middle row) and 200 Cycles/33 Minutes (bottom row) are Shown. 90
Figure 58: Electrical Bias Cycling Optical Microscopy Results (left column) and Continuous Bias Optical Microscopy Results (right column) Applied using 0.8V and 0.7 mA. 100 Cycles/17 Minutes (top row), 200 Cycles/33 Minutes (middle row) and 400 Cycles/67 Minutes (bottom row) are Shown. 91
Figure 59: EDS Data for Platinum Sputter Coated PEM Material Samples Applied with a 0.8V Electrical Bias Applied using Cycles (left column) and Applied Continuously (right column). Electrical Bias Cycles were Applied for 100 (top left), 200 (middle left) and 400 (bottom left) Times, while the Continuously Applied Bias was Applied for 17 min (top right), 33 min (middle right) and 67 min (bottom right). All Samples were in Contact with 5 vol% Acetic Acid Solvent at Room Temperature. 93
Figure 60: EDS Data for Silicon Peaks Located on the Platinum Sputter Coated PEM Material Samples Applied with a 0.8V Electrical Bias Applied using Cycles (left column) and Applied Continuously (right column). Electrical Bias Cycles were Applied for 100 (top left), 200 (middle left) and 400 (bottom left) Time, while the Continuous Applied

Bias was Applied for 17 min (top right), 33 min (middle right) and 67 min (bottom right). All Samples were in Contact with 5 vol% Acetic Acid Solvent at Room Temperature... 94
Figure 61: Optical Microscopy Images of Platinum Sputter Coated onto Various Polymer Substrate Materials. Images of the Platinum Coating are Shown before (left column) and after (middle column) the Electrical Bias was Applied. Interior Cutouts (right column) after the Electrical Bias was Applied are also Shown. Polymer Materials used were: PEM Material (top row), Polyethylene (2nd from top), Polycarbonate (3rd from top), Polytetrafluoroethylene (4th from top), Polystyrene (bottom row). Electrical Bias was Applied for 100 Cycles using 15.5V and 20 mA in Contact with 5 vol% Acetic Acid. 96
Figure 62: Optical Microscopy Images of Platinum Sputter Coated onto Various Glass/Ceramic Substrate Materials. Images of the Platinum Coating are Shown Before (left column) and After (right column) the Electrical Bias was Applied. Materials used were: Amorphous Glass (top row) and Aluminum Oxide (bottom row). Electrical Bias was Applied for 100 Cycles using 15.5V and 20 mA in Contact with 5 vol% Acetic Acid. 97
Figure 63: Optical Microscopy Images of Platinum Sputter Coated onto Various Bulk Metal Substrate Materials. Images of the Platinum Coating are Shown Before (left column) and After (middle column) the Electrical Bias was Applied. Images of Substrate Materials before the Platinum Sputter Coating was Applied are Shown in the Right Column. Materials used were: Zinc Plated Steel (top row), Cadmium Plated Steel (middle row) and Aluminum (bottom row). Electrical Bias was Applied for 100 Cycles using 15.5V and 20 mA in Contact with 5 vol% Acetic Acid. 98
Figure 64: Optical Microscopy Images of Various Electrocatalyst/Coatings Sputter Coated onto the PEM Material Substrate. Images of each Coating are Shown Before (left column) and After (right column) the Electrical Bias was Applied. Coating Materials used were: Platinum (top row), Gold (2nd row), Copper (3rd row) and Carbon (bottom row). Electrical Bias was Applied for 100 Cycles using 15.5V and 20 mA in Contact with 5 vol% Acetic Acid. 100
Figure 65: Optical Microscopy Images of Various Electrocatalyst/Coatings Sputter Coated onto the PEM Material Substrate with Coating Thicknesses of 6nm and 50nm. Images of each Coating are Shown Before (left column) and After (right column) the Electrical Bias was Applied. Coating Materials used were: Platinum (top two rows) and Gold (bottom two rows). Electrical Bias was Applied for 100 Cycles using 15.5V and 20 mA in Contact with 5 vol% Acetic Acid. 102
Figure 66: Optical Microscopy Images of Various Electrocatalyst/Coatings Sputter Coated onto the PEM Material Substrate with Coating Thicknesses of 6nm, 8nm, 20nm

and 50nm. Images of each Coating are Shown Before (left column) and After (right column) the Electrical Bias was Applied. Coating Materials used were: Copper (top two rows) and Carbon (bottom two rows). Electrical Bias was Applied for 100 Cycles using 15.5V and 20 mA in Contact with 5 vol% Acetic Acid. 103
Figure 67: Optical Microscopy Images of Platinum/Gold and Platinum/Carbon Sputtered Coated on to PEM Material Substrates Before (left column) and After (right column) a 15.5V Electrical Bias was Applied for 100 Cycles in Contact with 5 vol% Acetic Acid. Gold was Applied at 5nm (top row) and 15nm (middle row) Thicknesses. Carbon was Applied at 5nm (bottom row) Thickness. Platinum was Applied at 6nm for all Experiments. 105
Figure 68: EDS Scan Results from Polymer Substrate Materials 114
Figure 69: EDS Scan Results from Glass/Ceramic Substrate Materials 114
Figure 70: External EDS Scan Results from Bulk Metal Substrate Materials 115
Figure 71: Interior EDS Scan Results from Zinc and Cadmium Plated Steel Substrate Materials 115
Figure 72: Copper in Glacial Acetic Acid for 69hrs (right) and Pure Glacial Acetic Acid (left) 116
Figure 73: Optical Microscopy Image of Precipitate Power from Copper in Glacial Acetic Acid 117
Figure 74: EDS Scan Results (top) and Scanning Electron Microscopy Image (bottom) of Precipitate from Copper in Glacial Acetic Acid. 118
Figure 75: XRD Scan of Precipitate Powder from Copper in Glacial Acetic Acid. Δ= Copper (II) Acetate and ◊ =Copper (II) Acetate Monohydrate 119

1. Abbreviations List

EDS: Energy Dispersive Spectroscopy

FCATT: Fuel Cell All-Terrain Transport

FTIR: Fourier-Transform Infrared

GC: Gas Chromatography

MS: Mass Spectroscopy

MEA: Membrane Electrode Assembly

NIST: National Institute of Standards and Technology

PBI: Polybenzimidazole

PEM: Proton Exchange Membrane

SEM: Scanning Electron Microscopy

SwRI: Southwest Research Institute

TARDEC: Tank Automotive Research Development and Engineering Center

TGA: Thermo-Gravimetric Analysis

XRD: X-ray Diffraction

2. Introduction

This purpose of this paper is to report on the investigation and characterization of the degradation mechanisms of the FCATT PEM fuel cell. The "FCATT PEM Fuel Cell Failure Analysis Report" [1] identified two potential degradation processes occurring in the fuel cell, which were: 1. Both the Proton Exchange Membrane (PEM) material (located in the Membrane Electrode Assembly (MEA)) and MEA produced acetic acid when heated to 65°C or greater temperatures in deionized water and, 2. The total area of platinum nanoparticle electrocatalyst that coated the inside of the cathode MEA was significantly lower than its anode counterpart for each cell. This lack of platinum on the cathode side was especially apparent in the lowest performing cell, which was also producing the greatest amount of acetic acid on the cathode side of the cell. While the production of acetic acid from the thermal decomposition of the PEM material by itself appears to have a limited impact on performance, I hypothesize that the production of acetic acid (in combination with heat and/or applied electrical bias through the platinum) contributed to the degradation of the platinum nanoparticle electrocatalyst. The degradation and/or loss of the electrocatalyst would have a significant impact on stack performance, so understanding the mechanism behind each process is important to preventing stack damage.

The report compares ThermoGravimetric Analysis-Fourier Transform Infrared (TGA-FTIR) spectroscopy, Scanning Electron Microscopy (SEM), Energy Dispersive Spectroscopy (EDS), X-ray Diffraction (XRD), Optical Microscopy (OM) and Gas Chromatography (GC)/Mass Spectroscopy (MS) characterization results from the PEM material and the platinum electrocatalyst material in the FCATT fuel cell to determine the underlying mechanisms that caused the production of acetic acid and degradation of the platinum electrocatalyst on the cathode.

3. Experimental Operating Conditions

3.1. Introduction

Four different characterization techniques were used to characterize the degradation mechanisms proposed. These techniques were TGA-FTIR, SEM, EDS and GC/MS. These techniques are described in more detail later in this chapter.

The PEM material located in the FCATT fuel cell was found to produce acetic acid. PEM material samples were acquired from Membrane Electrode Assemblies (MEAs) located at the front (cell closest to the stack manifold) and back (cell furthest from the stack manifold) of the FCATT PEM stack, shown in Figure 1**.** The front MEA is referred to as Cell 1 and the back MEA is referred to as Cell 31. Approximately 100mg of PEM material, from the outer edges of Cell 1 and 31 each, was shipped to the Southwest Research Institute (SwRI) (San Antonia, TX) for analysis using the TGA-FTIR characterization technique to analyze the off-gases produced during the thermal decomposition process.

Figure 1: Gen 2 Membrane Electrode Assembly Sheet.

The degradation of PEM platinum electrocatalyst was analyzed by sputtering between 5.0-6.5nm of platinum onto ½ inch x ½ inch square pieces of PEM material cut from stack MEA sheets, shown in Figure 1. The platinum target (Figure 2) used was 57mm in diameter, had a thickness of 0.1mm, and was 99.99% pure. The target was purchased from Electron Microscopy Sciences (Hatfield, PA, USA).

Figure 2: Platinum Sputtering Target

Figure 3 shows the both non-sputtered (left) and platinum sputtered (right) PEM material samples. The platinum can be observed clearly on the right sample since the non-sputtered PEM material is fairly optically transparent.

Different operating conditions which the platinum nano-coating may have experienced inside the MEA were reproduced as experimental variables. These varying conditions included: 1. acetic acid concentration, 2. operating temperature, 3. applied electrical bias, 4. solution conductivity, and 5. operating temperature in combination with applied electrical bias. To simulate these individual conditions, or a combination of these conditions, the following experimental setups were used. EDS scans of the platinum, at multiple locations per sample, were taken before and after experiments to determine whether platinum levels were statistically lowered.

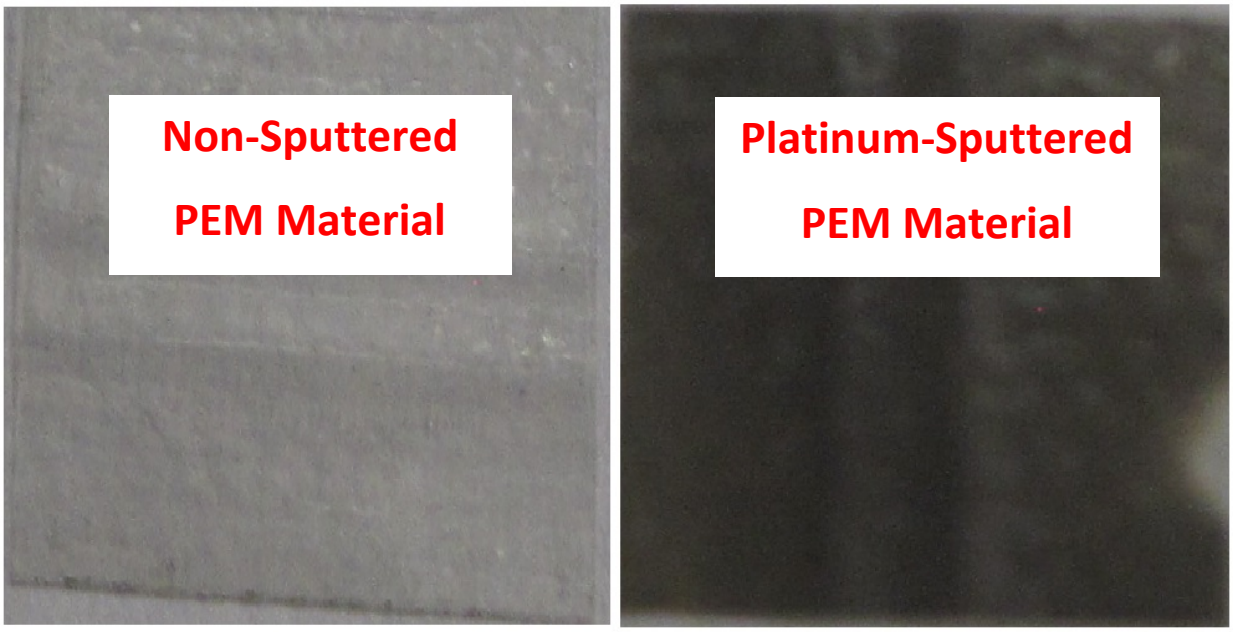

Figure 3: Non-sputtered (left) and Platinum Sputtered (right) FCATT Fuel Cell PEM Materials

3.2. Platinum Degradation Experimental Setup

3.2.1. Acetic Acid Concentration Effects

Three platinum sputter coated PEM material samples were immersed in 10mL of either deionized water, 5 vol% acetic acid solution (95 parts deionized water and 5 parts acetic acid), or 99.7 vol% glacial acetic acid solution inside 50mL beakers, as shown in Figure 4. Each sample remained submerged in their respective solution for at least 38 hours at room temperature (~21°C).

Samples were submerged under the solution to increase the contact area between the platinum sputter coating and the solution using tweezers. Making physical contact with each sample was previously characterized and found to not result in platinum loss. 2-3 mL (at most) of each solution was added once per day to maintain a constant solution level at 10mL.

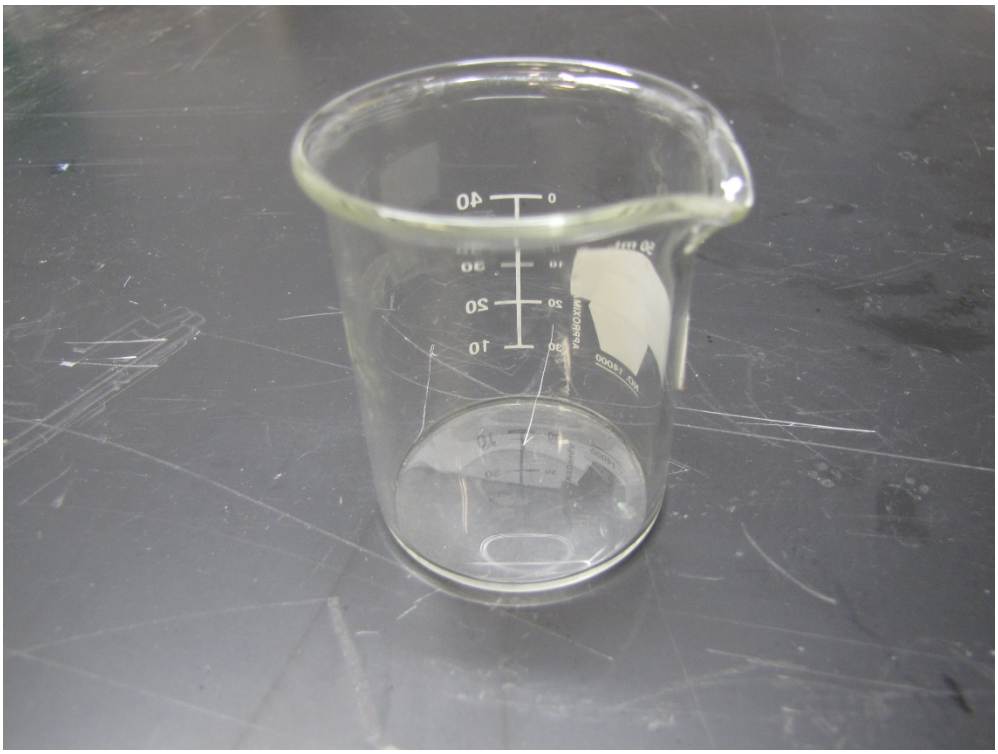

Figure 4: Beaker used to Hold PEM Material Sample for Temperature Experiments

3.2.2. Temperature Effects

Platinum sputter coated PEM material samples were first immersed in 10mL of either deionized water, 5 vol% acetic acid solution (95 parts deionized water and 5 parts acetic acid) or 99.7 vol% glacial acetic acid solution inside 50mL beakers, which was the same as the acetic acid concentration experimental setup. The three beakers were then placed on a Corning PC-420D (Corning, Corning, NY, USA) hotplate and heated to temperatures between 46-103°C for at least 38 hours each, shown in Figure 5. Different material samples were placed inside each beaker for each temperature evaluation.

Samples were submerged under the solution using glass beads to increase the contact area between the sputtered platinum sputter coating and the solution. As with the acetic acid concentration experiments 2-3 mL of solution was added to maintain a constant solution level at 10mL. The time between needing to add additional solution depended on the temperature setpoint and the solution being used. The glacial acetic acid has a higher boiling point and did not require additional solution to be added as frequently, for example.

Figure 5: Heating Equipment Setup.

3.2.1. Electrical Bias Effects

Samples of the PEM material were cut from different cells, similar to what is shown in Figure 1, and a thin strip of platinum was produced by masking off sections of the PEM materials. A small fiduciary was placed on one corner to identify which side the platinum was located on. A diagram of this is shown in Figure 6. The platinum layer was between 5.0-6.5nm thick and was 3/32 inch (2,380um) wide.

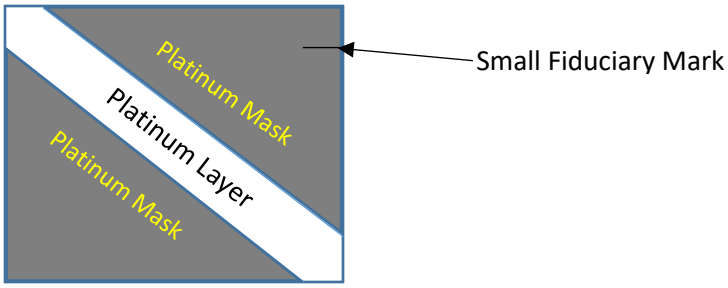

Figure 6: Diagram of Platinum Layer for Electrical Bias Experiments

Each sample then had a high-temperature ceramic doughnut spacer attached to the PEM material surface on top of the platinum layer. The center of the spacer had a ¼ inch diameter hole and the spacer was ½ inch in height. The center hole of the spacer had solution placed inside while the electrical bias was being applied, and electrical leads were attached to both ends of the platinum layer which came from the power supply. A diagram of this is shown in Figure 7.

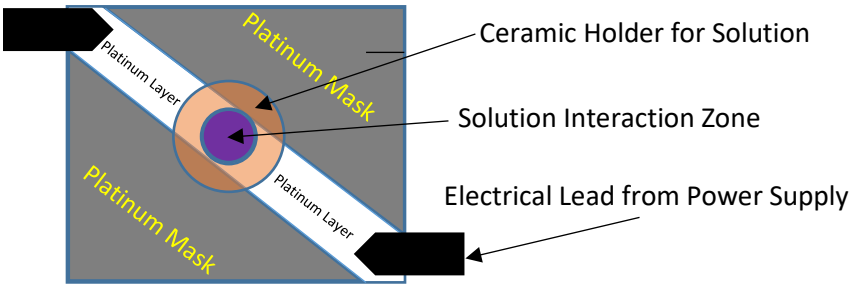

Figure 7: Diagram of Ceramic Spacer and Electrical Leads for Electrical Bias Experiments

A second ceramic spacer, identical to the one described above, was placed under the PEM material to raise the sample high to allow enough room attach the electrical leads from the power supply. A weight was also placed on top of the spacers to minimize spacer movement that may have occurred from the electrical leads. A picture of the final experimental setup is shown in Figure 8.

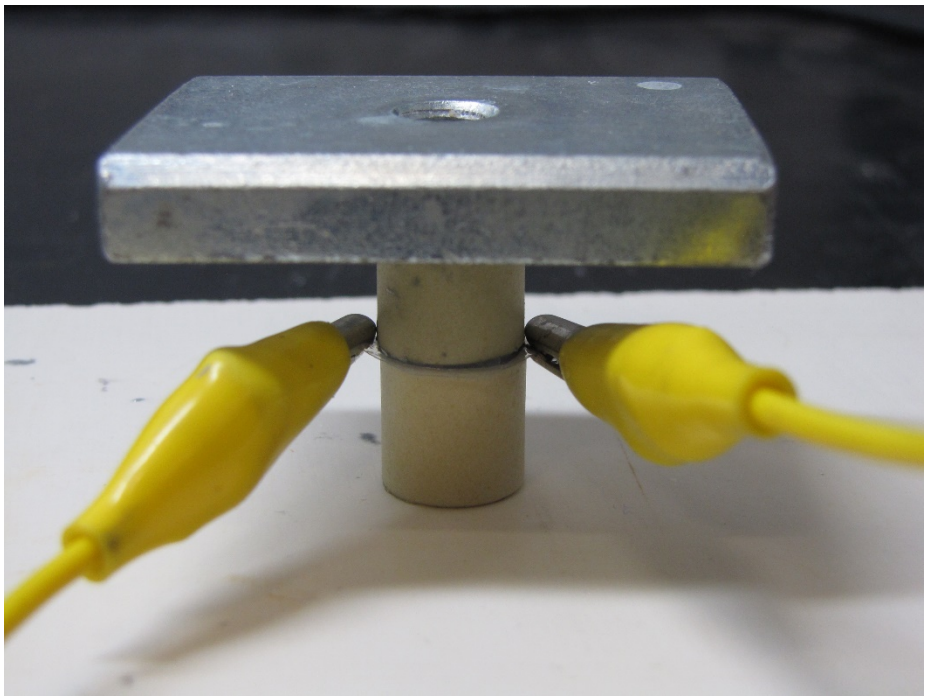

Figure 8: Electrical Bias at Room Temperature Experimental Setup

Samples were tested by one of two approaches: 1. Cycling the electrical bias on for 5 seconds and then turning off the electric bias for 5 seconds which counted for one bias cycle step. This process was repeated for the duration of the experiment and 2. Continuously holding the bias for the entire duration of the experiment. Samples tested using the first approach were cycled for 50, 100, 200 or, 400 times, where the time to perform 50 cycles was approximately 8 minutes, 100 cycles was approximately 17 minutes, 200 cycles was approximately 33 minutes and, 400 cycles was approximately 67 minutes. Samples tested using the second approach were constantly held (the bias was not turned on and off) at their bias value for the same total amount of time as the samples that were cycled. Samples using a constant bias were held for 17 minutes, 33 minutes or 67 minutes.

3.2.2. Solution Conductivity Effects

Solution mixtures of 10 mL, using deionized water mixed with 99.7 vol% acetic acid, 99 vol% propionic acid or 99 vol% butyric acid in ratios between 0-100 vol%, were made and placed into 50 mL beakers. Solution mixture molarity and conductivity values were compared and solutions with similar molarity and conductivity values were used in the same experimental setup used for the electrical bias effects. Each solution mixture used a separate sample and a 15.5V electrical bias was applied for each sample for 100 cycles each.

Images of the platinum were taken using the optical microscope before and after each experiment to document platinum loss.

3.3. Characterization Techniques

3.3.1. Gas Chromatography and Mass Spectroscopy

Gas Chromatography (GC) and Mass Spectroscopy were performed using a PerkinElmer Clarus 600T GC/ Clarus 600 MS system (PerkinElmer; Waltham, MA, USA). Liquid samples were injected into the GC using an auto sampler with a 1µL injection volume, which were then passed through an Elite-1 GC column (part number N9316008) with a 0.25mm column ID, 15m column length, and 340°C maximum column temperature.

The following parameters were used for the GC and MS to characterize the following sample types.

Deionized Water and Acetic Acid

Inlet Line Temperature: **200°C**

Mass Spectrometer Source Temperature: **200°C**

Injection Port: **A**

Injector Temperature: **150°C**

Gas Chromatograph Oven Temperature Profile:

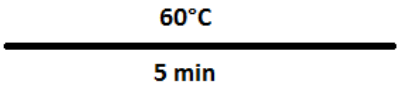

Figure 9: Deionized Water and Acetic Acid GC Oven Temperature Profile

Gas Chromatograph Carrier Gas Flow Rate: **1.5 mL/min**

Gas Chromatograph Split Injection Mode (Flow or Ratio): **Ratio**

Gas Chromatograph Split Injection Ratio: **300:1**

Mass Spectrometer Solvent Delay: **0 min**

Mass Spectrometer Mass Number Range: **5 to 600**

Propionic Acid

Inlet Line Temperature: **200°C**

Mass Spectrometer Source Temperature: **200°C**

Injection Port: **A**

Injector Temperature: **175°C**

Gas Chromatograph Oven Temperature Profile:

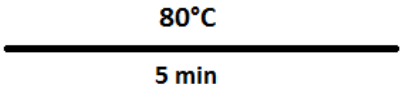

Figure 10: Propionic Acid GC Oven Temperature Profile

Gas Chromatograph Carrier Gas Flow Rate: **1.5 mL/min**

Gas Chromatograph Split Injection Mode (Flow or Ratio): **Ratio**

Gas Chromatograph Split Injection Ratio: **300:1**

Mass Spectrometer Solvent Delay: **0 min**

Mass Spectrometer Mass Number Range: **5 to 600**

Butyric Acid

Inlet Line Temperature: **200°C**

Mass Spectrometer Source Temperature: **200°C**

Injection Port: **A**

Injector Temperature: **200°C**

Gas Chromatograph Oven Temperature Profile:

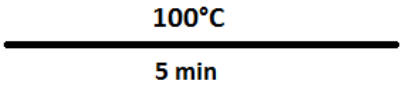

Figure 11: Butyric Acid GC Oven Temperature Profile

Gas Chromatograph Carrier Gas Flow Rate: **1.5 mL/min**

Gas Chromatograph Split Injection Mode (Flow or Ratio): **Ratio**

Gas Chromatograph Split Injection Ratio: **300:1**

Mass Spectrometer Solvent Delay: **0 min**

Mass Spectrometer Mass Number Range: **5 to 600**

3.3.2. Scanning Electron Microscopy (SEM) and Electron Dispersive Spectroscopy (EDS)

Scanning Electron Microscopy (SEM) was performed using a Hitachi system (Hitachi; Krefeld, Germany) with an electron voltage of 30.0kV, a magnification range of 200x, and a working distance of 10 mm. Energy Dispersive Spectroscopy (EDS) was performed using an Oxford Instruments system (Oxford Instruments; Concord, MA, USA) with an electron voltage of 30.0kV, a magnification range of 200x and a working distance of 10 mm. Samples were made electronically conductive by sputtering between 5.0-6.5.0nm of platinum onto the top side of each PEM material sample.

3.3.3. X-Ray Diffraction (XRD)

X-Ray Diffraction (XRD) was performed using a SmartLab X-ray Diffraction (XRD) system (Rigaku Americas Corporation; The Woodlands, TX, USA). Broad material scans were conducted from 10° ≤ 2θ°≤90° with a 0.040 step, 1.00°/min scan speed, a copper filament and nickel filter, and at 20 kV. Focused scans around a single peak were taken from 18° ≤ 2θ°≤33° with a 0.010 step width, 0.10°/min scan speed, a copper filament and nickel filter, and was operated at 20 kV.

3.3.4. Fourier-Transform Infrared Spectroscopy (FTIR)

The FCATT PEM material was analyzed, at room temperature, using an FTIR at the Elastomer, Isomer, Polymer laboratory located at TARDEC in building 215.

Fourier-Transform Infrared Spectroscopy (FTIR) was performed using a Thermo Scientific Nicolet 6700 system (Thermo Scientific Instruments Corporation; Madison, WI, USA). FTIR scans were performed between 4000 and 500 cm^{-1} wavenumbers and 64 scans were performed per sample.

3.3.5. Thermo-Gravimetric Analysis – Fourier Transform Infrared Spectroscopy (TGA-FTIR)

The off-gas produced from the FCATT PEM material samples was analyzed using a TGA-FTIR from Southwest Research Institute (SwRI) (San Antonia, TX).

Thermo-Gravimetric Analysis (TGA) was performed using a TA Instruments TGA Q5600 SDT system (TA Instruments; New Castle, DE, USA). Between 17.4060 mg and 23.4950 mg of sample was used and was heated from 21°C to 700°C using a ramp rate of 30°C/min in a nitrogen atmosphere.

Fourier-Transform Infrared Spectroscopy (FTIR) was performed on using a Nicolet iS50 system (Thermo Scientific Instruments Corporation; Madison, WI, USA). FTIR scans were performed between 4000 and 500 cm^{-1} wavenumbers and 16 scans were performed per data point.

3.3.6. Conductivity Measurements

Conductivity from solutions was determined using an Extech ExStik II EC400 (Extech, Nashua, NH) conductivity probe. Pure solutions and solution mixtures were created to be ~20mL, which was enough to submerge the probe electrodes and obtain conductivity values. Measurements were records from the probe once the conductivity value stopped changing.

4. Fuel Cell All-Terrain Transport (FCATT) Proton Exchange Membrane (PEM) Material Acetic Acid Production Mechanism Characterization

4.1. Introduction

This section will characterize the FCATT PEM material to determine its chemical composition before thermal decomposition and the chemical composition of its off-gas, which will provide useful information into the production mechanism of acetic acid.

4.2. FCATT Exhaust Water Characterization and Discussion

Figure 12 shows the cathode and anode exhaust water analysis results, previously reported [1], which demonstrates that acetic acid was being produced in both samples. (The issue was first noted when the odor of vinegar was smelled while the FCATT was being operated.)

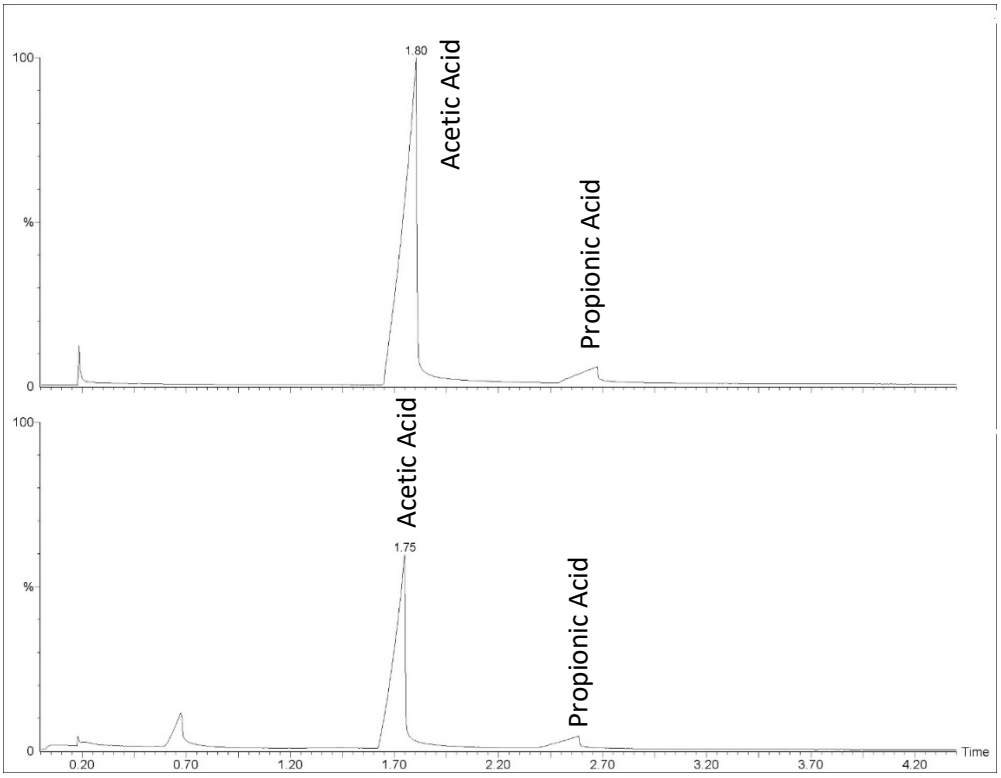

Figure 12: FCATT PEM Stack Cathode Exhaust Water (top) and Anode Exhaust Water (bottom)

The presence of any compound other than water is a clear indication that the PEM fuel cell is not operating correctly.

Figure 13 and Figure 14, also reported previously [1], show that acetic acid was identified being produced from the both the MEA and PEM material itself (in three separate locations within the stack) when heated to at least 65°C. Cell 1 was closest to the stack manifold and Cell 31 was farthest away from the stack manifold.

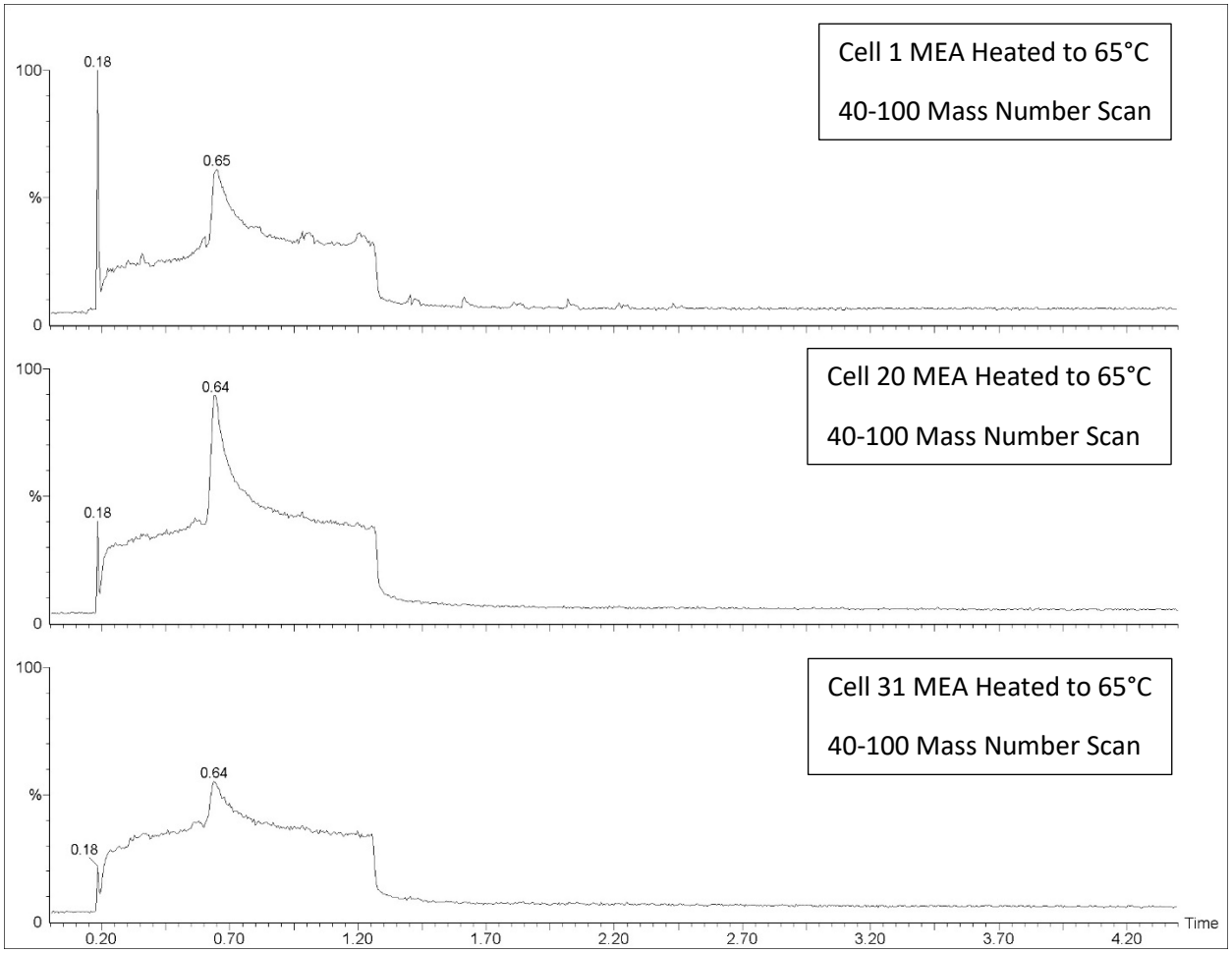

Figure 13: Chromatographs of PEM Stack Membrane Electrode Assembly's (MEA) for Cell 1 (top), Cell 20 (middle) and Cell 31 (bottom) Heated to 65°C.

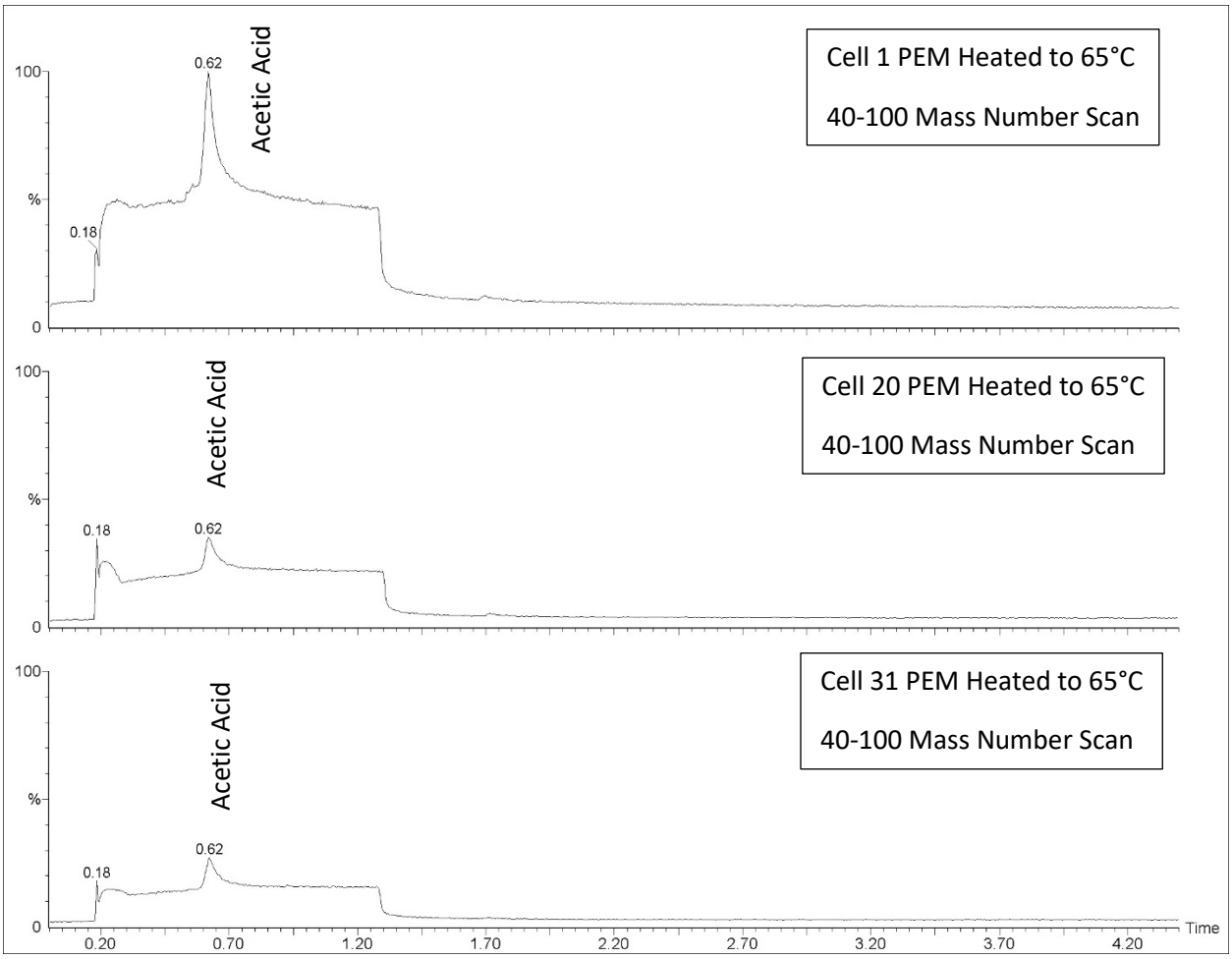

Figure 14: Chromatographs of Proton Exchange Membrane (PEM) for Cell 1 (top), Cell 20 (middle) and Cell 31 (bottom) Heated to 65°C.

Up to this point the previous report only showed that heating the PEM material produced the acetic acid, but the reaction mechanism for the formation of the acetic acid was still unknown. The following section will take a closer look at the PEM material composition and what compounds are produced when heated, and a reaction mechanism will be proposed.

4.3. FCATT PEM Material FTIR and TGA-FTIR Characterization

Figure 15 shows FTIR scan results reported previously [1] using the Cell 1 PEM material.

Literature studies identified the peaks at 3333.00 cm^{-1} and 2930.00 cm^{-1} to be from silicon, which was contained within the PEM material [2, 3, 4]. Further comparison of Figure 15 against literature results only revealed partial or close (but not exact) matches. Acetic acid (or acetic acid with different side groups) results reported in literature studies [5, 6, 7, 8, 9, 10, 11, 12] have main peaks that match or are close to the PEM material at 1712.99 cm^{-1} and 1250.00 cm^{-1}. A few additional acetate compounds are reported in literature studies [13, 14]. From these results it appears that an ester or acetate compound could be eluting from the PEM material to react and form acetic acid. It is also possible, based on these literature results, that acetic acid could be directly eluting from the PEM material.

These results present two problems that need to be resolved, which are: 1. there are a number of possible compounds that may have been added during the formulation of the PEM material, but none of these compounds make a close enough match to identify which is present at room temperature and 2. The specific compound(s), if any, which are produced during thermal decomposition is unknown.

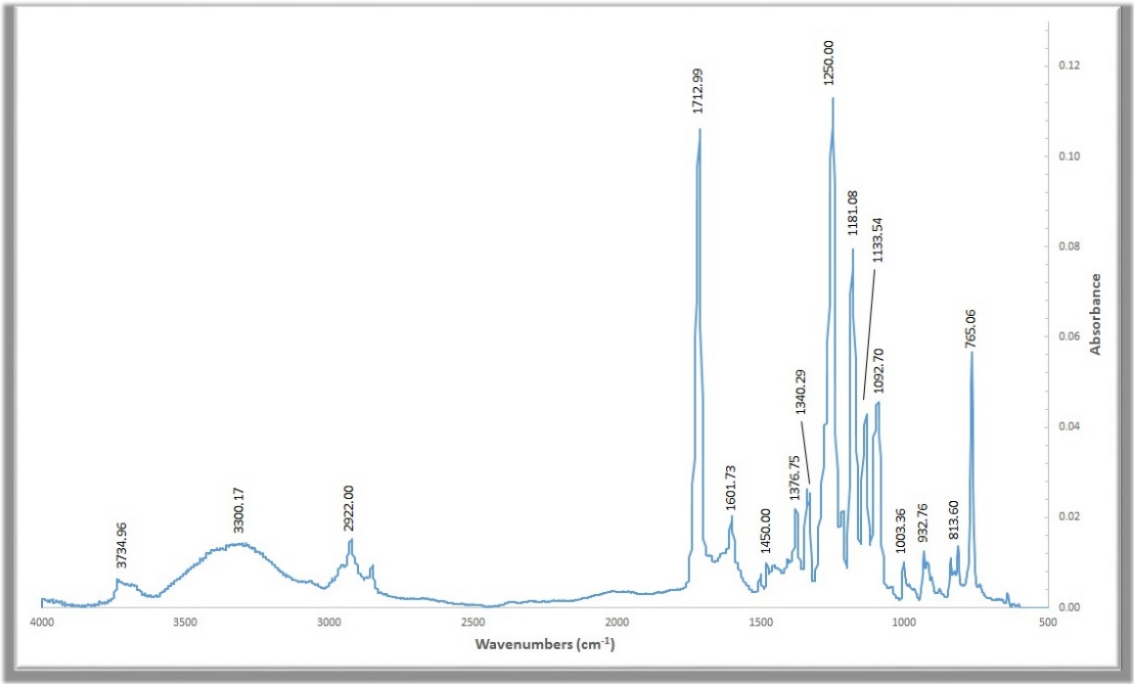

Figure 15: Fourier-Transform Infrared Spectroscopy Scan Results for PEM Material within Cell 1 and Cell 31.

Additional information to answer these two questions can be gained by using the TGA-FTIR characterization technique. Any chemical compounds produced during thermal decomposition of the PEM material (using the TGA) are analyzed by an FTIR, which is referred to as TGA-FTIR analysis. Samples of the PEM material from Cell 1 and 31 were sent to Southwest Research Institute for TGA-FTIR characterization.

Figure 16 shows the TGA mass loss (left vertical scale-bar) and derivative of the mass loss raw data (right vertical scale-bar) for Cell 1. The mass loss data is shown as the blue line and the derivative is shown as the orange line. Overall one large decomposition event occurred which started around 400°C.

Figure 17, Figure 18, and Figure 19 show the FTIR results for the characterization of the Cell 1 PEM material off-gas and their respective compound database match results. At lower decomposition temperatures (around 188°C) the only detectable compound was water. Later, at elevated temperatures (around 402°C), two compounds were detected which were ethanal (aka. Acetaldehyde) and carbon dioxide (CO_2).

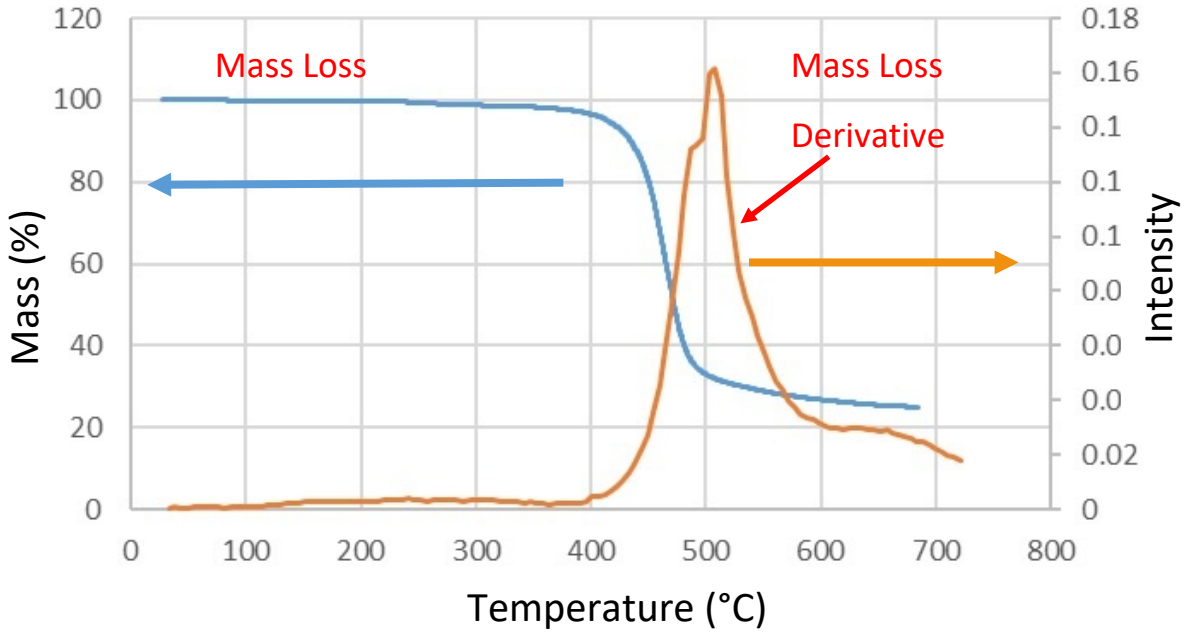

Figure 16: Cell 1 TGA Mass Loss and Derivative Raw Data Plots

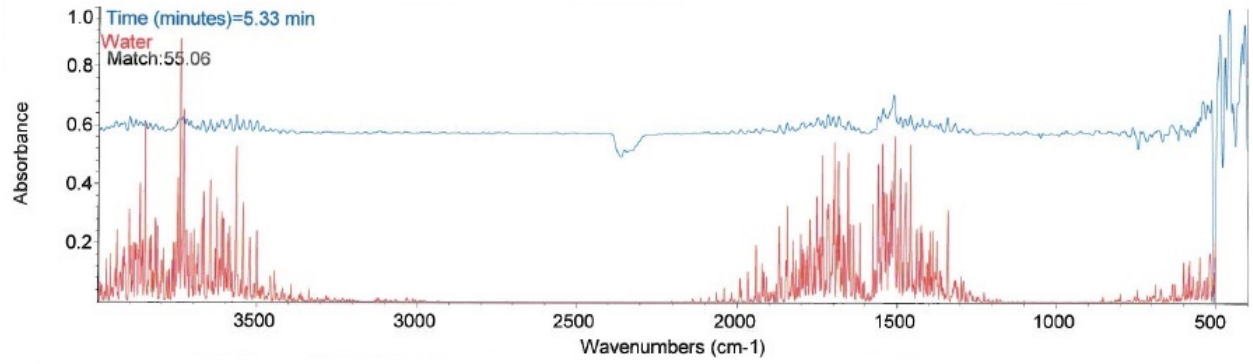

Figure 17: Cell 1 FTIR Scan Raw Data and Database Results at 5.33min (188°C)

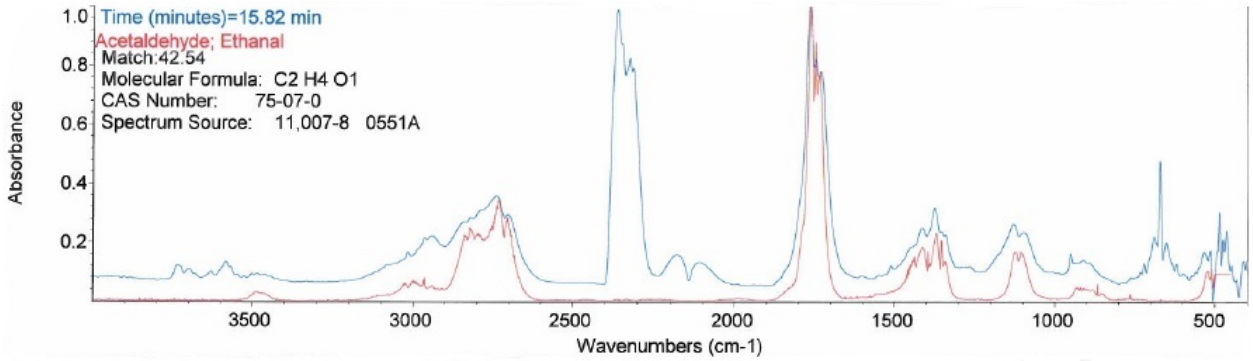

Figure 18: Cell 1 FTIR Scan Raw Data and Database Results at 15.82min (502°C)

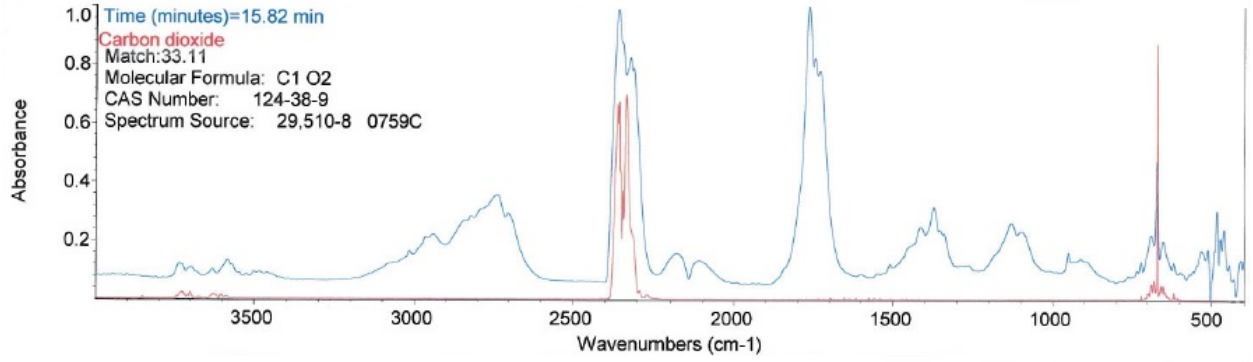

Figure 19: Cell 1 FTIR Scan Raw Data and Database Results at 15.82min (502°C)

Figure 20 shows the TGA mass loss (left vertical scale-bar) and derivative of the mass loss raw data (right vertical scale-bar) for Cell 31. The mass loss data is shown as the blue line and the derivative is shown as the orange line. Overall there occurred two decomposition events which started around 400°C, similar to Cell 1. The Cell 31 PEM material thermal decomposition has a much more defined second decomposition event shown in the derivative plot.

Figure 21, Figure 22, Figure 23 and Figure 24 show the FTIR results for the characterization of the Cell 31 PEM material off-gas and their respective compound database match results. Similar to Cell 1 at lower decomposition temperatures (around 267°C) the only detectable compound was water. Later, at elevated temperatures (around 407°C, 513°C and 529°C), two compounds were detected, which were ethanal and butanoic acid (aka. Butyric acid).

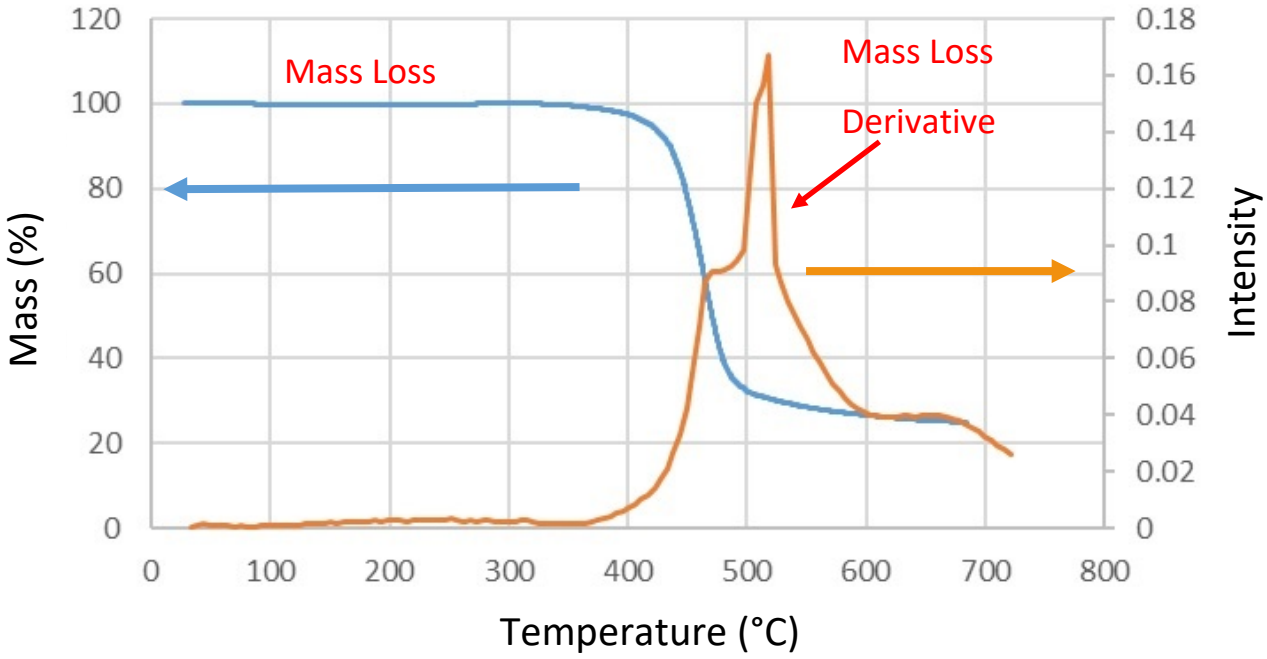

Figure 20: Cell 31 TGA Mass Loss and Derivative Raw Data Plots

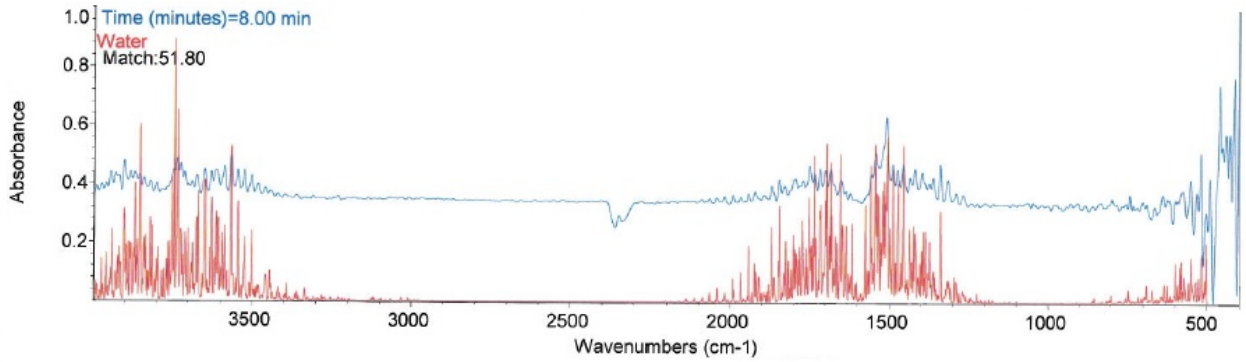

Figure 21: Cell 31 FTIR Scan Raw Data and Database Results at 8.00min (267°C)

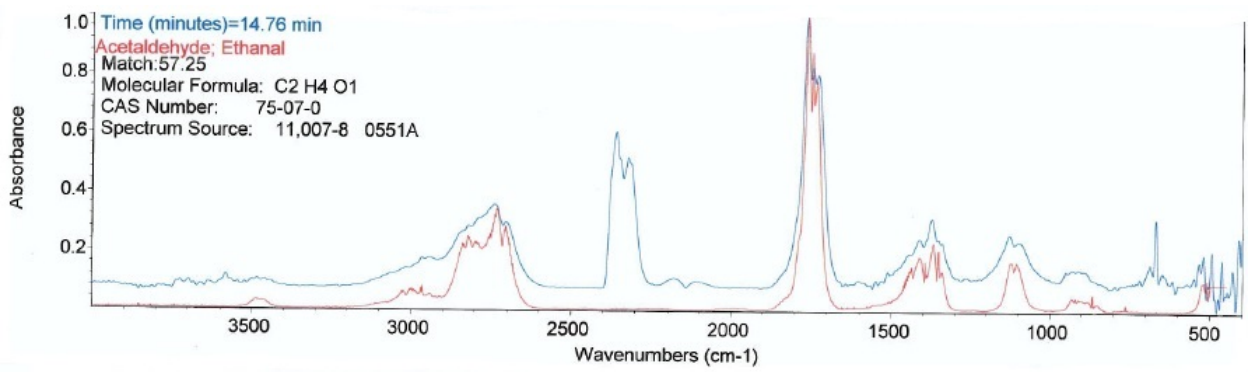

Figure 22: Cell 31 FTIR Scan Raw Data and Database Results at 14.76min (407°C)

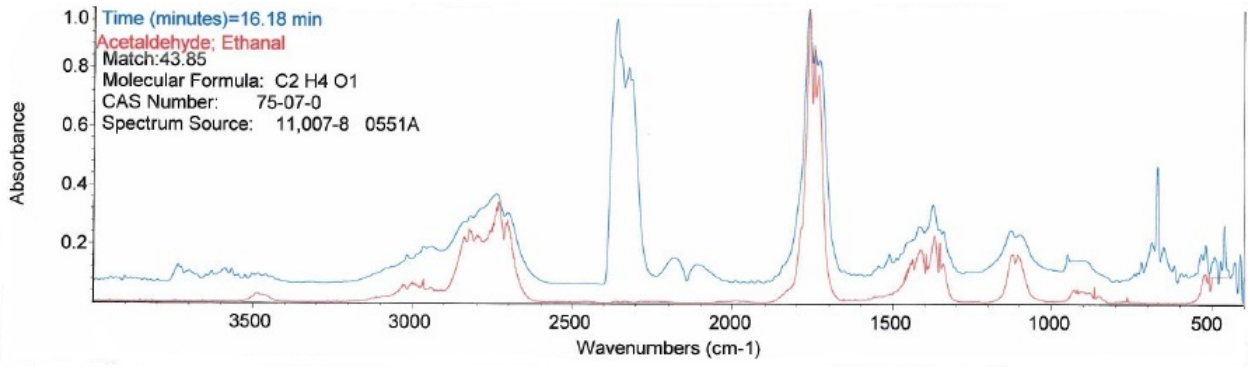

Figure 23: Cell 31 FTIR Scan Raw Data and Database Results at 16.18min (513°C)

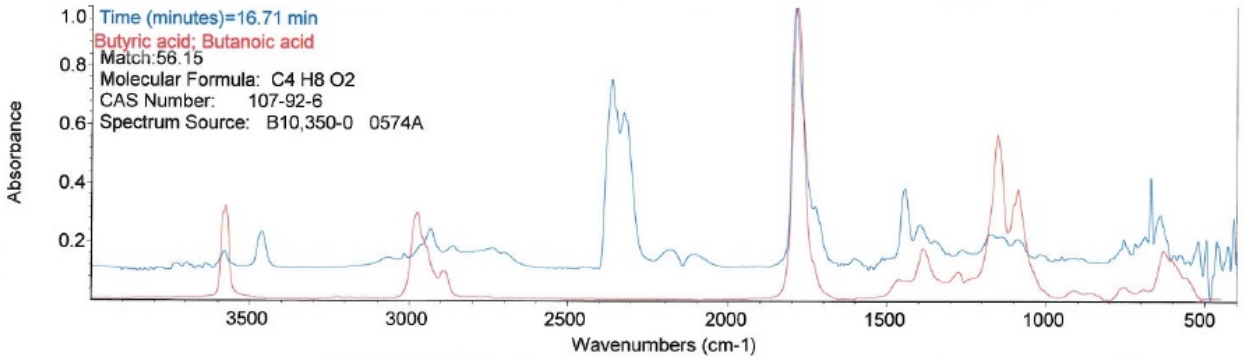

Figure 24: Cell 31 FTIR Scan Raw Data and Database Results at 16.71min (529°C)

Overall the water, ethanal, and CO_2 appear to have a clear match between the peaks in the database FTIR plot and the PEM material off-gas FTIR raw data. The butanoic acid, despite having a match of 56%, does not appear to have a clear match between the database and PEM material off-gas FTIR raw data.

Based on these results the next section will propose reaction mechanism(s) that describe how the acetic acid was produced in both the MEA and the PEM material examples.

4.4. Industrial Acetic Acid Production Reactions

Two different material samples, with greatly different material compositions, were shown to produce acetic acid when thermally decomposed, which were samples of MEA and PEM material from the FCATT fuel cell stack. Before analysis of the TGA-FTIR data can be conducted a comprehensive list of the different reactions that produce acetic acid needs to be generated. There are a few different methods used produce acetic acid found in industry, which now will be quickly explored to determine whether any match the raw data presented thus far.

4.4.1. Methanol Carbonylation

Acetic acid can be produced through the reaction between methanol and carbon monoxide using metal carbonyl or metal rhodium catalysts [15, 16, 17], shown in the reactions below:

1. CH_3OH (methanol) + HI (hydrogen iodide) $\xrightarrow{catalyst}$ CH_3I (methyl Iodide) + H_2O
2. CH_3I (methyl Iodide) + CO $\xrightarrow{catalyst}$ CH_3COI
3. CH_3COI + H_2O $\xrightarrow{catalyst}$ CH_3COOH (acetic acid) + HI (hydrogen iodide)

This process of producing acetic acid regenerates the hydrogen iodide, which was used as a reagent in the first step. Additional steps would need to be taken to remove the hydrogen iodide.

4.4.2. Acetaldehyde Oxidation

Acetic acid can be produced through the oxidation of acetaldehyde using oxygen from the air, metal catalysts, high temperatures (150°C) and high pressures (55 atm) [18], shown in the reaction below:

1. CH_3COH (acetaldehyde) + O $\xrightarrow{150°C,\ 55atm,\ catalyst}$ CH_3COOH (acetic acid)

This reaction also has a number of side-products that are formed such as: butanone, ethyl acetate, formic acid and propionic acid.

4.4.3. Ethylene Oxidation

Acetic acid can be produced through the oxidation of ethylene using a palladium catalyst supported on a heteropoly acid, shown in the reaction below:

1. C_2H_4 (ethylene) + O_2 $\xrightarrow{catalyst}$ CH_3COOH (acetic acid)

4.4.4. Oxidative Fermentation

Acetic acid can be produced through the oxidation of acetaldehyde using acetic acid bacteria of the genus Acetobacter as a biocatalyst [19, 20, 21] under temperatures between 20-30°C and natural aeration using oxygen from the air. This reaction is shown below:

1. CH_3COH (acetaldehyde) + O $\xrightarrow{Acetobacter\ Bacteria,\ 20-30°C}$ CH_3COOH (acetic acid)

The Acetobacter bacteria is commonly found in air and historically caused vinegar (dilute acetic acid) to be produced in wine if precautions were not taken.

The MEA sample will be investigated first since it was previously shown to contain platinum and cobalt [1] electrocatalyst materials and many of these different reactions use a metal catalyst of some type.

4.5. FCATT Stack MEA Acetic Acid Reaction Mechanisms

The TGA-FTIR results collected from SwRI showed that acetaldehyde was produced from the thermal decomposition of the PEM material. The acetaldehyde was produced at higher temperatures than the 65°C previously shown in Figure 13, but it is not unreasonable to anticipate that a lower concentration of acetaldehyde would be produced at lower operating temperatures. The use of acetaldehyde excludes the methanol carbonylation and ethylene oxidation reactions, and leaves the acetaldehyde oxidation and oxidative fermentation reactions as possibilities.

As stated previously [1] EDS results from the MEA electrocatalyst material showed the presence of platinum in the cathode catalyst layer. The fact that a metal catalyst is present highly suggests that acetic acid was produced through the acetaldehyde oxidation reaction. The lower temperature used by the PEM stack (65°C) instead of the 150°C desired by the reaction would probably lower the yield of acetic acid produced, which had low concentrations when tested. One final point that strengthens the conclusion that acetaldehyde oxidation is the reaction mechanism used for acetic acid production with the MEA is that propionic acid was also detected in low concentrations, shown in Figure 12, directly from the FCATT exhaust. Propionic acid is one possible side-product of the acetaldehyde oxidation reaction and matches the characterization results.

4.6. FCATT Stack PEM Material Acetic Acid Reaction Mechanisms

Acetic acid was also produced directly from the PEM material itself, but that did not contain any electrocatalyst materials, which suggests a different mechanism was present for this scenario.

As mentioned above the oxidative fermentation reaction uses acetaldehyde and does not require the use of metal catalysts. The temperature required for this reaction to proceed is also similar to the 65°C used in the characterization experiments. The literature sources also mention that the Acetobacter bacteria is commonly found in air.

The oxidative fermentation reaction sounds the most plausible since Acetobacter bacteria was likely introduced into the deionized water bath used to heat the sample to 65°C. Oxygen, dissolved in the deionized water, was the source of oxygen that oxidized the acetaldehyde as it was produced from the PEM material thermal decomposition.

The next section will explore whether acetic acid (combined with temperature and electrical bias) could result in the degradation of the platinum electrocatalyst material, and what that mechanism would be.

4.7. Fuel Cell All-Terrain Transport (FCATT) Proton Exchange Membrane (PEM) Material Acetic Acid Production Mechanism Summary

Characterization of the FCATT MEA and PEM material shows the following results:

1. The PEM material in both Cell 1 and 31, when characterized by TGA-FTIR, showed the one major component of the off-gas was acetaldehyde.
2. The MEA samples most likely produced acetic acid by the acetaldehyde oxidation reaction.
3. The PEM material samples most likely produced acetic acid by the oxidative fermentation reaction.

5. Platinum Electrocatalyst Loss Degradation Investigation

5.1. Introduction

As mentioned in Section 2, the acetic acid being produced by Cell 1 is hypothesized to promote cell degradation through the loss of the platinum electrocatalyst on the cathodes (specifically) in the stack. This hypothesis is based on Scanning Electron Microscopy (SEM) images from the cathode and anode from Cell 1 and Cell 31, shown in Figure 25 below, which show a noticeably smaller amount of platinum on both the cathode and anode for Cell 1 compared to Cell 31. Since each cell is assumed to be manufactured in a uniform, similar manner a difference in electrocatalyst loading between cells is unlikely due to a processing/manufacturing flaw. If a processing/manufacturing flaw existed then that would be expected to be shown in cell performance plots when the stack was original. Original performance plots, which compare Cell 1 and Cell 31 [1] voltages, show no significant performance differences between those two cells, which indicate this was not a manufacturing issue or a deliberate design choice. Based on these assumptions and performance results, degradation is a certainly a possible explanation and will be investigated in this section.

The Cell 1 cathode appeared to have noticeably more platinum loss in its cathode compared to its anode than what Cell 31 showed. This observed difference in platinum loss is hypothesized to be connected to the acetic acid production, shown in Section 4 to be primarily produced in the Cell 1 cathode.

The following experimental results will independently simulate the different operating conditions the platinum in the cell experienced so as to determine if platinum loss is possible and if so what is that mechanism. Even though Section 2 states acetic acid concentration effects would be investigated separately, they have been grouped together with all the other experiments to save time and identify trends more easily.

5.2. Solvent Purity Characterization

The following experiments used four different solvents which were: 1. Deionized water, 2. 99.7 vol% glacial acetic acid, 3. 99 vol% propionic acid, and 4. 99 vol% butyric acid. To ensure that these solvents were pure, and contaminants were not present, they were all characterized using the GC/MS using the parameters outlined in Section 3. Chromatogram and Mass Spectrogram results, for each solvent, are shown in Figure 26 and Figure 27, respectively.

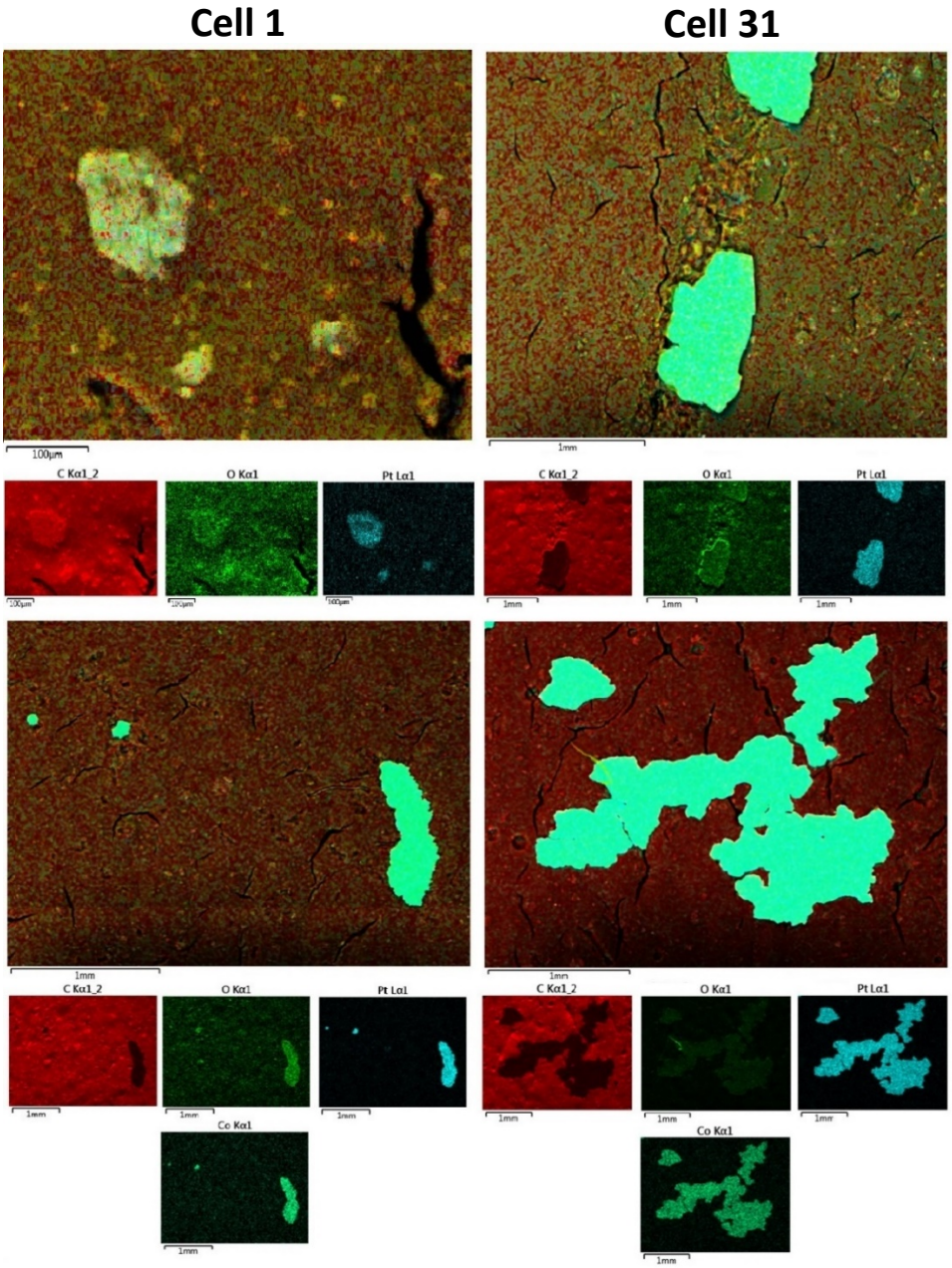

Figure 25: Cell 1 Cathode (top left)/Anode (bottom left) and Cell 31 Cathode (top right)/Anode (bottom right) Energy Dispersive Spectroscopy Platinum Electrocatalyst Elemental Map

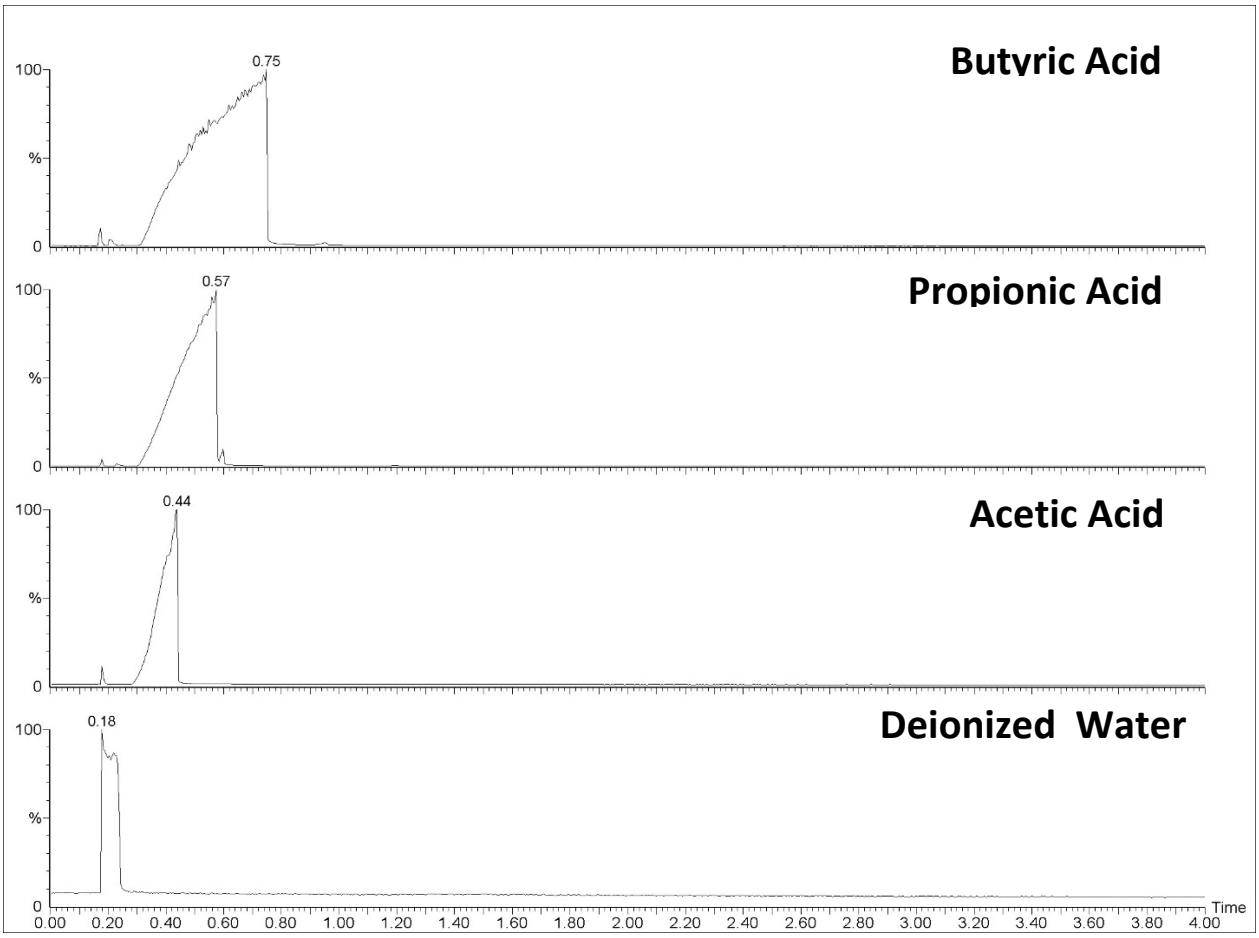

Figure 26: Deionized Water (bottom), 99.7 vol% Acetic Acid, 99 vol% Propionic Acid and 99 vol% Butyric Acid (top) Chromatograms Comparison Plot

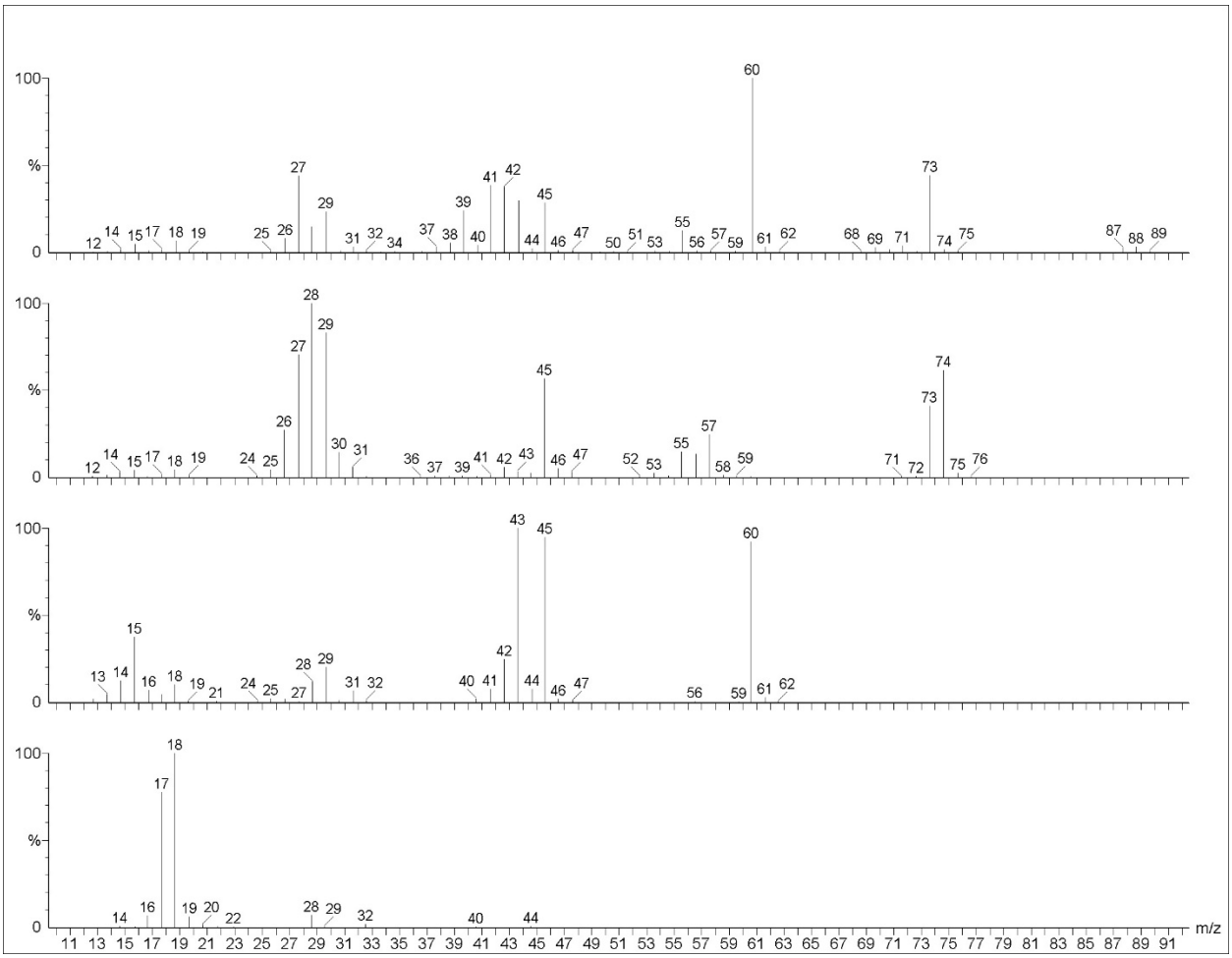

Figure 27: Deionized Water (bottom), 99.7 vol% Acetic Acid, 99 vol% Propionic Acid and 99 vol% Butyric Acid (top) Mass Spectrogram Comparison Plot

The results all show that each solvent contains no significant amounts of contaminants and any mass numbers present in significant quantities are from the carrier gas. Table 1 outlines the major compounds found in Figure 26.

Table 1: Deionized Water, 99.7 vol% Acetic Acid, 99vol% Propionic Acid and 99vol% Butyric Acid Compounds in Figure 26

Compound Tested	Compound Identified	Mass Number (m/z)	Elution Time (min)	CAS #
Deionized Water	Water	18	0.18	7732-18-5
Acetic Acid	Acetic Acid	60	0.44	64-19-7
Propionic Acid	Propanoic Acid	74	0.57	79-09-4
Butyric Acid	Butanoic Acid	88	0.75	107-92-6

Some of the lower mass numbers in each mass scan have elevated levels than what would be expected for a pure compound. This is due to the carrier gas contributing to those lower mass numbers in each mass scan. Table 2 shows a list of the common mass numbers located in the carrier gas:

Table 2: Common Gas Chromatograph/Mass Spectrometer Carrier Gas Mass Numbers

Compound Name	Mass Number (m/z)
Water (H_2O)	18
Carbon Monoxide (CO)	28
Nitrogen Gas (N_2)	28
Methanol (CH_3OH)	32
Oxygen Gas (O_2)	32
Carbon Dioxide (CO_2)	44

Now that the compounds used in this report are shown to be pure, and any results can be attributed directly to those specific compounds and nothing else, the following sections will outline the results found in determining whether it is possible to remove platinum from the PEM material using various operating parameters.

5.3. Impact of Temperature and Acetic Acid Concentration

As mentioned in Section 3 samples were heated between 46-103°C for 38 hrs each (the total duration the PEM stack was in operation) in either 10mL of deionized water (now referred to as 0 vol% acetic acid), 5 vol% acetic acid (a mixture of 5 vol% acetic acid and 95 vol% deionized water) and 99.7 vol% glacial acetic acid (now referred to as 99.7 vol% acetic acid).

These tests attempt to simulate the heat applied to the PEM material and platinum electrocatalyst during operation. Heating may occur on a macro scale due to normal operation or on a local level (molecular level) due to increased heating from increased cell inefficiencies (reported previously [1] possibly due to the manifold cooling Cell 1). EDS measurements were taken before and after each experiment to measure whether heating had an impact on the amount of platinum sputter coated on the PEM material.

Figure 28 shows an SEM image of a typical sample location to collect EDS data before and after experimental conditions are applied to each sample. The surface is relatively free of features or other forms of debris that may impact the EDS results.

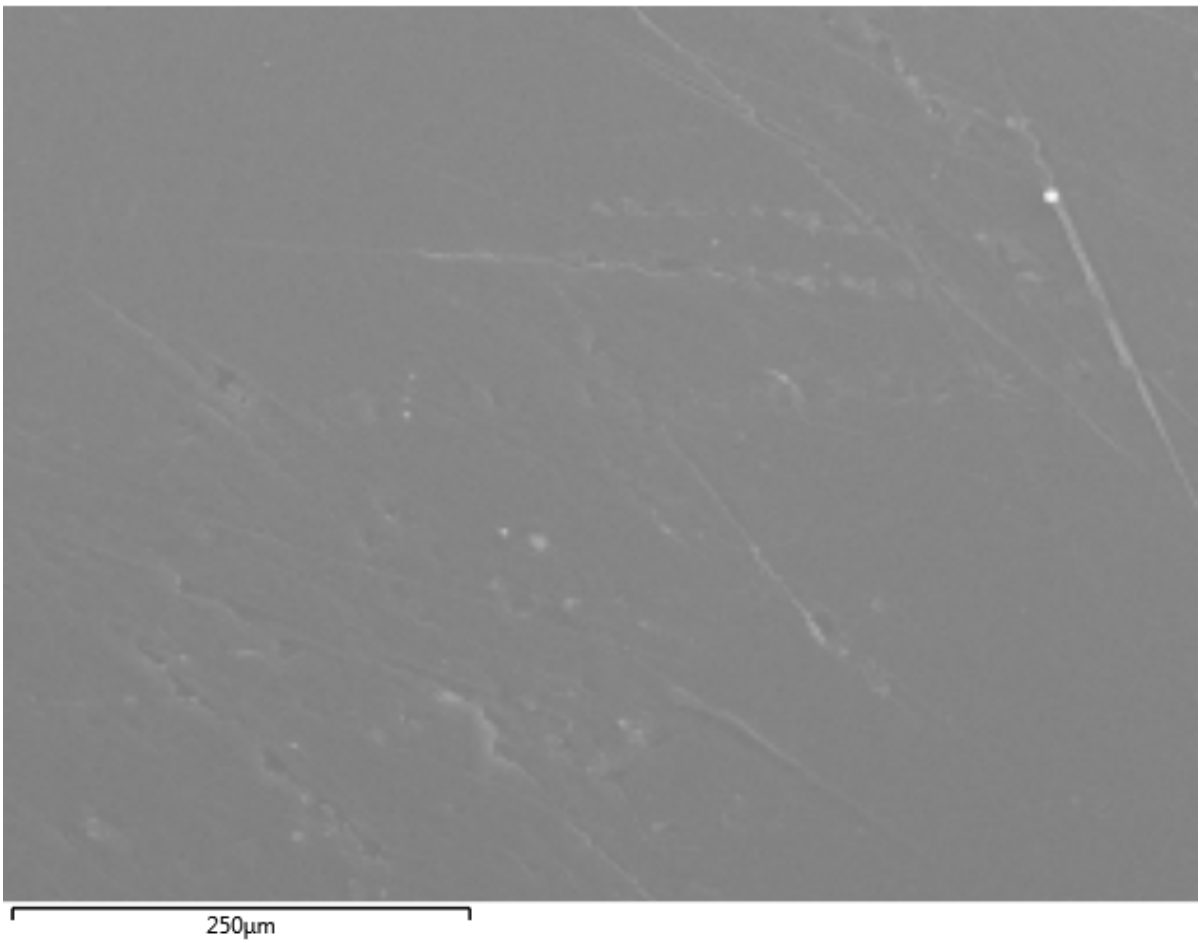

Figure 28: PEM Material Typical Scanning Electron Microscopy Image of EDS Sample Location

Figure 29 shows a typical EDS scan, taken before experimentation. The peak located at 2.048 keV is the main platinum peak and will be used for determination if platinum is being removed, since any changes would be the most noticeable in that peak. The copper peaks are from the copper tape used to hold the sample inside the SEM and the silicon is from quartz located in the PEM material [1]. Changes to the silicon peak height (located at 1.739 keV) also was monitored and reported.

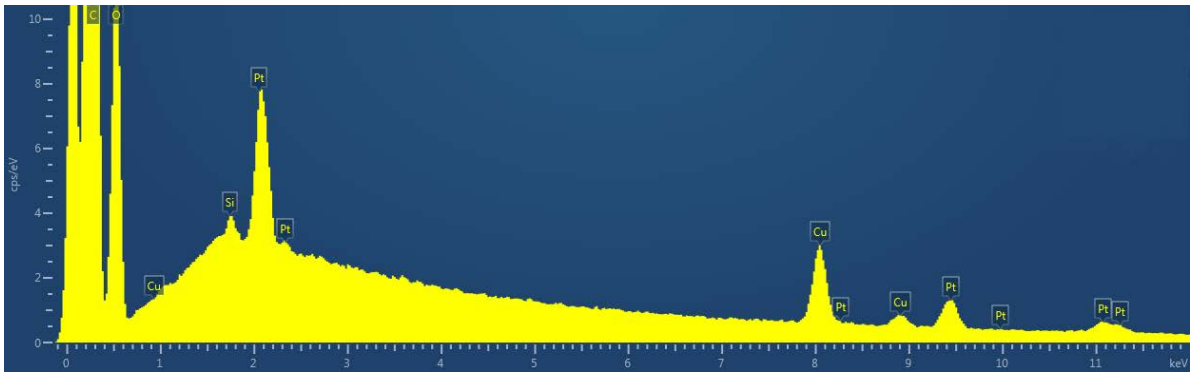

Figure 29: Typical Initial Energy Dispersive Spectroscopy Scan of PEM Material Sputter Coated with Platinum

Figure 30 shows an enlarged view of Figure 29 to demonstrate how peak height was calculated. The bottom point of the peak is read off the y-axis and then the top point of the peak is read off the y-axis. The difference between the two points was calculated to determine the peak height for each EDS scan taken.

Each sample had three scans taken before and three scans taken after each experiment at different locations across the sample. This ensured any possible localized effects would not represent the entire sample and changes, due to experimental conditions, would be identified in many different locations. Standard deviations (shown as vertical bars) for each experiment before and after were generated from the three scans.

Since an average is used, all future EDS plots will be as close to the average as possible and provide a representative picture, but may not be completely the same as the average reported. Figures that report peak height comparisons or ratio data between different experimental conditions use the average peak height from all three sample locations.

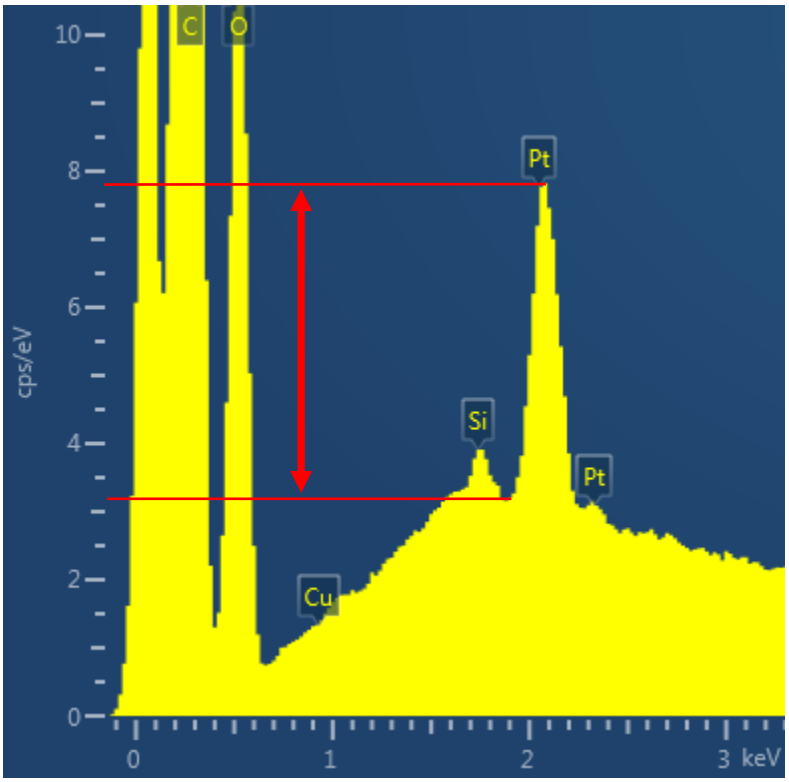

Figure 30: Enlarged Section of Typical Initial Energy Dispersive Spectroscopy Scan from PEM Material Sputter Coated with Platinum

Figure 31 shows the platinum loss results for the various samples heated at temperature below the normal stack operating temperature of 65°C and above that temperature up to a maximum of ~103°C. The left column shows data for samples heated in 0 vol% acetic acid solution, the middle shows data for samples heated in 5 vol% acetic acid solution and the right column shows data for samples heated in 99.7 vol% acetic acid. The top row shows the average platinum peak height before (blue bars) and after (orange bars) heating was applied. The bottom row shows the delta platinum peak height between the before and after data sets in the top row, which helps to evaluate trends that may occur, since the initial and final peak height values change slightly between samples.

Positive values in the bottom row indicate there was a decrease in the peak height from the initial EDS data, while negative values indicate there was an increase in the peak height from the initial EDS data.

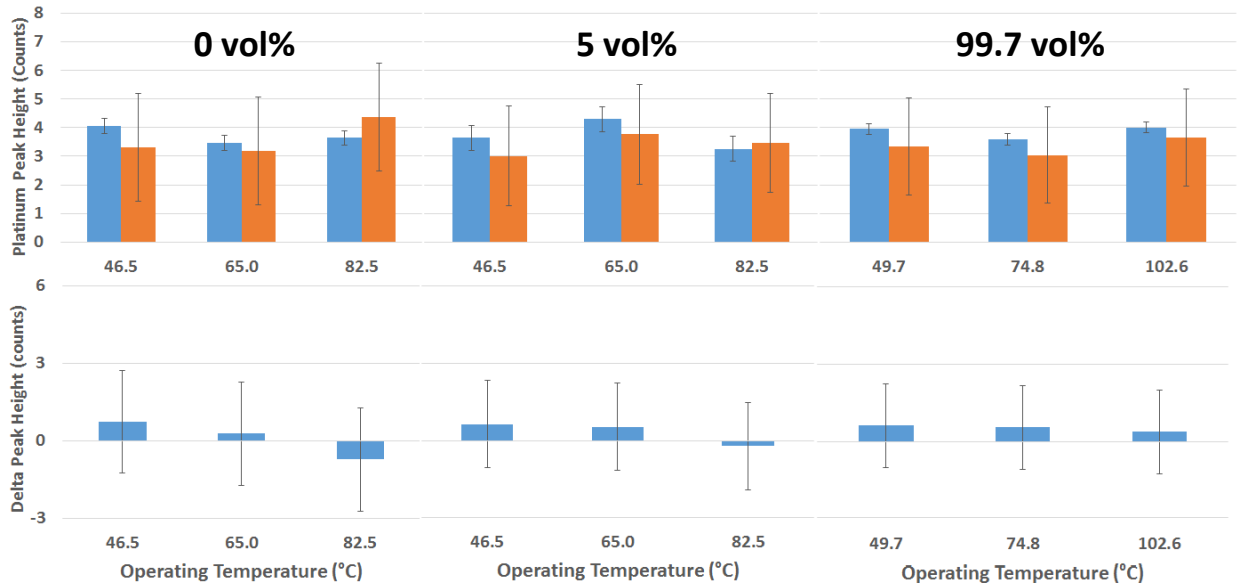

Figure 31: Before (blue bars, top row) and After (orange bars, top row) Platinum Peak Height Comparison for Heating Effects in 0 vol% Acetic Acid (left column), 5 vol% Acetic Acid (middle column) and 99.7 vol% Acetic Acid (right column). Bottom Row Shows Delta Values between Before and After.

Heating the samples for a prolonged period of time show the following information. First, there does not appear to be any difference in the platinum loss results as the temperature is increased. Second, there also does not appear to be any difference in the in the platinum loss results between the different solvents used.

Any platinum loss detected can be attributed to possibly one or more of the following reasons: 1. variations in the EDS detector readings, 2. variations in platinum levels between the different locations characterized. Each sample had different locations characterized before and after heating, so it is possible platinum sputtered levels would be slightly different across the sample, and 3. minimal platinum loss due to handling of each sample. Platinum loss due to sample handling was investigated and found to be undetectable.

Increases in platinum levels can be simply attributed to either variations in the EDS detector readings, which usually for heavier elements (such as platinum) would have a 1% variation, or from variations in the sputtered platinum levels. All values are within the standard deviation of all other samples, so no trends are statistically significant.

Despite the platinum peak height values not changing there was one effect heating had on the samples detected by the EDS scans, which was an increase in the silicon peak height, shown next.

Figure 32 shows the EDS determined silicon peak height before and after heating each sample. The plot is arranged the same as Figure 31.

Unlike the platinum results, the silicon does show some trends when heated. The 0 vol% and 5 vol% solvents appear to show gradual increases in average silicon peak height with increasing temperature. The 5 vol% acetic acid solution clearly showed the most noticeable increase in average silicon peak height with increasing temperature. Despite the average peak height increasing, all changes were still within the standard deviation and thus were not statistically significant. It is possible this is a real trend but the results are uncertain at the moment.

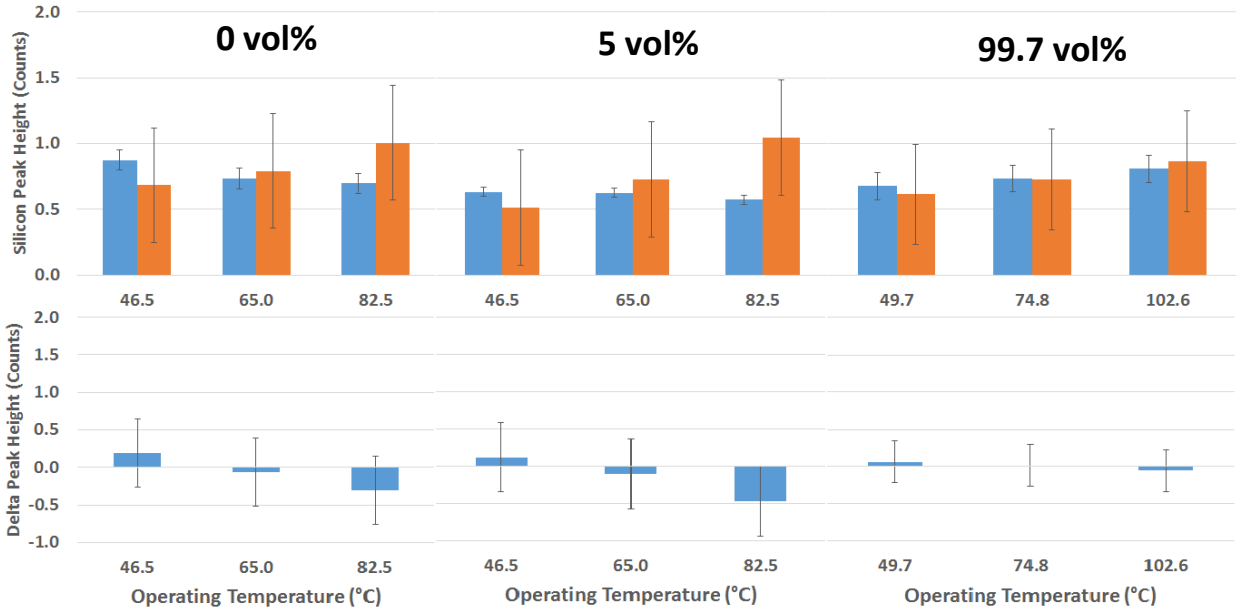

Figure 32: Before (blue bars, top row) and After (orange bars, top row) Silicon Peak Height Comparison for Heating Effects in 0 vol% Acetic Acid (left column), 5 vol% Acetic Acid (middle column) and 99.7 vol% Acetic Acid (right column). Bottom Row Shows Delta Values between Before and After.

Since the results do point to possible sample change from heating, one additional data manipulation technique was used to refine the data into a common data set which now includes changes in both the platinum peak and silicon peaks. The initial and final platinum/silicon peak height ratios were calculated and plotted in a similar manner to the previous two plots, which helps remove variation differences in data results.

Figure 33 shows the platinum/silicon peak ratio data for each heating experiment. The ratio data collected from samples before each experiment is shown in the blue bars and the data collected after each experiment is shown in the orange bars. The left column shows the 0 vol% solvent data, the middle column shows the 5 vol% data and the right column shows the 99.7 vol% data. The top row shows the ratio data before and after each experiment and the bottom row shows the delta between the initial and final ratio values.

A smaller ratio could indicate there was an increase in the silicon peak, a decrease in the platinum peak or a combination of both.

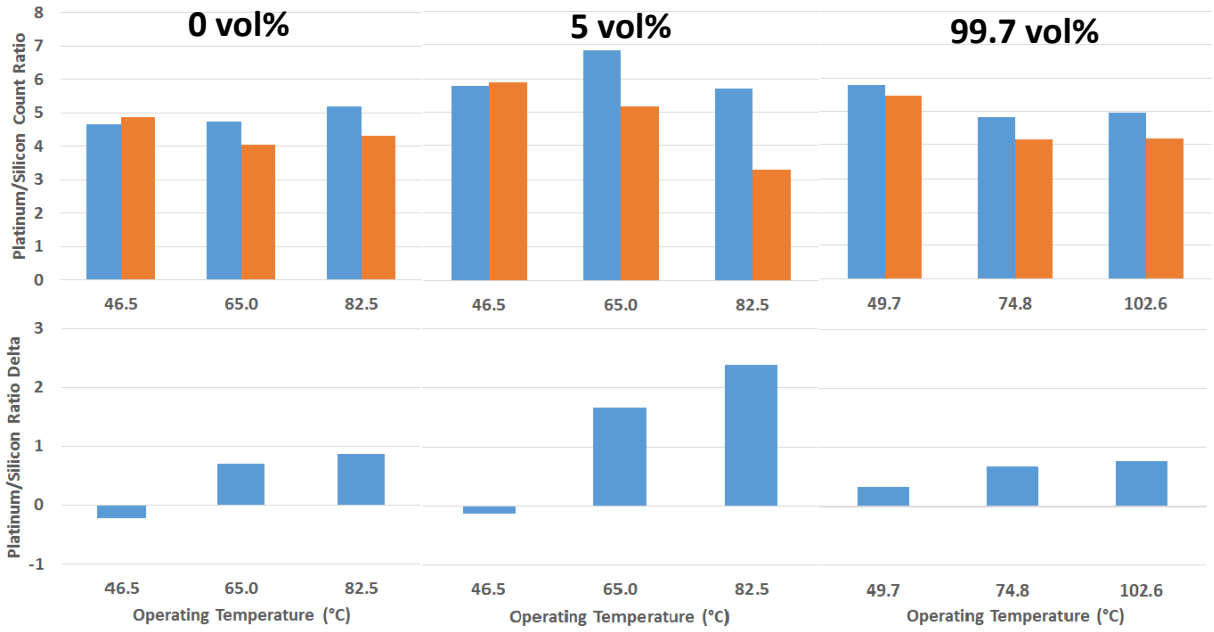

Figure 33: Before (blue bars, top row) and After (orange bars, top row) Platinum/Silicon Peak Height Ratio Comparisons for Heating Effects in 0 vol% Acetic Acid (left column), 5 vol% Acetic Acid (middle column) and 99.7 vol% Acetic Acid (right column) Calculated from Figure 31 and Figure 32. Bottom Row Shows Delta Values between Before and After.

The results show that both the 0 vol% and 99.7 vol% solvent result in a slight reduction of the platinum/silicon ratio, they are very similar. The 5 vol% solvent shows a significant decrease to the ratio value, which primarily was seen to be the result of increased silicon peak height. While no platinum loss was observed the increased silicon may be important to take note of and will be monitored in the future to determine whether there is any correlation between increased silicon levels and platinum loss using different experimental conditions.

The platinum electrocatalyst inside the stack also generated an electrical bias, which traveled through the platinum inside the stack. The next section will simulate the effect of an applied electrical bias on sputter coated platinum while in contact with the different solvents.

5.4. Impact of Electrical Bias and Acetic Acid Concentration

5.4.1. Resistivity Comparison between Samples and Literature Results

Before an electrical bias was applied to the platinum sputter coating the samples were characterized as to whether an electrical current would pass through the platinum and how would the intrinsic resistivity compare to literature results. Sputtered platinum has been documented in literature studies [22, 23, 24] to have a lower resistivity than bulk metal samples of the same material. It is important to determine the difference in resistivity since higher resistivity potentially could prevent current from flowing through the sputtered platinum at all or in sufficient amounts that would not be representative of the platinum in the FCATT PEM cells.

To determine the platinum sputter coating resistivity six samples were coated with a platinum strip similar to the illustration shown in Section 3, Figure 6. Platinum sputter coating strips were made with varying widths and lengths, but all coatings were 6.0nm in thickness. A 15.5V electrical bias was applied to each sample, at room temperature, and a multimeter was used to measure the current passing through each sample. Additional resistance, which may have manifested itself as increased resistivity, was included in the measurement through the use of the multimeter and contact resistance between the wire cable connections. Table 3 shows the values recorded for each of the six samples.

Table 3: Platinum Sputter Coating Resistivity Calculation Parameters

Sample #	Applied Voltage (V)	Measured Current (mA)	Platinum Sputter Coating Thickness (nm)	Platinum Sputter Coating Width (in)	Platinum Sputter Coating Length (in)
1	15.5	31.80	6.0	0.1895	0.7950
2	15.5	18.60	6.0	0.1300	0.8585
3	15.5	25.80	6.0	0.1530	0.7650
4	15.5	25.60	6.0	0.1470	0.8485
5	15.5	35.60	6.0	0.2105	0.8240
6	15.5	28.25	6.0	0.1760	0.8095

Figure 34 shows the calculated resistivity values (blue dots) from the sputtered platinum coating using the parameters reported in Table 3 at room temperature. The calculated values are also compared to

reported intrinsic platinum resistivity values (green dots) from literature [25]. The data is plotted on a logarithmic vertical axis.

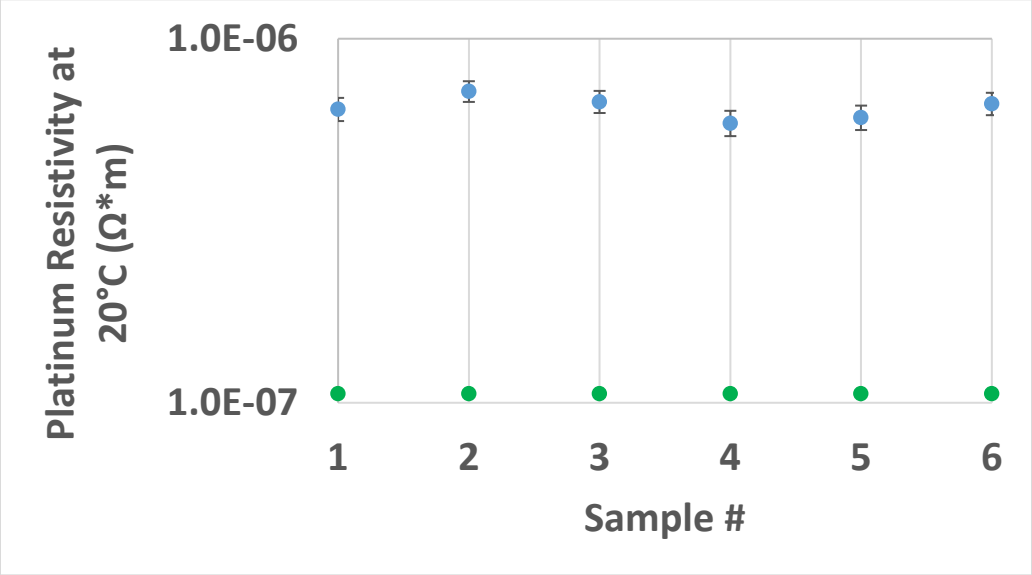

Figure 34: Platinum Sputter Coating Resistivity Calculations (blue dots) using Parameters in Table 3 Compared to Reported Intrinsic Platinum Resistivity from Literature (green dots).

The data shows three important results, which are: 1. The sputter coating resistivity data was reproducible and was generally consistent between each sample, 2. The sputter coating resistivity values were only 6 times greater than the intrinsic resistivity from literature and 3. The sputter coating was capable of flowing current in the mA range, which is sufficient to measure.

These results, compared to reported literature studies, was determine to be greater by an average of 6.0 times. A significant portion of this increased resistivity could have been due to the internal resistance if the multimeter and the contact resistance between the wires used in the measurement. Even if these additional sources of resistance were small, a factor of 6 increase is considered minimal when literature studies have reported orders of magnitude differences [26] between the sputtered material and bulk resistivity values.

Since previous samples with sputtered platinum have been shown to be capable to passing a current through the platinum layer, and those previous platinum layers also have shown similar (less than an order of magnitude difference) resistivity values to bulk platinum metal, one final analysis was to determine whether sputtering platinum onto the polymer changed the lattice strain applied to the silicon in each PEM material sample. Changing the strain applied to the silicon lattice in the PEM material, using the sputtering process, could potentially influence how easily the platinum is removed from the PEM material

results and should be accounted for, if present. Different platinum deposition processes may induce different amounts of strain so similar results between tests can be compared.

5.4.2. Sample Strain Induced by Platinum Sputtering Process

Strain values from PEM material samples, prior to and after sputtering platinum, were determined from XRD scans using the Williamson-Hall method.

The Williamson-Hall method takes into account XRD peak broadening could be caused by particle size changes and/or strain changes in the sample, based on the following formulas:

$$\beta_L = \frac{K*\lambda}{L*Cos(\theta)} \quad \text{(Equation 1)}$$

Where,

β_L = Peak broadening from particle size (nm)

K = Shape factor (typically between 0.7 and 1.1)

λ = Monochromatic X-ray wavelength (nm) (1.54nm for copper target used in these experiments)

L = Peak broadening at half the maximum intensity (Full-Width Half-Max (FWHM)) (radians)

Θ = Bragg angle (radians)

$$\beta_e = C\varepsilon * \tan(\theta) \quad \text{(Equation 2)}$$

Where,

β_ε = Peak broadening from strain

C = Multiplication factor (typically 4)

ε = Strain

Θ = Bragg angle (radians)

Equations 1 and 2 can then be combined to form Equation 3.

$$\beta_{tot} = \beta_L + \beta_e = C\varepsilon \tan(\theta) + \frac{K*\lambda}{L*Cos(\theta)} \quad \text{(Equation 3)}$$

Equation 3 can then be rearranged to form Equation 4.

$$\beta_{tot}Cos(\theta) = C\varepsilon Sin(\theta) + \frac{K*\lambda}{L} \quad \text{(Equation 4)}$$

Since Equation 4 is same form as the standard equation for a straight line (y=mx + b) it can be plotted to determine the slope and intercept. $B_{tot}Cos(\theta)$ is plotted on the y-axis and Sin(θ) is plotted on the x-axis from at least two peaks to generate a straight line. More peaks, if available, are better as the accuracy of the slope and intercept increases. The slope is equal to Cε and strain can be calculated from the slope, while the intercept is equal to (K*λ/L) and particle size can be calculated from the intercept.

As previously determined [1] the PEM material contains quartz inside the polymer material. The mean peak was the (1, 0, 1) miller index located at 26.9° 2-Theta with a small peak with the (2, 0, 2) miller index located at 55.9° 2-Theta. Since no other peaks were present these two peaks were used to calculate strain before and after the sputter coating process. No additional peaks were detected after sputtering the platinum either because the sputtered platinum was either amorphous or had such a small peak height that it was obscured by the background noise.

Results showed the average particle size and strain from each sample prior to sputter coating was 5.6 nm and 0.51%, respectively. The average particle size and strain afterwards were 6.0 nm and 0.53%, respectively. Since the particle size and strain were essentially unchanged this shows that any results detected were independent of the sputtering process.

The next variable to check is whether the applied electrical bias is realistic of what the FCATT PEM cells would experience on a macro or nano-scale.

5.4.3. Current Density Comparison between Samples and FCATT Cells

To accurately simulate the electrical bias generated by the stack, the different stack electrical parameters need to be determined.

Table 4 shows the FCATT PEM stack voltage, current, and current density on a per cell basis. Each cell had a 537.79 cm^2 active area and the stack contained 31 cells total, which were both used to calculate the cell current density. The cell current density can be determined both on a macro-scale (which spreads current across the entire cell area) or on a micro-scale or nano-scale (which spreads the current across individual platinum nanoparticles or agglomerated platinum clusters. The cross-sectional area for a typical agglomerated platinum cluster (using a conservative approach) was determined to be between 0.0002 cm^2 (2.0 x 10^{10} nm^2) and 0.0017 cm^2 (1.7 x 10^{11} nm^2).

Table 4: FCATT PEM Stack Operating Voltage, Current and Current Density Values

	5 kW Power	13 kW Power
Cell Voltage (V)	0.794	0.666
Cell Current (A)	3.19	10.13
Cell Current Density (macroscale) (mA/cm^2)	5.93	18.84
Cell Current Density (nanoscale) (mA/cm^2)	$1.87*10^6$ to $1.59*10^7$	$5.95*10^6$ to $5.06*10^7$

The following applied electrical bias experiments first use an elevated voltage to determine whether applied bias has an impact on the platinum levels, then uses a voltage of 0.8V that simulates the FCATT PEM stack cells more closely. The current density in each sample was compared to determine whether these experiments also simulate the cell current density too, which is shown in Table 5.

Table 5: PEM Material Sputter Coated with Platinum Operating Voltage, Current and Current Density Values

	Minimum Values	Maximum Values
Cell Voltage (V)	0.8	15.5
Cell Current (A)	0.0007	0.02
Cell Current Density (nanoscale) (mA/cm^2)	$4.901*10^6$	$1.40*10^8$

Overall at first comparison the current density in the sputtered platinum samples appears to be exponentially greater than what each cell would experience. The platinum electrocatalyst in the FCATT stack cells would have a much smaller current density on a macro-scale, but on a nano-scale the platinum in both cases fall within the same current density range. Experimental results obtained from the sputter coated PEM material samples, with an electrical bias applied at room temperature, were assumed to represent a similar response in the FCATT cells based on both samples having similar current densities on a nano-scale.

Since both the resistivity and current density of the platinum sputter coating are close to reported literature results and operating conditions found within the FCATT PEM stack any results obtained were assumed to be a close approximation of the FCATT PEM stack behavior. The following results illustrate the effects, first, from using a 15.5V electrical bias applied to each sample, to determine if it is possible to remove the sputtered platinum using a combination of an applied electrical bias with different acetic acid solution concentrations.

5.4.4. Impact of 15.5V Electrical Bias Effects and Acetic Acid Concentration

Since applying an electrical bias while in contact with a solution composed with and without acetic acid is very similar to the operating conditions experienced by the cells in the stack, optical microscopy photographs of each sample were taken before and after each experiment to document any changes to each sample.

The first three samples were in contact with 0 vol% acetic acid solvent while a 15.5V electrical bias was applied while at room temperature. As mentioned earlier in this paper the electrical bias was turned on and off to simulate thermal cycling of the stack. Samples were cycled for 50 times, 100 times, 200 times and finally for 400 times. One cycle event applied the electrical bias for 5 seconds followed by a 5 second period of rest.

Figure 35 shows optical microscopy pictures of the samples before (left column) and after (right column) an electrical bias of 15.5V was applied for 100 (top row), 200 (middle row) and 400 (bottom row) cycles, in contact with 0 vol% acetic acid solvent. The results do not show any changes to the platinum levels that could be detected visually, but changes still may have occurred that the EDS would detect.

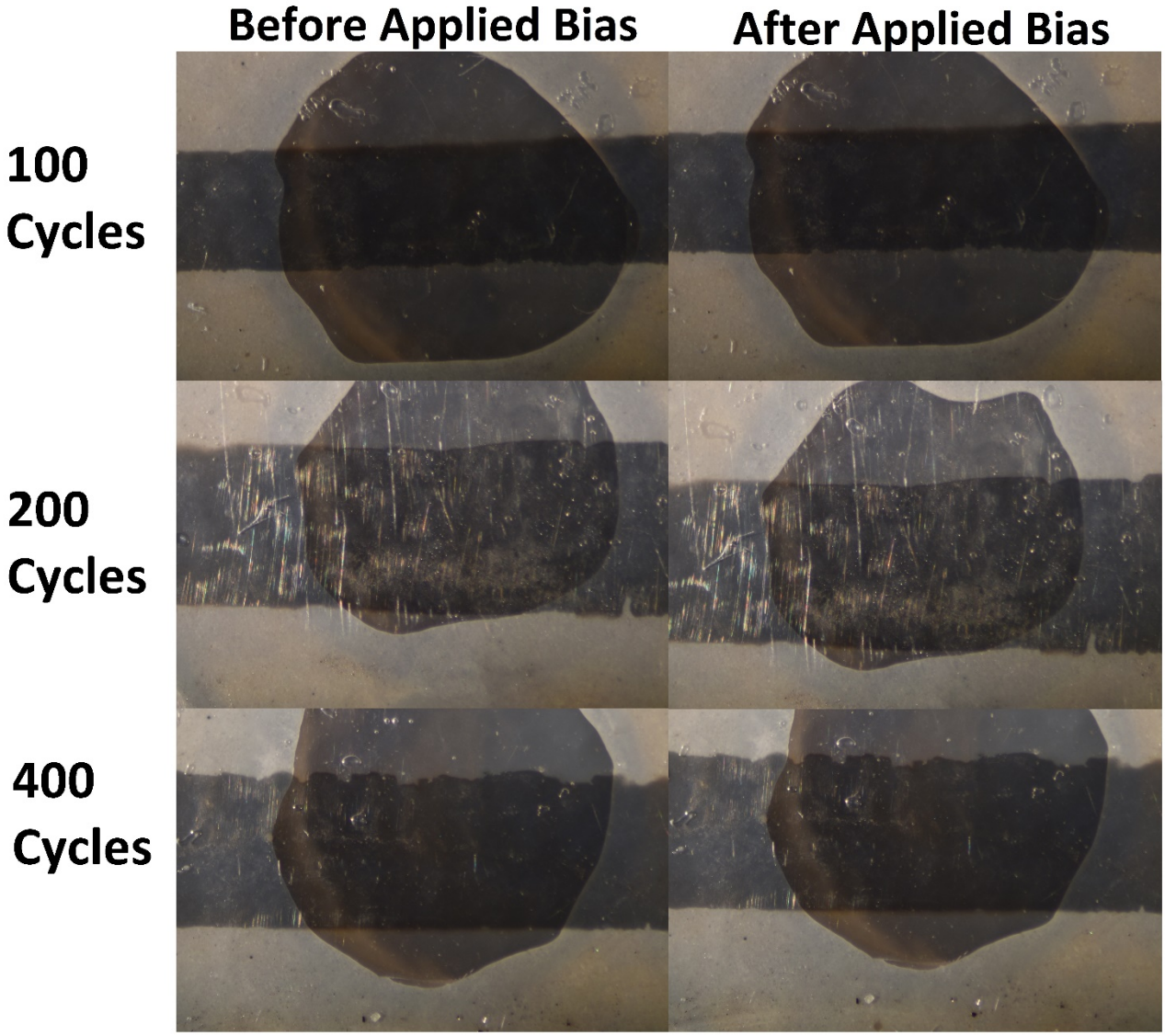

Figure 35: Optical Microscopy Images of Platinum Sputter Coated PEM Material Samples Before (left column) and After (right column) 15.5V Electrical Bias for 100 (top row), 200 (middle row) and 400 (bottom row) Cycles in Contact with 0 vol% Acetic Acid Solvent at Room Temperature.

Figure 36 shows both the platinum and silicon EDS detector counts from each sample shown in Figure 35. The left-most column shows the EDS data for the platinum in contact with the 0 vol% acetic acid solvent, the next column over shows data for the platinum outside the solvent (just exposed to air), the next column over is for the silicon in contact with the solvent and the column farthest to the right is for silicon outside the solvent. The top row is for the sample which had 100 cycles, the middle row is for the sample which had 200 cycles and the bottom row is for the sample which 400 cycles applied.

Figure 37 shows optical microscopy pictures of the samples before (left column), after (middle column) and an interior image afterwards (right column) an electrical bias of 15.5V was applied for 50 (top row), 100 (middle row) and 200 (bottom row) cycles, in contact with 5 vol% acetic acid solvent. The results show dramatic changes to the platinum where a section of platinum in all cases was completely removed. The results are so dramatic that after completing the 100 and 200 cycle experiments it was clear the 400 cycles would be the same, so 50 cycles was investigated to see if that could produce similar results, which it did.

Figure 38 shows both the platinum and silicon EDS detector counts from each sample shown in Figure 37. The left-most column shows the platinum EDS data for the region where platinum was not removed, the next column over shows platinum EDS data for the region where platinum was removed, the next column over shows silicon EDS data for the region where platinum was not removed and the column farthest to the right shows silicon EDS data for the region where platinum was removed. The top row is for the sample which had 100 cycles, the middle row is for the sample which had 200 cycles and the bottom row is for the sample which 400 cycles applied.

Figure 39 shows optical microscopy pictures of the samples before (left column) and after (right column) an electrical bias of 15.5V was applied for 100 (top row), 200 (middle row) and 400 (bottom row) cycles, in contact with 99.7 vol% acetic acid solvent. Similar to the 0 vol% acetic acid samples these results do not show any changes to the platinum levels that could be detected visually. These samples will also be characterized by EDS do determine if platinum and/or silicon levels have changed.

Figure 40 shows both the platinum and silicon EDS detector counts from each sample shown in Figure 39. The left column shows the EDS data for the platinum and the right column shows the EDS data for the silicon in contact with the 99.7 vol% acetic acid solvent. The top row is for the sample which had 100 cycles, the middle row is for the sample which had 200 cycles and the bottom row is for the sample which 400 cycles applied.

The EDS data collected was converted to a graphical form so trends in the data could be more easily observed and is shown below.

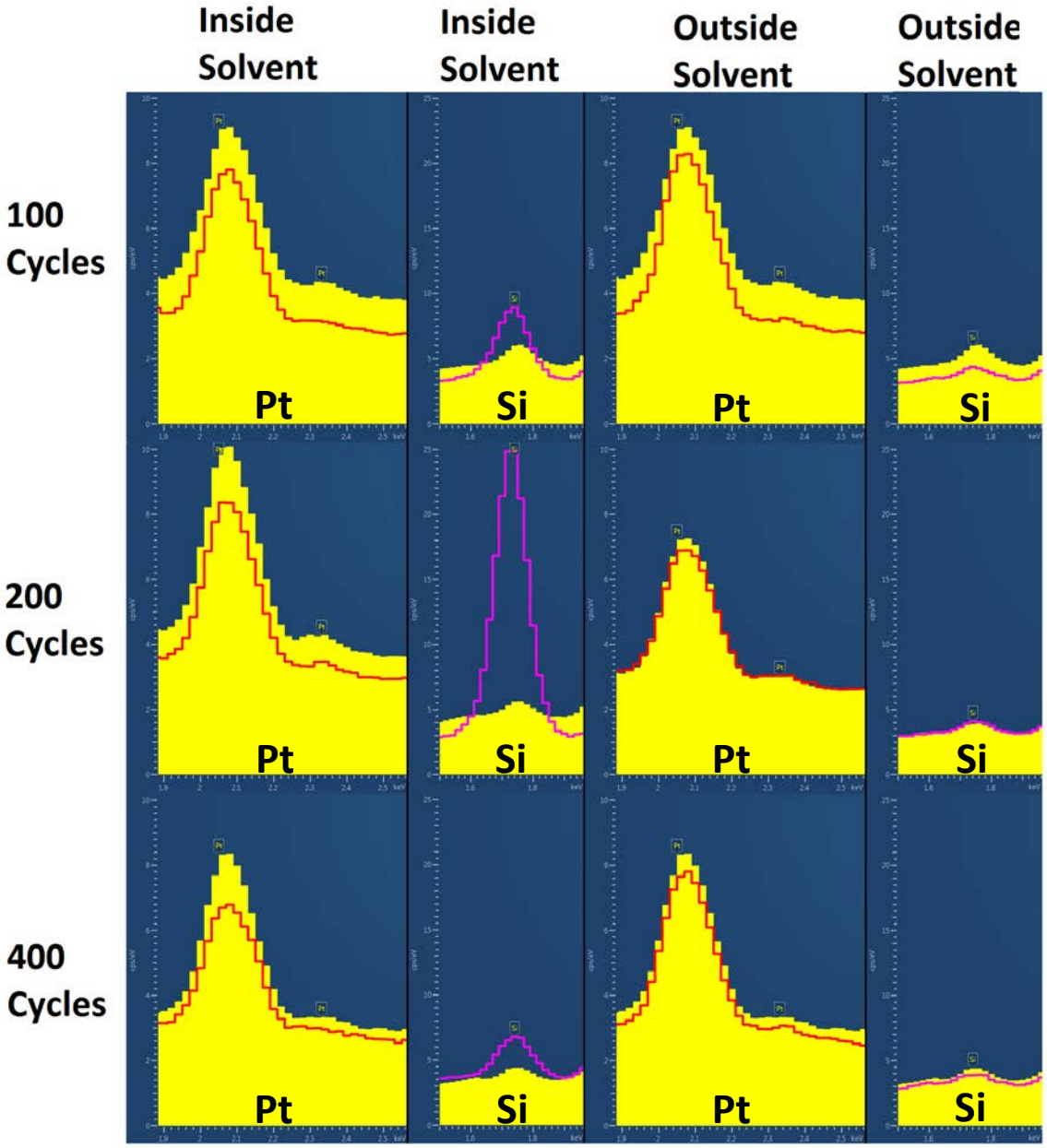

Figure 36: EDS Data for Platinum Sputter Coated PEM Material Samples with a 15.5V Electrical Bias for 100 (top row), 200 (middle row) and 400 (bottom row) Cycles in Contact with 0 vol% Acetic Acid Solvent at Room Temperature. Platinum (left column) and Silicon (right column) EDS Data Before (yellow) and After (red and purple) Cycling is Reported too.

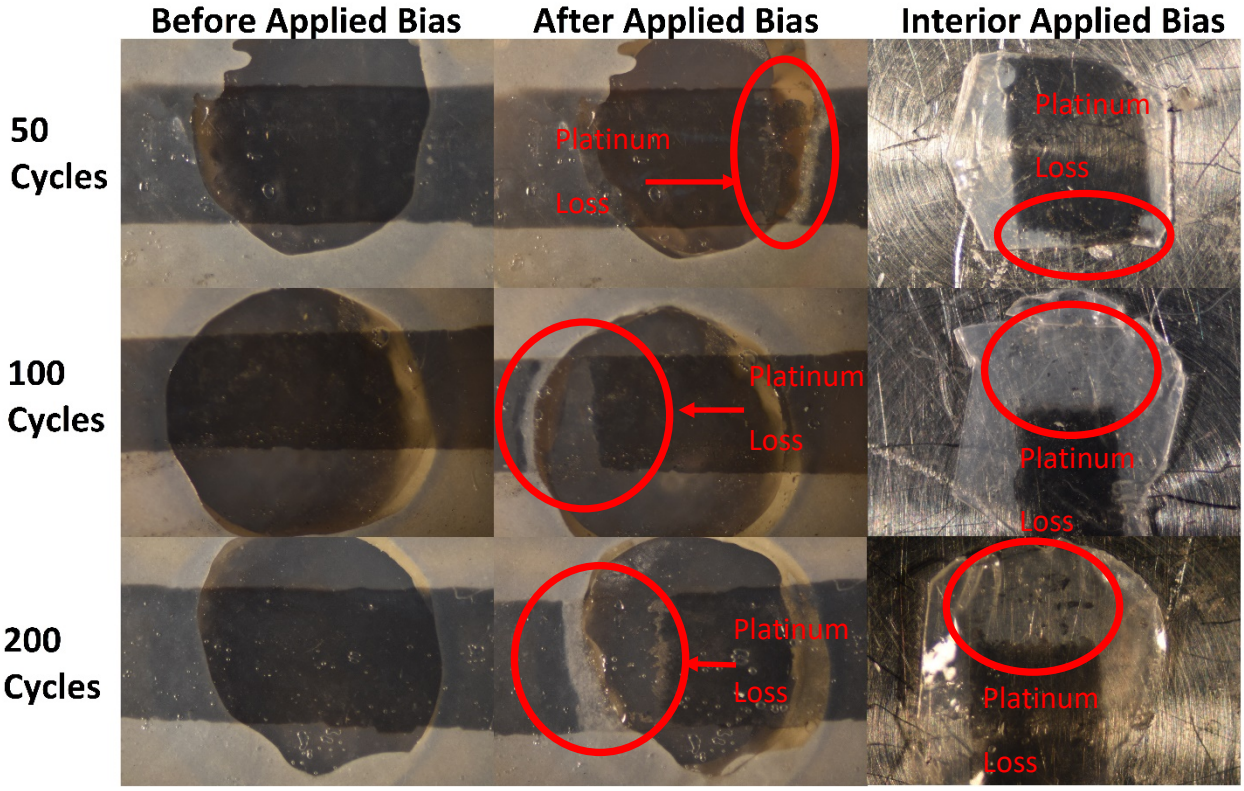

Figure 37: Optical Microscopy Images of Platinum Sputter Coated PEM Material Samples Before Cycling (left column), After Cycling (middle column) and Solution Interaction Area Cutout After Cycling (right column) on Samples with a 15.5V Electrical Bias Applied for 50 (top row), 100 (middle row) and 200 (bottom row) Cycles in Contact with 5 vol% Acetic Acid Solvent at Room Temperature.

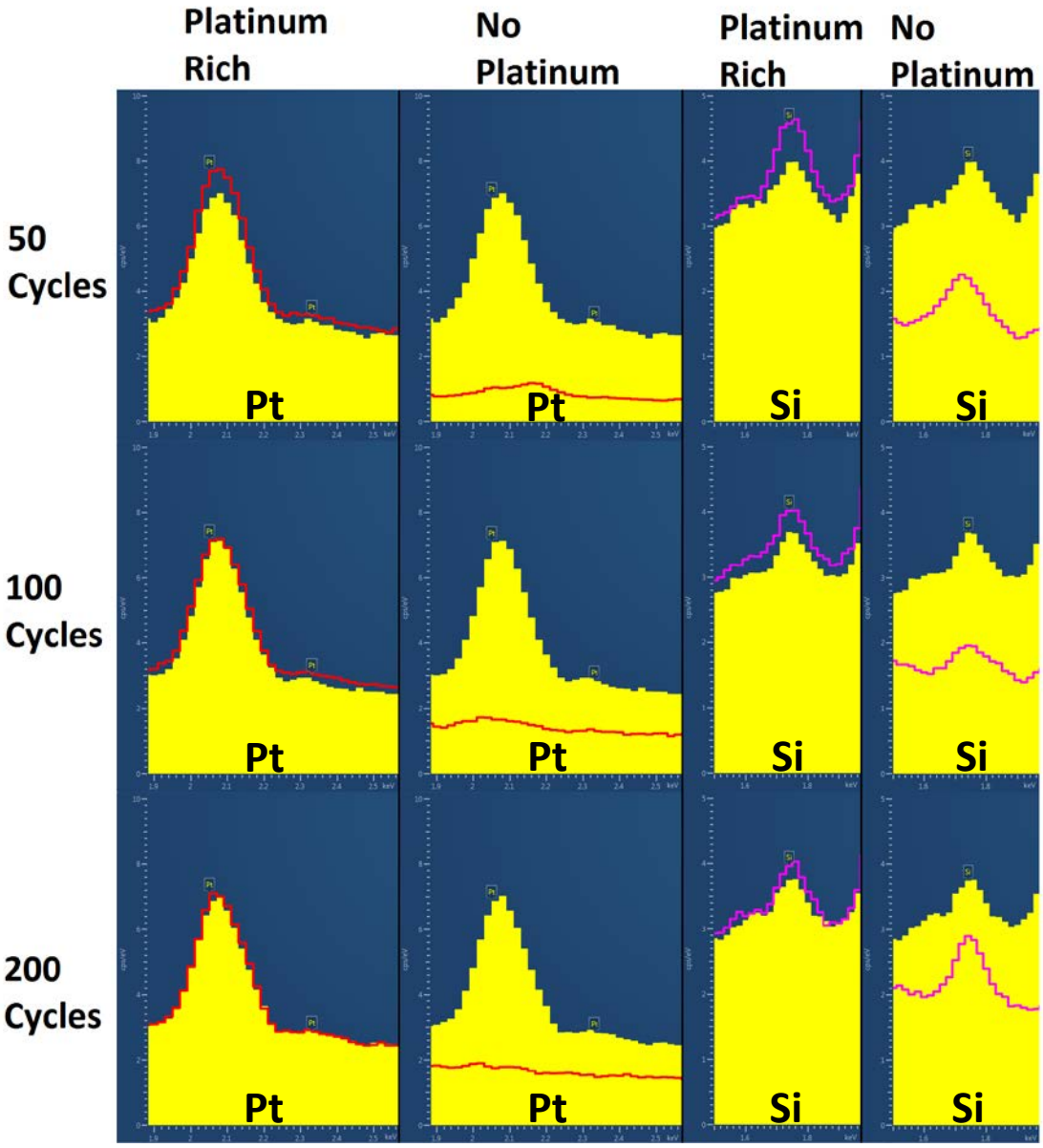

Figure 38: EDS Data for Platinum Sputter Coated PEM Material Samples with a 15.5V Electrical Bias for 50 (top row), 100 (middle row) and 200 (bottom row) Cycles in Contact with 5 vol% Acetic Acid Solvent at Room Temperature. Platinum Levels are Reported in the Platinum Rich (left column) and No Platinum (2nd from left column) Regions and Silicon Levels in the Platinum Rich (2nd from right column) and No Platinum (right column) are as well. EDS Data Before (yellow) and After (red and purple) Cycling is Reported too.

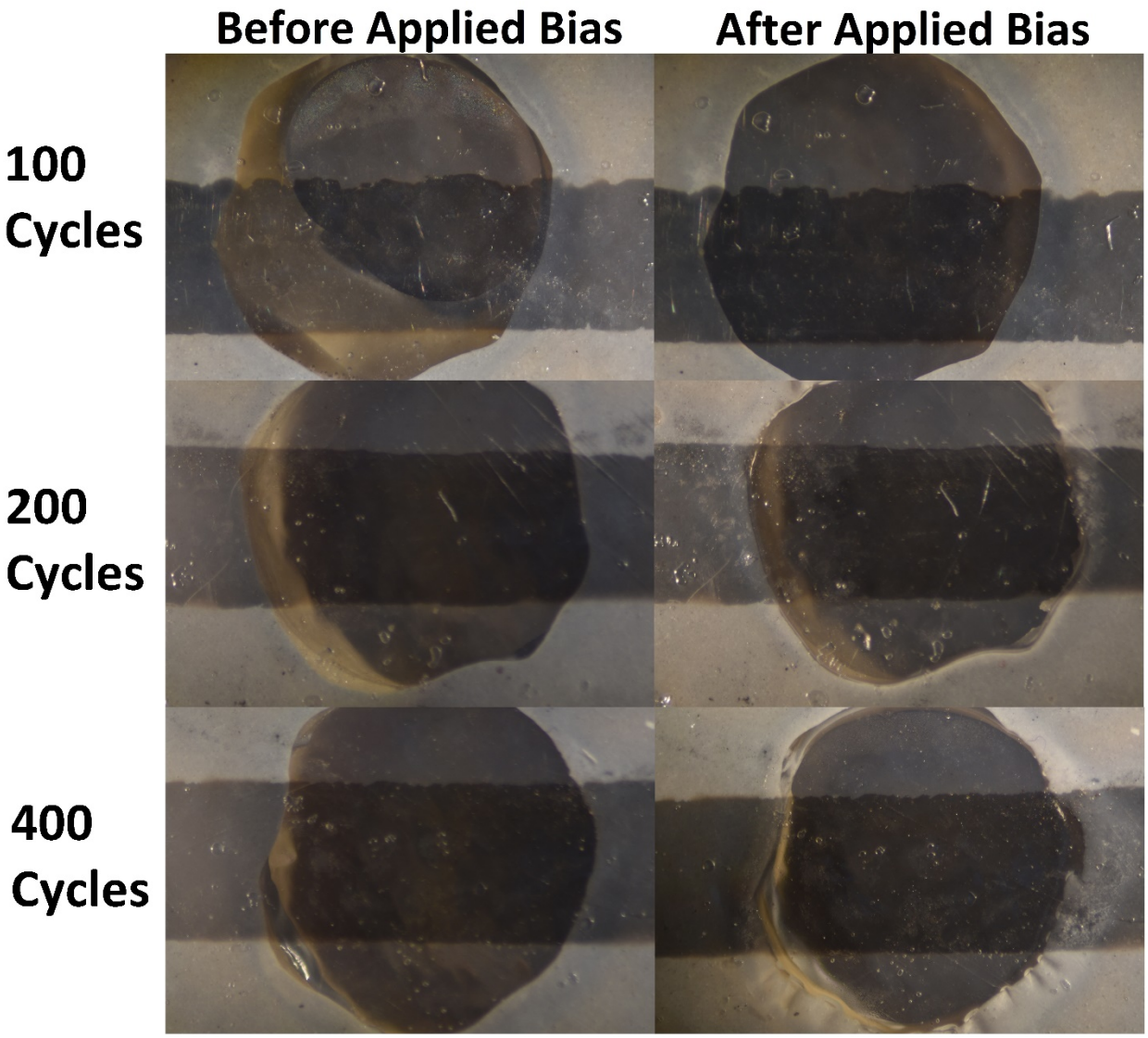

Figure 39: Optical Microscopy Images of Platinum Sputter Coated PEM Material Samples Before (left column) and After (right column) on Samples with a 15.5V Electrical Bias Applied for 100 (top row), 200 (middle row) and 400 (bottom row) Cycles in Contact with 99.7 vol% Acetic Acid Solvent at Room Temperature.

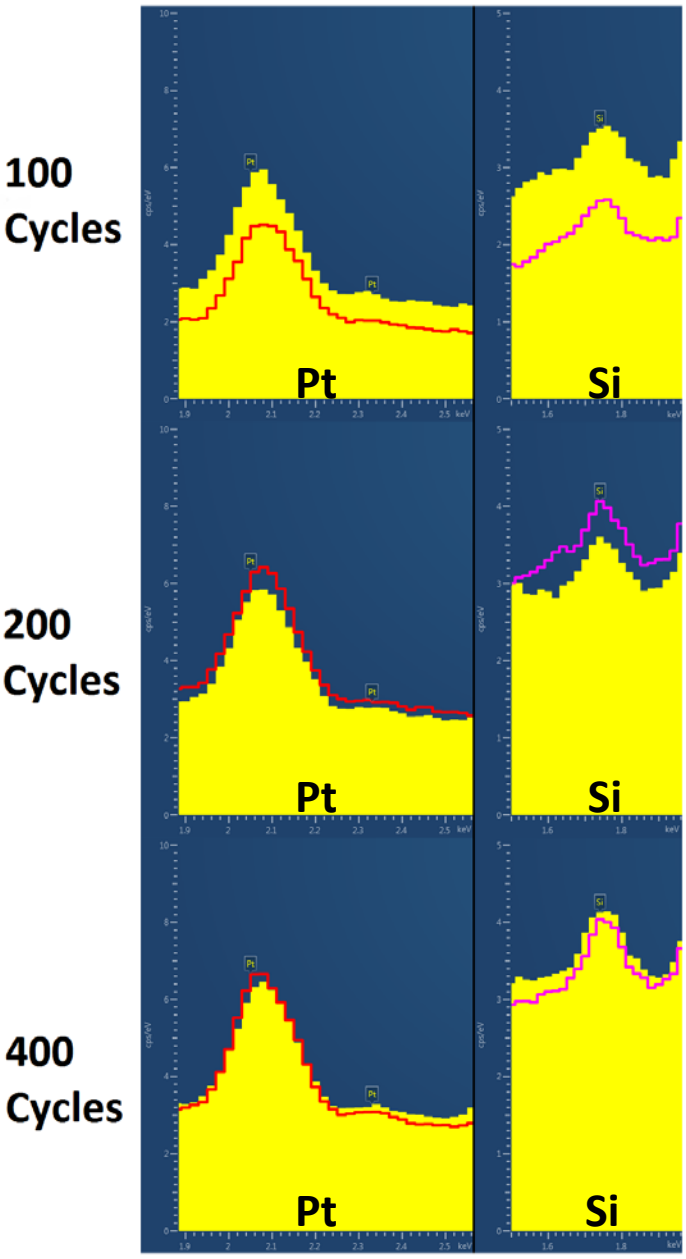

Figure 40: EDS Data for Platinum Sputter Coated PEM Material Samples with a 15.5V Electrical Bias Applied for 100 (top row), 200 (middle row) and 400 (bottom row) Cycles in Contact with 99.7 vol% Acetic Acid Solvent at Room Temperature. Platinum (left column) and Silicon (right column) EDS Data is Reported Before (yellow) and After (red and purple) Cycling.

Figure 41 shows the changes to platinum and silicon values, not in contact with solvent, before (blue bars, top row) and after (orange bars, top row) a 15.5V electrical bias was applied for 100, 200 and 400 cycles. The bottom two plots show the delta value between the before and after platinum and silicon values. Data was extracted from Figure 36. Overall, there does not appear to be noticeable trends associated with applying a 15.5V electrical bias by itself.

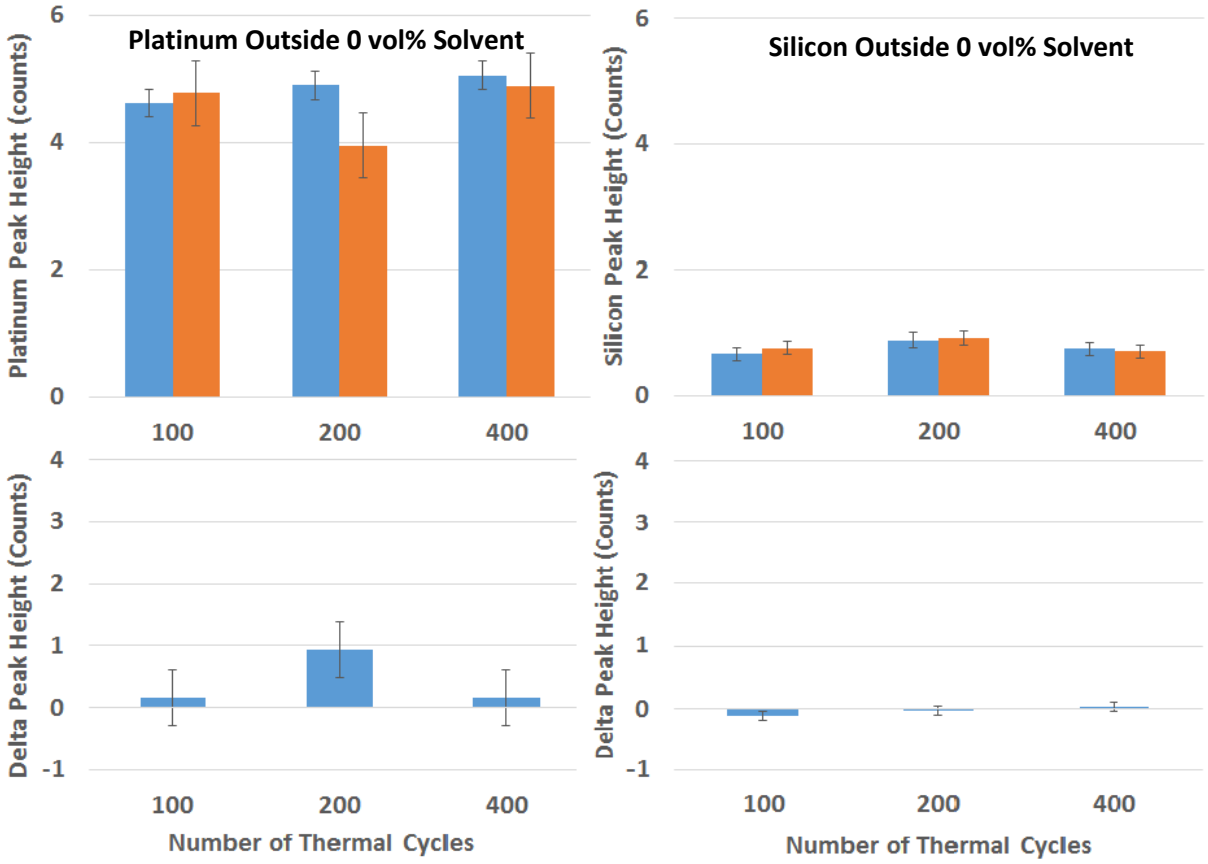

Figure 41: Before Cycling (blue bars, top row) and After Cycling (orange bars, top row) Comparison for 15.5V Electrical Bias Effects Outside Solvent Interaction Area for 100, 200 and 400 Cycles. Changes in Platinum (left column) and Silicon (right column) Values are Shown from EDS Data in Figure 36. Bottom Row Shows Delta Values between Before and After.

Figure 42 shows the changes to platinum values, in contact with 0 vol% acetic acid (left column), 5 vol% acetic acid (middle two columns) and 99.7 vol% acetic acid (right column) before (blue bars, top row) and after (orange bars, top row) a 15.5V electrical bias was applied for 50, 100, 200 and/or 400 cycles. The bottom two plots show the delta value between the before and after platinum and silicon values. Data was extracted from Figure 36, Figure 38 and Figure 40, respectively. Overall the following trends were observed. The 0 vol% acetic acid data shows a gradual decrease in platinum with increasing cycles. The 5 vol% acetic acid data shows a significant reduction in platinum (within a section of the platinum strip) to the point where platinum is nearly eliminated. The remaining platinum with the 5 vol% acetic acid samples did not show any significant loss. Finally, the 99.7 vol% acetic acid data did not show any change to its platinum levels.

Figure 43 shows the changes to silicon values, in contact with 0 vol% acetic acid (left column), 5 vol% acetic acid (middle two columns) and 99.7 vol% acetic acid (right column) before (blue bars, top row) and after (orange bars, top row) a 15.5V electrical bias was applied for 50, 100, 200 and/or 400 cycles. The bottom two plots show the delta value between the before and after platinum and silicon values. Data was extracted from Figure 36, Figure 38 and Figure 40, respectively. Overall the following trends were observed. The 0 vol% acetic acid data shows a significant increase in silicon for the 100 and 200 cycles. The 5 vol% acetic acid data shows no change in the silicon levels anywhere on the entire sample. Finally, the 99.7 vol% acetic acid data did not show any change to its silicon levels either.

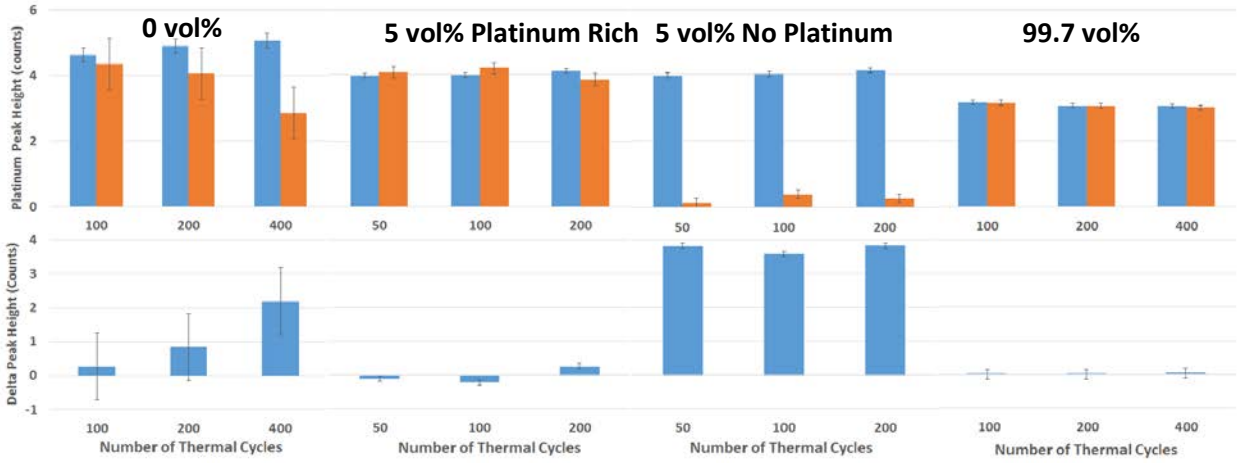

Figure 42: Before Cycling (blue bars, top row) and After Cycling (orange bars, top row) Platinum Peak Comparison for Electrical Bias Effects using 15.5V in 0 vol% Acetic Acid (left column), 5 vol% Acetic Acid Platinum Rich (2nd from left column), 5 vol% Acetic Acid no Platinum (2nd from right column) and 99.7 vol% Acetic Acid (right column) which was Extracted from Figure 36, Figure 38 and Figure 40, Respectively. Bottom Row Shows Delta Values between Before and After.

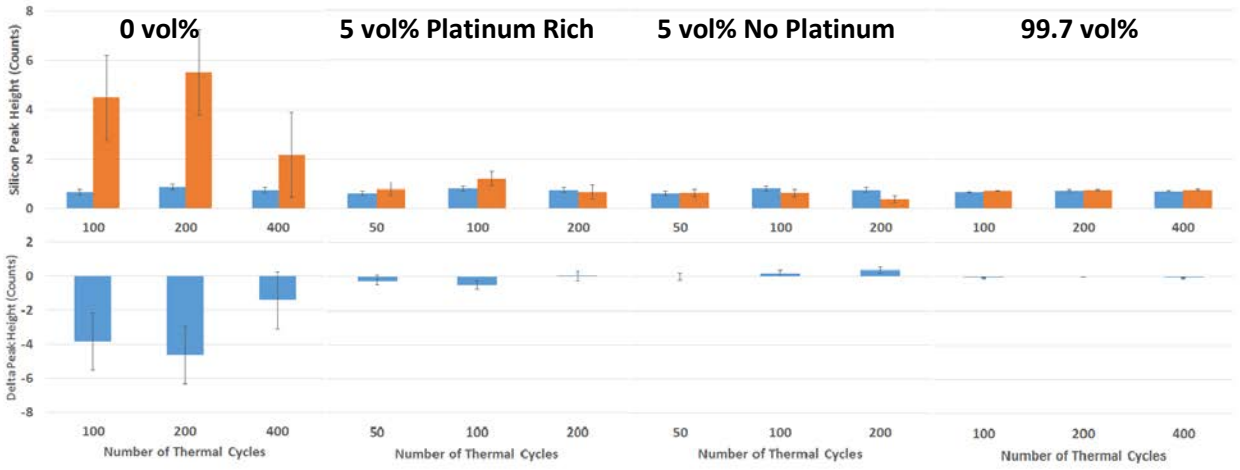

Figure 43: Before Cycling and After Cycling Silicon Peak Comparison for Electrical Bias Effects using 15.5V in 0 vol% Acetic Acid (left column), 5 vol% Acetic Acid Platinum Rich (2nd from left column), 5 vol% Acetic Acid no Platinum (2nd from right column) and 99.7 vol% Acetic Acid (right column) which was Extracted from Figure 38. Bottom Row Shows Delta Values between Before and After.

Figure 44 shows the changes to platinum/silicon ratio values, in contact with 0 vol% acetic acid (left column), 5 vol% acetic acid (middle two columns) and 99.7 vol% acetic acid (right column) before (blue bars, top row) and after (orange bars, top row) a 15.5V electrical bias was applied for 50, 100, 200 and/or 400 cycles. The bottom two plots show the delta value between the before and after platinum and silicon values. Data was calculated from Figure 42 and Figure 43. Overall the following trends were observed. Solvents that showed platinum loss to any degree, such as the 0 vol% and 5 vol% acetic acid solvents, had significantly lower platinum/silicon ratios after the electrical bias was applied. In the 0 vol% acetic acid case the ratio was initially lowered due to a significantly increased silicon level then, at 400 cycles, a combination of decreased platinum and increased silicon levels. In the 5 vol% acetic acid case the ratio was lowered only in the sample regions where platinum had been removed, which resulted in the lower ratio value.

The data indicate that as the platinum/silicon ratio become lower (post experiment) platinum loss was more likely to occur (in the 100 and 200 cycle 0 vol% acetic acid cases) or that platinum loss had already occurred (in the 400 cycle 0 vol% acetic acid case and 50,100 and 200 cycle 5 vol% acetic acid cases). The fundamental connection between the increased silicon levels and platinum loss (and the trends within that data) will be discussed in greater detail in Section 6.

The next set of data will look at the platinum and silicon levels when only a 0.8V electrical bias is applied to samples for 100, 200 and 400 cycles when in contact with 5 vol% acetic acid, now that platinum

loss is possible using an applied electrical bias. The electrical bias and current density will also be within the same range as the FCATT PEM cell and this will give the closest electrical approximation.

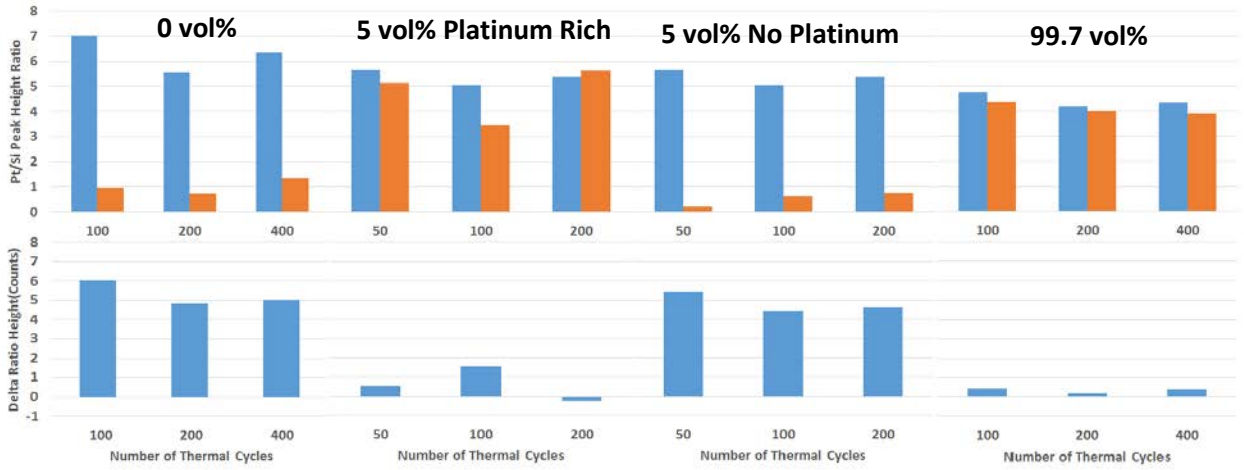

Figure 44: Before Cycling (blue bars, top row) and After Cycling (orange bars, top row) Platinum/Silicon Peak Ratio Comparison for Electrical Bias Effects using 15.5V in 0 vol% Acetic Acid (left column), 5 vol% Acetic Acid Platinum Rich (2nd from left column), 5 vol% Acetic Acid no Platinum (2nd from right column) and 99.7 vol% Acetic Acid (right column) which was Calculated from Figure 42 and Figure 43. Bottom Row Shows Delta Value between Before and After.

5.4.1. Impact of 0.8V Electrical Bias Effects using 5 vol% Acetic Acid

The following set of data looks at the platinum levels using a 0.8V electrical bias while in contact with the 5 vol% acetic acid solution. The same experimental setup was used as with the 15.5V electrical bias and the same number of cycles (and cycle duration) were as before.

Figure 45 shows optical microscopy images before (left column) and after (right column) the electrical bias was applied for 100 (top row), 200 (middle row) and 400 (bottom row) cycles. The images show that no noticeable platinum loss was observed, but as with the 15.5V 0 vol% acetic acid experiments, platinum loss may still have occurred. The significantly lower electrical bias would also most likely produce a lower loss of platinum, so these results are not unexpected.

Figure 46 shows the EDS data from the optical microscopy samples for platinum and silicon before (yellow, both platinum and silicon) and after (red for platinum and purple for silicon). The platinum levels appear lower for all three samples, while the silicon levels appear very close to their original values for all the samples.

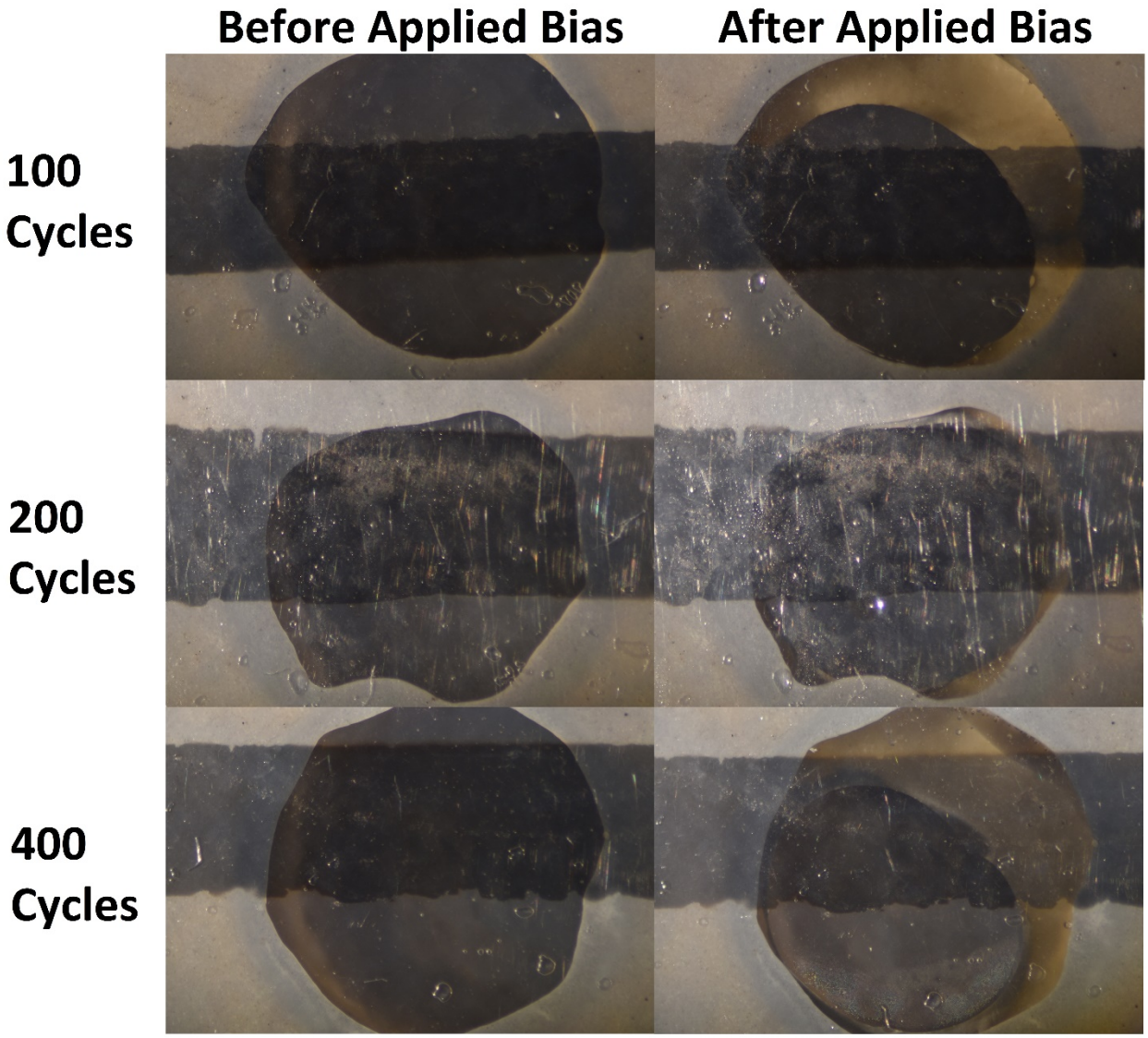

Figure 45: Optical Microscopy Images of Platinum Sputter Coated on PEM Material Samples Before (left column) and After (right column) on Samples with a 0.8V Electrical Bias Applied for 100 (top row), 200 (middle row) and 400 (bottom row) Cycles in Contact with 5 vol% Acetic Acid Solvent at Room Temperature.

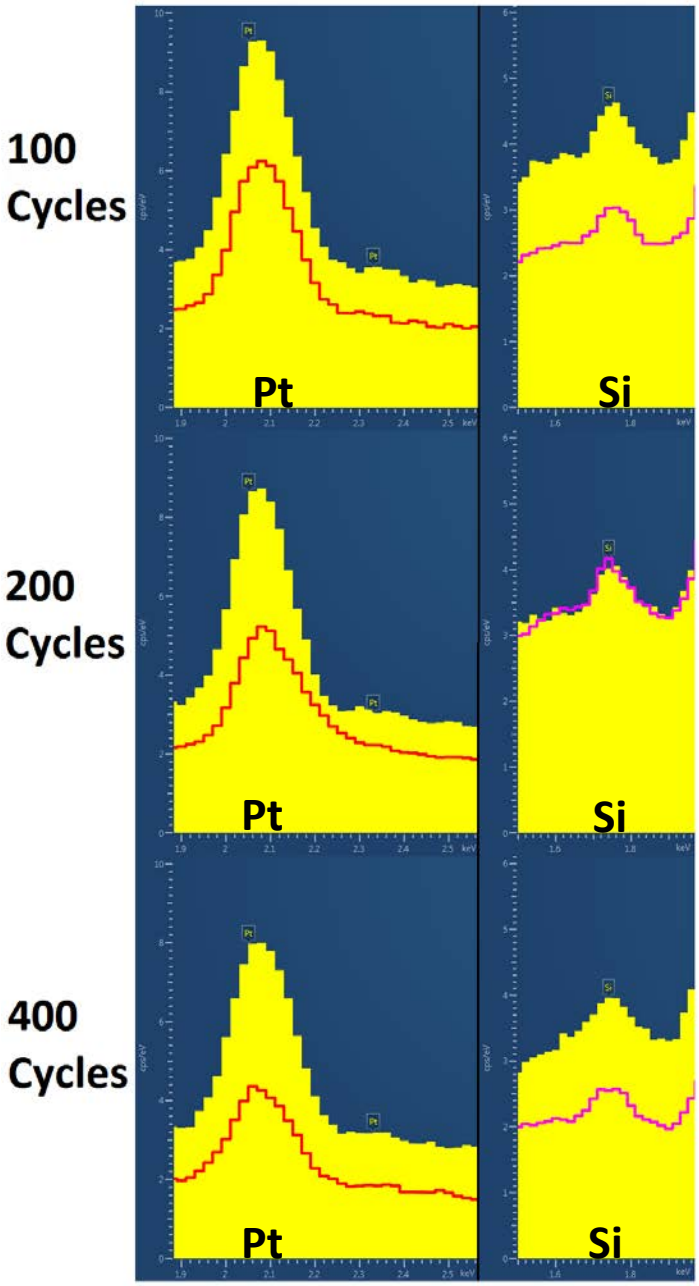

Figure 46: EDS Data for Platinum Sputter Coated on PEM Material Samples with a 0.8V Electrical Bias Applied for 100 (top row), 200 (middle row) and 400 (bottom row) Cycles in Contact with 5 vol% Acetic Acid Solvent at Room Temperature. Platinum (left column) and Silicon (right column) EDS Data are Shown Before (yellow) and After (red and purple) Cycling.

Figure 47 shows the platinum levels (left column) before (blue bars) and after (orange bars) and the silicon levels (right column) before (blue bars) and after (orange bars) from the EDS data in Figure 46. The delta values between before and after each experiment (for platinum and silicon) are shown in the bottom row.

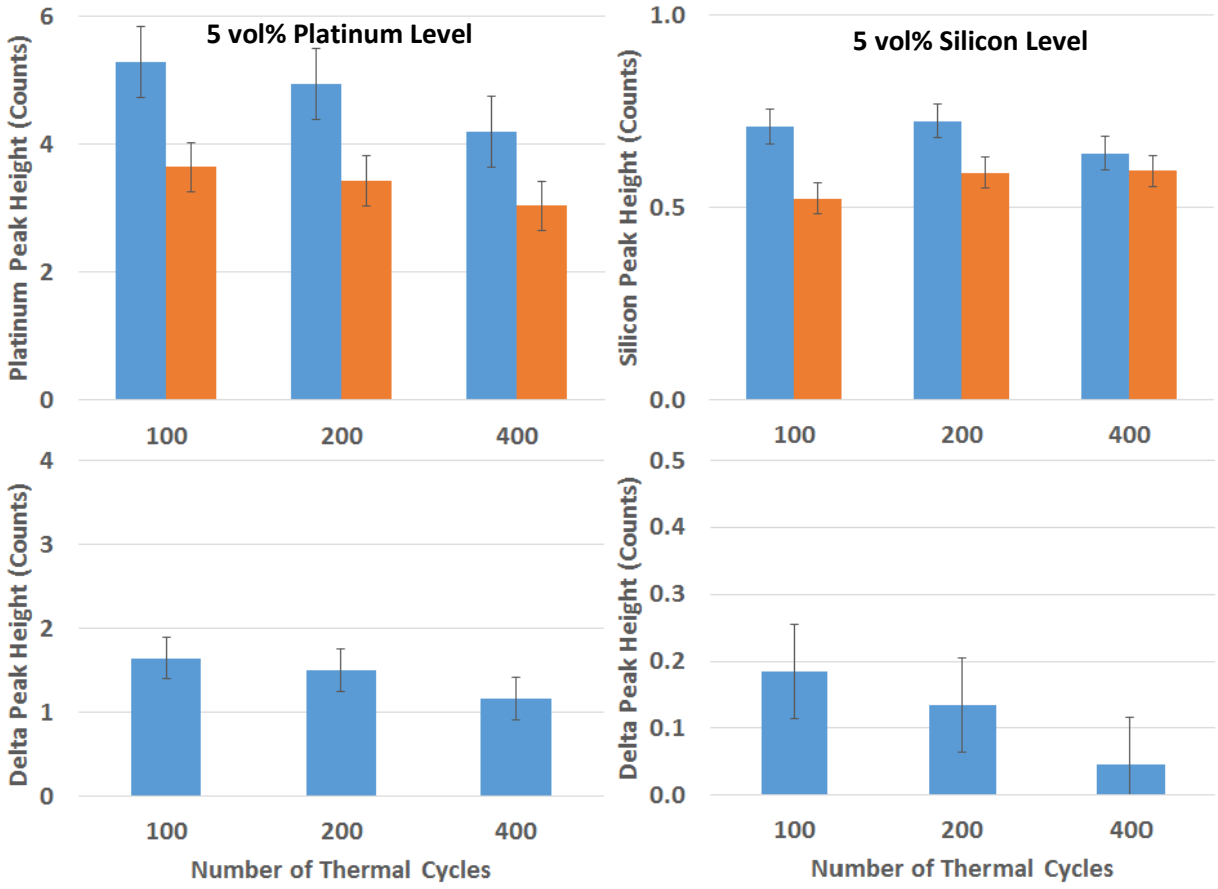

Figure 47: Before (blue bars, top row) and After (orange bars, top row) Platinum (top left plot) and Silicon (top right plot) Comparison for Electrical Bias Effects using a 0.8V in 5 vol% Acetic Acid which was Extracted from Figure 46. Bottom Row Shows Delta Value between Before and After.

The data shows that the platinum levels are statistically and consistently lower for all experiments. The silicon levels appear fairly consistent between the different experiments and do not deviate significantly based on the number of cycles.

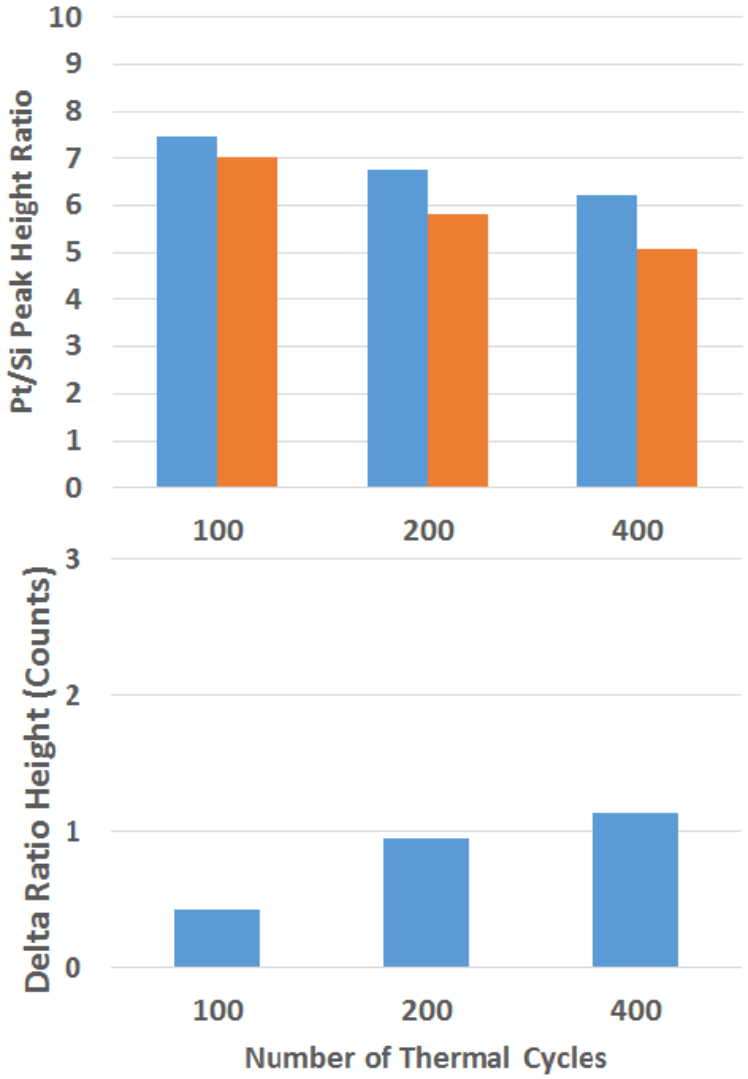

Figure 48: Before (blue bars, top row) and After (orange bars, top row) Platinum/Silicon Peak Ratio Comparison for Electrical Bias Effects using a 0.8V in 5 vol% Acetic Acid which was Calculated from Figure 47. Bottom Row Shows Delta Value between Before and After.

Figure 48 shows the platinum/silicon ratio values (top row) calculated from Figure 47 using the before (blue bars) and after (orange bars) EDS values. The delta values between the before and after values are shown in the bottom row. The delta values consistently increase as the number of cycles increase, similar to the data from the 15.5V 5 vol% acetic acid experiments.

The results from the 0.8V experiments show some similarities and some differences from the data presented in the 15.5V 5 vol% acetic acid experiments. Similarities were that: 1. platinum loss was observed and the silicon levels stay relatively constant and 2. The delta between the platinum/silicon ratio values consistently became greater as the number of cycles increased. As previously mentioned a higher delta platinum/silicon ratio indicated platinum loss was more likely to have occurred.

The main difference between these results and the 15.5V results was that the magnitude of platinum loss and the delta platinum/silicon ratio was lower. This can be explained by the fact a significantly lower electrical bias being used, so lower result values would be expected.

5.5. Platinum Electrocatalyst Loss Degradation Investigation Summary

Results from applying either a 15.5V or 0.8V electrical bias across the platinum sputter coating are very dramatic, as clearly platinum was shown to be removed using the 15.5V and 0.8V 5 vol% acetic acid samples. There are a few overarching observations that were taken from these results, which were:

1. Platinum loss was not observed where no solution was in contact with the platinum. This indicates that simply applying an electrical bias is not enough to remove the platinum.
2. Platinum loss was observed in both the 15.5V 0 vol% and 5 vol% acetic acid solutions, but the 5 vol% acetic acid solution was far more aggressive at removing platinum from the PEM material. This implies that solution chemistry is not the only driving force and a common element between both solvents exists which promotes platinum loss.
3. Platinum loss was also observed with the 0.8V 5 vol% acetic acid solution. The magnitude of platinum loss was ~35-40% from the original starting value. The lower amount of platinum loss, compared to the 15.5V experiments, is explained due to the reduced electrical bias.
4. Platinum loss was only observed at the edge where solvent started touching the platinum, for the 15.5V 5 vol% acetic acid samples. The center of the solution interaction area, where platinum was not visibly removed, did not show any significant loss in platinum content when also characterized using the EDS. This indicates that that the platinum needs to have be in contact with a solvent and have an electrical bias applied, simultaneously, for any effect to occur. Once platinum was removed from the edge, to such a degree where current could not flow, then further platinum loss stopped. The fact platinum was removed only in one spot indicates this process is very quick to occur.
5. The samples in contact with 15.5V 99.7 vol% acetic acid did not show any platinum loss. This indicates that the platinum loss in the 5 vol% acetic acid samples was not, at least partially, the result of a reaction between platinum and acetic acid at standard operating conditions.
6. The 15.5V 0 vol% and 99.7 vol% acetic acid solutions, initially, have no electrical conductivity, while the 5 vol% acetic acid solution is electrically conductive. The 0 vol% solution can become electronically conductive over time due to, at least, gasses from the air diffusing into the solution. Since the 0 vol% and 5 vol% solutions are or can become electronically conductive this is potentially a common element that explains why both exhibited platinum loss. It is also possible that, in the 5 vol% acetic acid case, the increased electronic conductivity is potentially lowering the activation energy for platinum to react with acetic acid, thus promoting that reaction.
7. Samples that used either the 0 vol% or 5 vol% acetic acid solutions showed a reduced platinum/silicon ratio after the experiment, compared to their initial platinum/silicon ratio. This decreased ratio was determined to be either the result of a significantly increased silicon level, a reduced platinum level or a combination of both. Decreased ratio values also appeared to

indicate statistically significant platinum levels were shortly going to occur or had already occurred.

Although these results are very interesting and promising there still are unanswered questions as to what the underlying mechanism is. Overall there appears to be a significance between the silicon levels and platinum levels in each sample in addition to their ratio values and the types of solution used was show to be dramatically important in the amount of platinum was removed. These questions will be investigated in more detail in Section 6.

6. Platinum Electrocatalyst Loss Degradation Mechanism Determination

The underlying mechanism for the platinum loss using the different solvents is not clear. The fact that the 0 vol% and 5 vol% solvents share the connection that both promote platinum loss under an electrical bias and either are or can become electronically conductive appears to be relevant. This indicates that solution conductivity may have a connection and should be characterized further.

A direct reaction between acetic acid and platinum does not appear to occur in a non-conductive solution, but the reaction barrier between the platinum and acetic acid may be lowered enough to promote a reaction when the solvent conductivity is high enough, instead of simply conductivity being the sole facilitator.

Deionized water (0 vol% acetic acid) is also, as a pure compound, not electronically conductive, but as stated earlier, can become conductive through gas diffusion. The magnitude of this conductivity increase over time will be investigated to see if it is significant enough to justify the platinum loss observed.

To determine whether solution conductivity or a reaction between platinum and acetic acid is the more dominant process two additional organic acid solvents were used while applying a 15.5V electrical bias for 100 cycles.

6.1. Conductivity or Reduction of Platinum/Acetic Acid Reaction Barrier Effects

As mentioned, two additional weak organic acids were used in place of acetic acid. These additional acids have a similar water solubility to acetic acid, have a similar molecular mass as acetic acid, have a similar density, have a similar pH to acetic acid and, all have a similar electronic conductivity. The hypothesis was that if a reaction was the dominant mechanism, to facilitate platinum loss using acetic acid, then these additional two solvents should not remove platinum since it is highly unlikely that a similar reaction would occur with chemically different compounds. If platinum loss did occur using all three acids then conductivity would likely be the dominant mechanism since that was a common factor between all three solvents.

Table 6 shows the solvent properties for the different weak acids used for the conductivity experiments. The additional two weak acids used were propionic acid and butyric acid. These two acids were decided upon since their molar masses, acidity values and solubility in water were very close to each other, which helps eliminate those variables as possible contributions to platinum loss.

Table 6: Weak Organic Acid Solvent Properties

Acid Properties	Acetic Acid	Propionic Acid	Butyric Acid
Molar Mass (g/mol)	60.05	74.08	88.11
Acidity (pK_a)	4.76	4.88	4.82
Water Solubility (21°C)	Miscible	Miscible	Miscible

The first task was to determine the conductivity ranges for each solvent at different molarity/volume % levels. Obtaining conductivity values across the entire range for each acid compound would allow for a comparison to be made using similar conductivities, molarity and/or volume % values. The following plots show how the conductivity of each solvent compared at different concentrations as a function of solvent molarity and solvent volume %.

Figure 49 and Figure 50 show the conductivity ranges for the acetic acid (blue triangles), propionic acid (orange squares) and butyric acid (black circles) as a function of solvent molarity and solution solvent fraction, respectively. The acetic acid had the highest conductivity while the butyric acid had the lowest conductivity at all molarity and solution solvent fraction values. The acetic acid maximum conductivity (at 15 vol%) was only 1.63 times larger than the maximum butyric acid value (at 10 vol%), so their conductivities are relatively similar. This difference is minimized as the solvent molarities and solution solvent fractions decrease, which also makes conductivity comparisons at higher dilution levels (near 5 vol%) easier.

Another result was that as the molar mass of the solvent increases the molarity or solution solvent fraction where the maximum conductivity value occurs decreases. This difference in conductivities only became prevalent at higher solution solvent fractions (>10 vol%). Conductivity values were used at solvent fractions around 5 vol% since deviations between the three solvents were minimal. The following table shows the solvent fraction, molarity and conductivity values used for the platinum loss conductivity experiments.

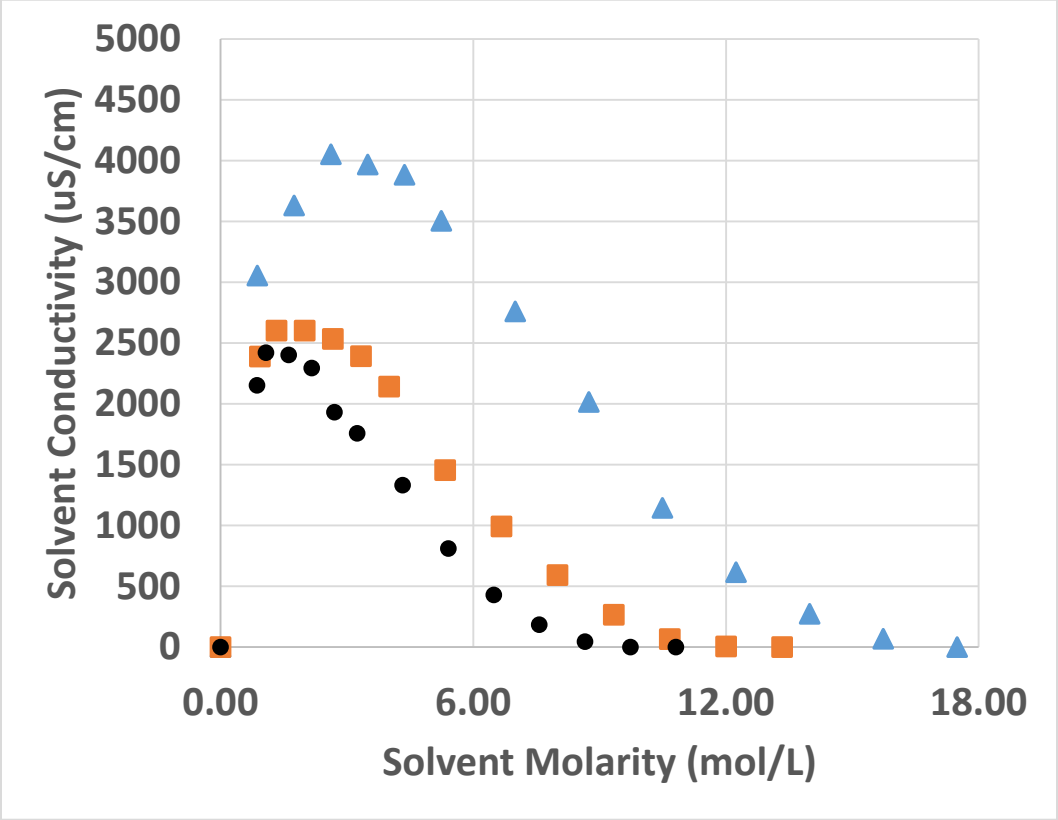

Figure 49: Acetic Acid (blue triangles), Propionic Acid (orange squares) and Butyric Acid (black circles) Conductivity Values across Entire Solution Molarity Range

Table 7 shows the solvent properties for the three different acids used in the platinum loss conductivity experiments. The three solvents used a 5 vol% solvent fraction which equated to similar molarity values close to 0.90 mol/L. Conductivity values were also similar with a 29% difference between the acetic acid and butyric acid. This difference in conductivities may result in slight differences in experimental results and will be taken into account when analyzing platinum and silicon post experiment data.

Table 7: Solvent Properties for Sputter Coated Platinum Loss Conductivity Experiments

Acid Name	Solution Solvent Fraction (vol%)	Solvent Molarity (mol/L)	Solvent Conductivity (uS/cm)
Acetic Acid	5.0	0.87	3,057
Propionic Acid	5.0	0.93	2,389
Butyric Acid	5.0	0.87	2,152

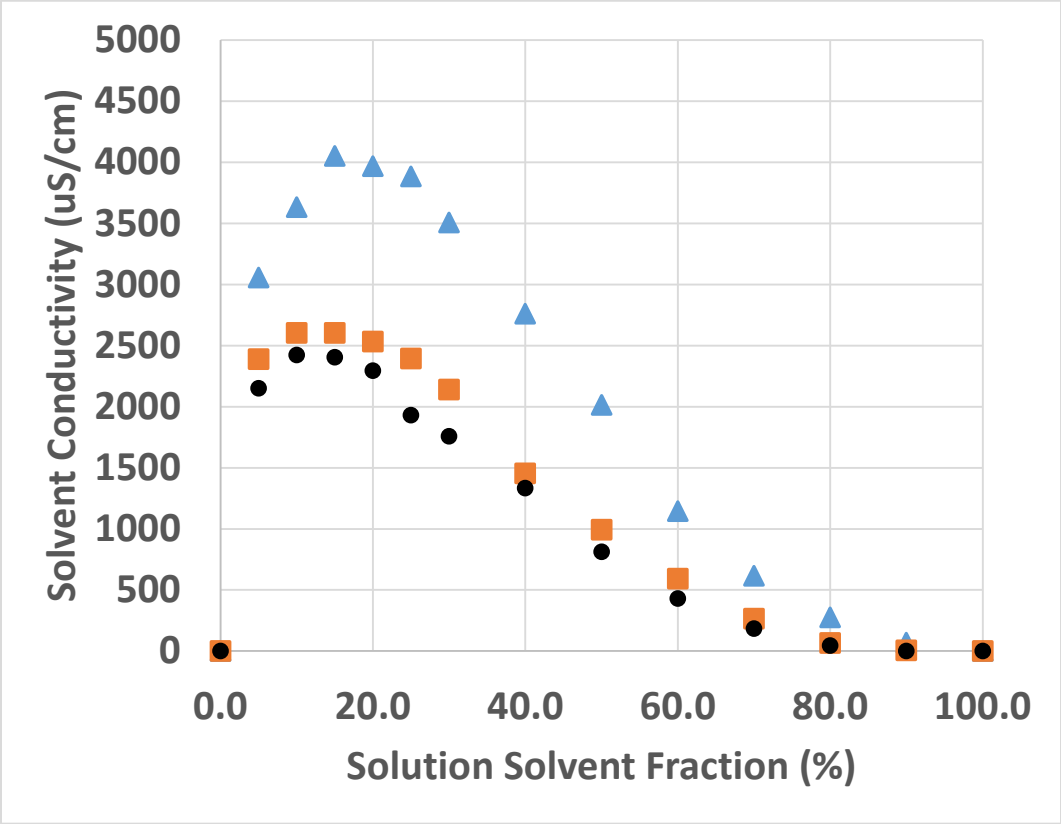

Figure 50: Acetic Acid (blue triangles), Propionic Acid (orange squares) and Butyric Acid (black circles) Conductivity Values across Entire Solution Solvent Fraction Range

The next set of data will show the results after applying a 15.5V electrical bias for 100 cycles across three samples in contact with 5 vol% acetic acid (data taken from Figure 37 and Figure 38), 5 vol% propionic acid and 5 vol% butyric acid. Optical microscopy images and EDS data will be compared to determine whether a noticeable difference in platinum was observed using different acid chemistries.

Figure 51 shows optical microscopy images of three samples which had 15.5V applied for 100 cycles using acetic acid (top row shown previously), propionic acid (middle row) and butyric acid (bottom row). Images before (left column) cycles were applied, after (middle column) cycles were applied and a close-up of the interior section (right column) after applying cycles are shown.

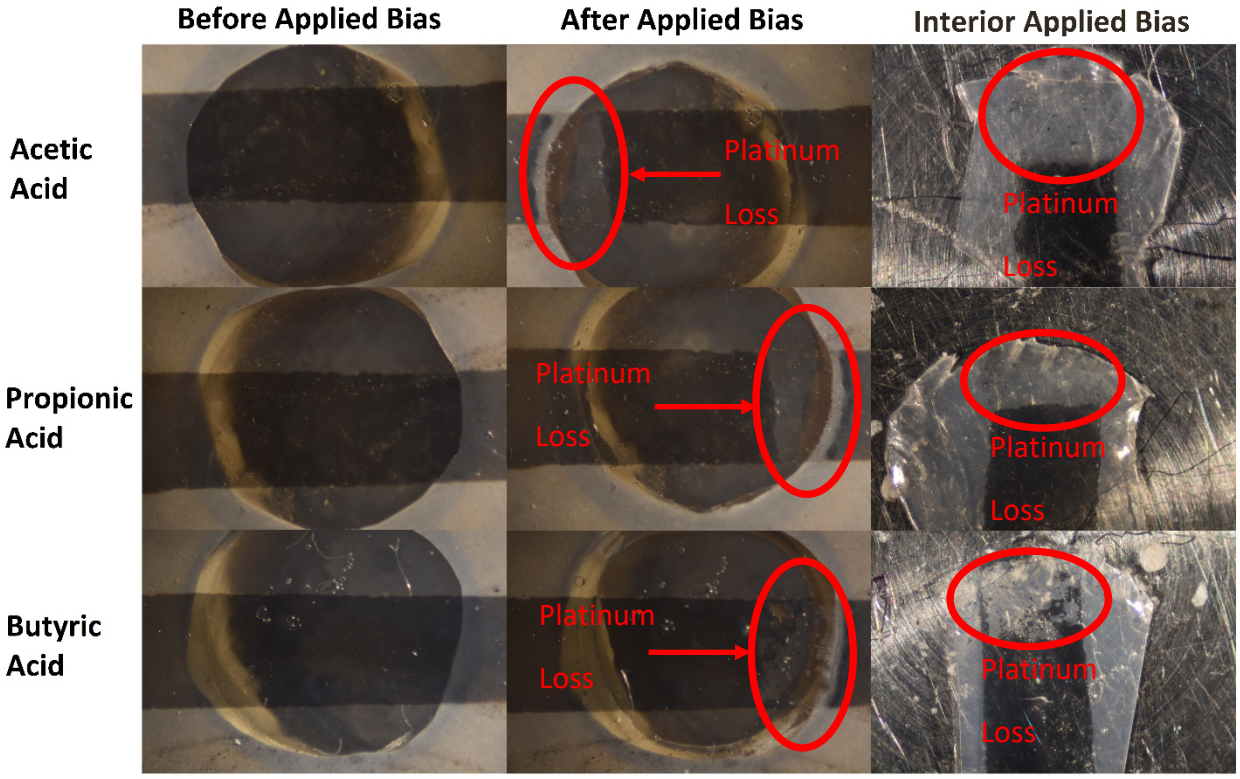

Figure 51: Platinum Sputter Coated PEM Material Samples in Contact with 5 vol% Acetic Acid (top row), 5 vol% Propionic Acid (middle row) and 5 vol% Butyric Acid (bottom row) for 100 Cycles with a 15.5V Electrical Bias Applied. Optical Microscopy Images are Shown Before Cycles were Applied (left column), After Cycles were Applied (middle column) and an Interior Image After Cycles were Applied (right column).

The results from all three samples clearly shows that platinum loss had occurred in a similar magnitude. There may be a slightly lesser amount of platinum removed in the propionic and butyric acid samples, which may be related to their lower conductivity values, but ultimately each sample suffered platinum loss to an extent where the sample would be unusable and would not produce power.

These results indicate that conductivity was the dominant process that resulted in the 15.5V and 0.8V 5 vol% acetic acid samples losing platinum, instead of a reaction between the acetic acid and platinum due to a lower reaction barrier. This lends credibility that the 0 vol% acetic acid sample may have lost its platinum due to the deionized water becoming conductive over time as mentioned earlier. The magnitude of this conductivity change over time will now be investigated to determine if its conductivity could be increased significantly within the 100, 200 and 400 cycle timeframes.

Figure 52 shows the 0 vol% acetic acid conductivity (red dots) as a function of time sitting idle in a glass beaker. The solvent conductivity was measured every 5 minutes to determine how quickly its conductivity naturally changed and how that magnitude in change compared to the conductivity of the 5 vol% acetic acid conductivity. Times that 100 (blue line), 200 (green line) and 400 (red line) cycle tests took to complete were superimposed over to the raw data to determine how they compared.

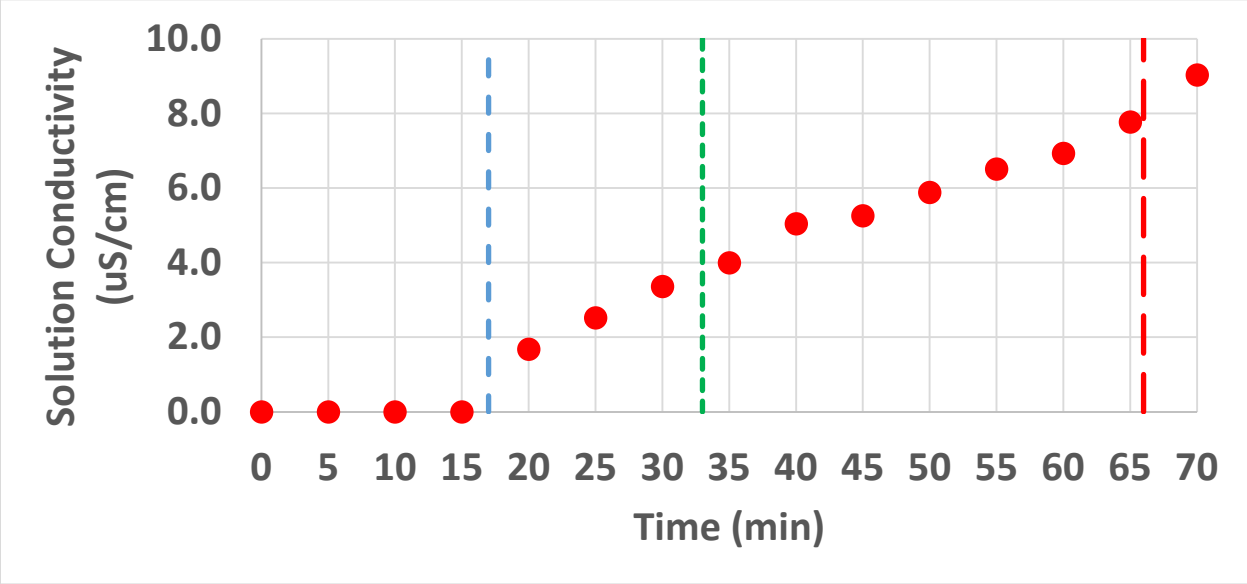

Figure 52: Deionized Water (0 vol% Acetic Acid) Conductivity Values over Time. Horizontal Dashed Lines Represent an Equivalent Amount of Time to Complete 100 (blue line), 200 (green line) and 400 (red line) Cycles and the Times those Measurements Occur on the Plot in Relation to the Reported Conductivity Values.

The results show that the 0 vol% acetic acid solvent did not change conductivity until around the 17 minute mark and then increased at a rate of 0.17 uS/cm per minute. The 100, 200 and 400 cycle experimental results also coincide with results too. The 100 cycle results showed no platinum loss and the results above show very minimal conductivity at that point. The 200 cycle results showed possibly some platinum loss but was still not statistically significant, which matches the data above where the conductivity had increased nearly 235% from the 17 minute mark. Finally the 400 cycle results showed noticeable platinum loss and the results above show a 530% increase in conductivity from the 17 minute mark.

Some additional observations to take away are the following. These results are not completely representative of the actual cell because the PEM material is not present. The PEM material could also increase the conductivity through the production of acetaldehyde (discussed in Chapter 4), which would only increase these results further. The second observation is that platinum loss appears to be sensitive to small changes in solvent conductivity. These recorded conductivities are, at most, only 0.30% (at the 65 minute mark) of the 5 vol% acetic acid conductivity. As mentioned, the actual results may be larger due to acetaldehyde production, but contributions from acetaldehyde would be expected to be minimal based on TGA data in Chapter 4. The 0 vol% acetic acid samples were not heated externally and the only heating would have occurred from local joule heating. Even with local joule heating TGA plots showed nearly no mass loss up to the 300°C temperature, which these samples did not reach. All this suggests that platinum loss is highly sensitive to small changes in the solvent conductivity.

Now that the platinum loss has been connected to increasing solvent conductivity (and not a chemical reaction) additional characterization is still needed to connect how the increased solution conductivity results in platinum being removed. Increasing solution conductivity can also increase the diffusion coefficient of different ions [27] by applying an external force where in this work the external force would be an electric field generated by the current flowing through the platinum.

This is also supported by the increased silicon concentrations at lower solution conductivities. Quartz is known to be a piezoelectric material, where piezoelectric materials accumulate a charge when stress is applied to the material. It is possible that quartz, when placed into an electric field, would diffuse more readily towards the platinum (due to the force being applied from the electric field) on the polymer surface. There are three different events that could be occurring, which need to be looked at closer, which may result in platinum being removed. The first possibility is that the quartz is accelerated (through an increased diffusion rate) through the polymer near the surface and collides with the platinum, thus breaking both the platinum and quartz free, where both elements enter the solvent. A second possibility is that, after the quartz diffused to the surface, then the platinum diffused into the quartz. The addition of platinum into the lattice structure of the quartz would increase the overall strain experienced by the quartz particles [28, 29, 30]. If the strain is increased enough the platinum doped quartz would attempt to reduce its strain by detaching from the PEM material, thus removing the platinum in the process. The

final possibility is that quartz diffuses to the surface through the electric field, but instead of platinum diffusing into the quartz lattice structure the platinum agglomerates onto the surface of the quartz. The addition of platinum on the quartz surface possibly could increase particle strain by constraining the quartz additionally, thus promoting the platinum-coated quartz to detach from the PEM material.

The next section will investigate changes in the samples using XRD to see if any crystallographic changes in the PEM material were observed, such as particle size or strain changes which would help explain the platinum loss mechanism.

6.2. Particle Size and Strain Effects

Each sample that had a 15.5V electrical bias applied was characterized using XRD to determine the quartz particle size and strain. Changes in particle size and/or strain would point towards the quartz being doped by the platinum.

Figure 53 shows a comparison between the XRD data of the platinum sputter coated PEM material before an electrical bias was applied (blue data) and after a 15.5V electrical bias was applied for 100 (red data), 200 (green data) and 400 (yellow data) cycles in contact with 0 vol% acetic acid. The intensity magnitude of all PEM material samples, which had an electrical bias applied, was similar and appeared to be independent of acetic acid percentage.

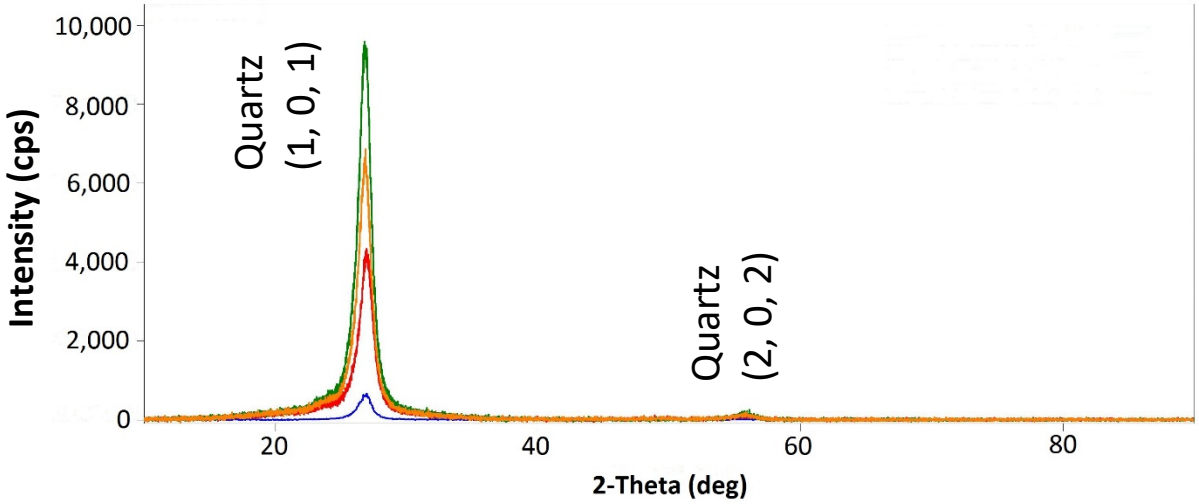

Figure 53: XRD Scan of Platinum Sputter Coated PEM Material Samples Before (blue data) and After Applying a 15.5V Electrical Bias for 100 (red data), 200 (green data) and 400 (yellow data) Cycles using 0 vol% Acetic Acid.

Figure 54 shows the XRD scan data from PEM material samples which had a 15.5V electrical bias (top) and 0.8V electrical bias (bottom) applied for 100, 200 and 400 cycles using a 5 vol% acetic acid solvent. Overall, the main peak intensities are larger than data from the PEM material prior to having an electrical bias applied, shown in Figure 53.

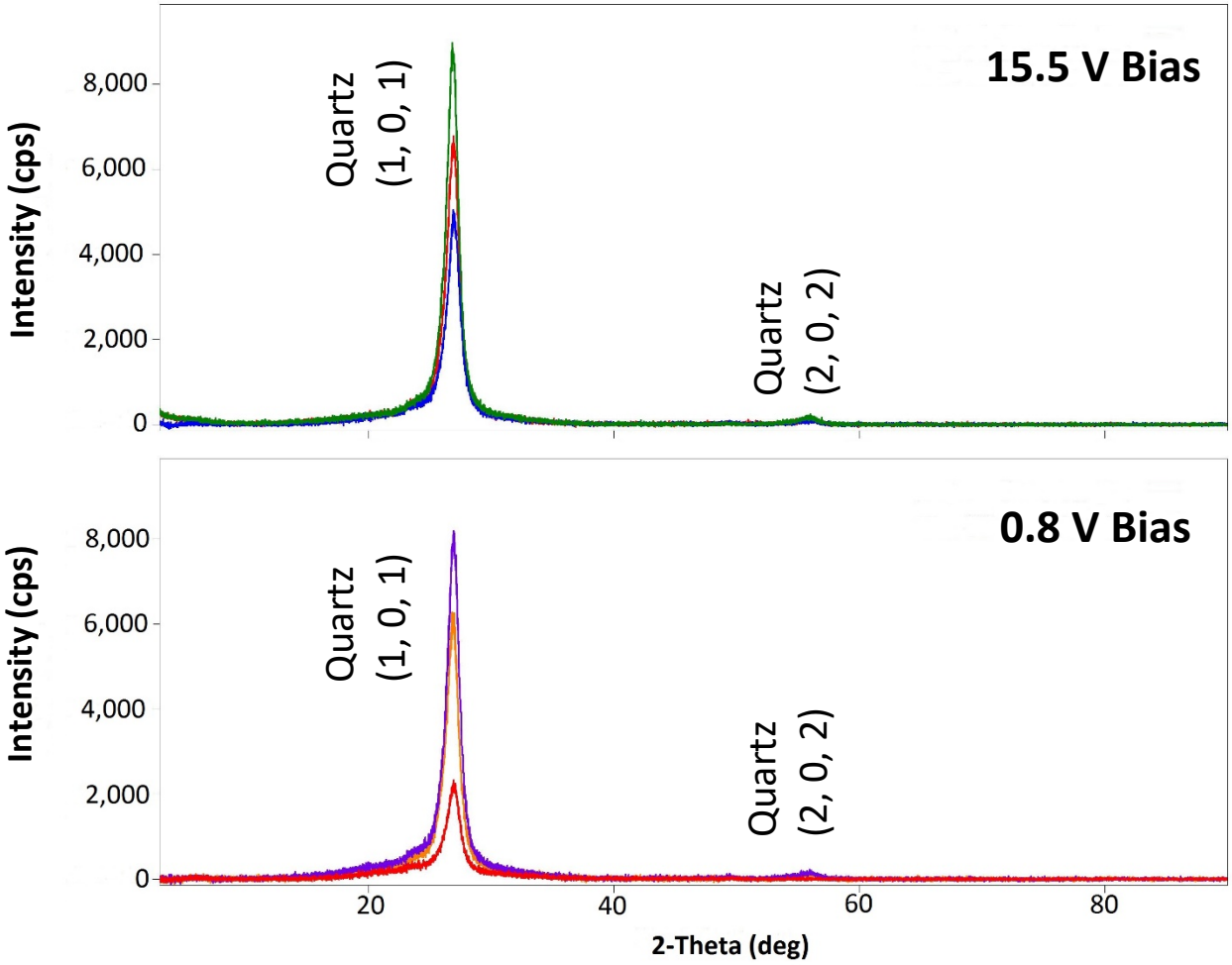

Figure 54: XRD Scan of Platinum Sputter Coated PEM Material Samples After Applying a 15.5V Electrical Bias for 50 (top, blue), 100 (top, red) and 200 (top, green) Cycles and a 0.8V Electrical Bias for 100 (bottom, orange), 200 (bottom, purple) and 400 (bottom, red) Cycles using 5 vol% Acetic Acid.

Figure 55 shows the quartz particle size (top) and strain (bottom) data after a various number of cycles were applied with a 15.5V bias. Particle size and strain data were collected from samples in contact with

0 vol% acetic acid (blue bars), 5 vol% acetic acid (red bars), 99.7 vol% (green bars) and the starting quartz value (purple bar). Particle size and strain values were calculated using the Williamson-Hall method explained in Section 5.4.2.

Results show that the particle sizes for the 0 vol% and 5 vol% acetic acid samples are statistically similar to each other but the average particle size for both did increase with the number of cycles, eventually becoming statistically greater than the starting quartz particle size. The particle size for the 99.7 vol% acetic acid samples remains relatively constant and does not significantly change from the starting quartz particle size.

The strain also follows a similar pattern to that of the particle sizes. The 0 vol% and 5 vol% acetic acid samples have statistically greater strain than the starting quartz strain and the 0 vol% acetic acid samples increase strain with number of cycles until their strain value is similar to that of the 5 vol% acetic acid samples. The 99.7 vol% acetic acid samples do not increase their strain and stay consistent with the starting strain value.

These trends in particle size and strain match closely to the trends observed earlier with solvent conductivity and platinum loss. The 0 vol% acetic acid gradually increased its solvent conductivity and platinum loss, the 5 vol% acetic acid consistently had the largest conductivity and platinum loss, and the 99.7 vol% acetic acid did not have any solvent conductivity or platinum loss.

Figure 56 shows the quartz particle size (top) and strain (bottom) data after a various number of cycles were applied with a 15.5V and 0.8V bias. Particle size and strain data were collected from samples in contact with 5 vol% acetic acid with a 15.5V bias applied (blue bars), 0.8V bias applied (red bars) and the starting values (purple bar). The 0.8V bias samples appeared to have statistically similar particle sizes and strain values to that of the 15.5V bias sample and were still elevated from the starting values. The 0.8V bias samples did seem to have slightly lower particle size and strain averages, which may be caused by the reduced electric field generated. The 0.8V bias data is missing the particle size and strain results for the 400 cycle test because the XRD data did not resolve more than one peak, which prevented the Williamson-Hall method from calculating particle size and strain data for that one sample.

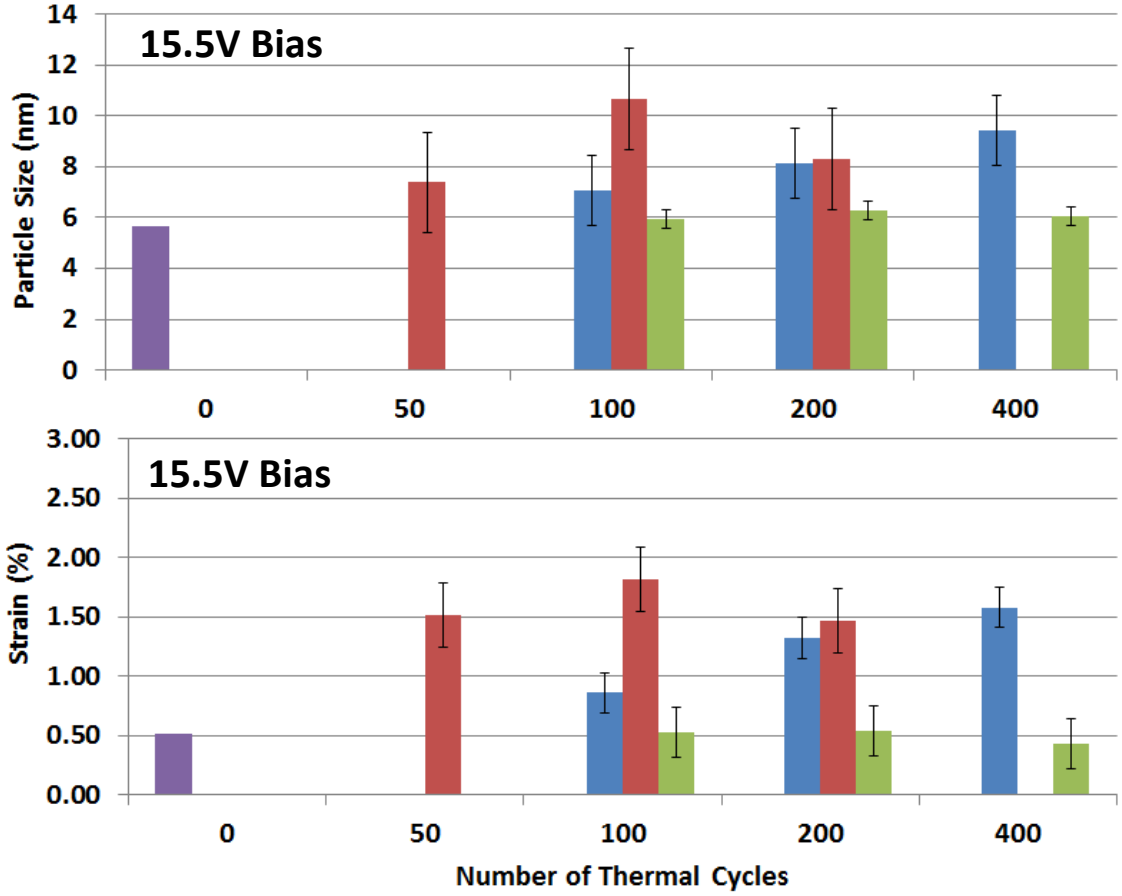

Figure 55: Particle Size Distribution (top) and Strain Distribution (bottom) Value Calculated from XRD Results for Platinum Sputter Coated PEM Material Samples with 15.5V Applied Bias in Contact with Different Solvent Acetic Acid Volume Fraction Values. Results are Shown before Experimentation (purple bar), with 0 vol% Acetic Acid (blue bars), with 5 vol% Acetic Acid (red bars) and 99.7 vol% Acetic Acid (green bars).

The trends observed with the 0.8V bias 5 vol% acetic acid particle size and strain data also match closely with the trends observed earlier. The magnitude of the electric field between these two sets of data appears to be the only statistically significant difference.

Since all the samples that have statistically significant amounts of platinum loss also have particle sizes of 8nm or larger and strain values of 1.00% or larger this points to possibly a change in the quartz lattice structure or unit cell volume. The exact values for each lattice parameter and unit cell volume were not able to be determined using the data collected, but the specific lattice parameter(s) that were changing can be investigated using the unit cell volume equation, shown below.

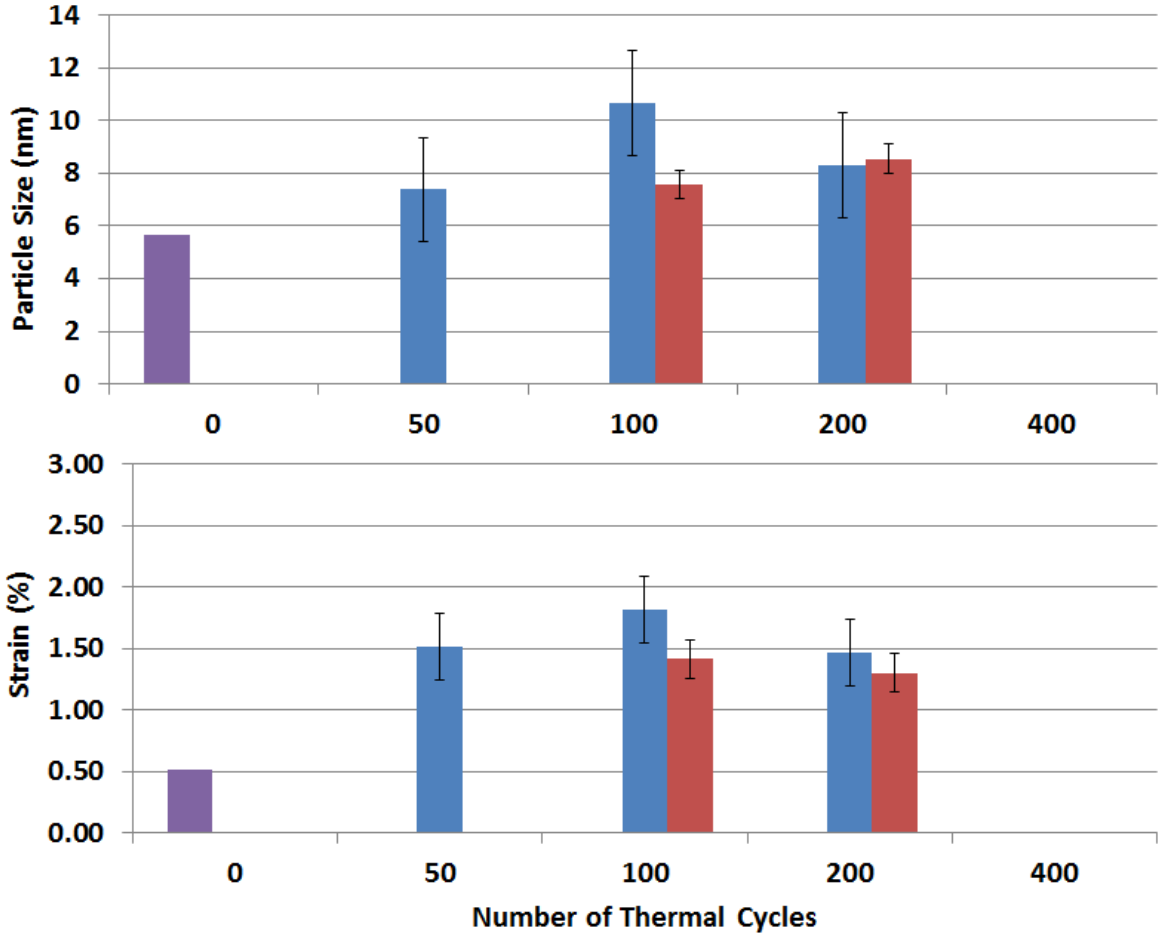

Figure 56: Particle Size Distribution (top) and Strain Distribution (bottom) Values Calculated from XRD Results for Platinum Sputter Coated PEM Material Samples with 15.5V (blue bars) and 0.8V (red bars) Applied Bias in contact with 5 vol% Acetic Acid. Starting values Before Experimentation are Shown in Purple.

The symmetry of the quartz was determined to be hexagonal using the Rigaku XRD reference database. The unit cell volume for the hexagonal structure is shown below in equation 5:

$$V = \frac{\sqrt{3} * a^2 * c}{2}$$ (Equation 5)

Where,

V = Unit cell volume ($Å^3$)

a = Hexagonal lattice parameter (Å)

c = Hexagonal lattice parameter (Å)

Since the particle size was found to increase (in the 0 vol% and 5 vol% acetic acid samples) with the number of cycles that indicates either platinum is agglomerating onto the surface of the quartz or platinum is diffusing into the quartz lattice structure. Agglomeration of platinum onto the surface of the quartz would increase its overall particle size seen by the XRD, but still could distort the hexagonal crystal structure of the quartz and increase its overall strain. Diffusion of platinum into the quartz lattice structure would also increase the volume (shown in Equation 5) since platinum has a larger atomic radius that silicon or oxygen and would increase the a-lattice parameter, the c-lattice parameter or both lattice parameters simultaneously. Determination which of these two mechanisms is actually occurring is not possible at this time, but both mechanisms involve quartz diffusing to the PEM material surface and interacting with the platinum.

6.3. Platinum Electrocatalyst Loss Degradation Mechanism Determination Summary

A much clearer picture of the overall mechanism promoting platinum loss from the FCATT PEM fuel cell is now understood. The following points were determined in this section:

1. The loss of platinum from the PEM material was found to be associated with the solvent having electronic conductivity. Solvents that did not conduct electrons did not show statistically significant losses in platinum levels.
2. The mechanism behind the loss of platinum was determined to not be a reaction between the solvent and the platinum, as three different electronically conductive acid solvents were used (which contained different chemistries) and resulted in similar levels of platinum loss.
3. An electric field, generated by current flowing through the platinum, improved the diffusion of quartz to the PEM material surface. The solvent electronic conductivity promoted increased interaction between the quartz and platinum at the PEM material surface.
4. Platinum is either agglomerating onto the quartz surface or diffusing into the quartz lattice structure resulting in increased quartz particle size and strain. The quartz attempts to reduce the strain by detaching itself and the platinum from the PEM material and enters the solvent. A strain value of 1.00% or greater appears to be where platinum loss is noticed.

Now that a clearer picture of what causes platinum loss in the FCATT PEM fuel cell has been determined the next section will attempt to determine methods of preventing or reducing platinum loss. These different approaches will try using different PEM materials, electrocatalyst materials, processing techniques, or bias application methods.

7. Stack Operating Techniques and Cell Fabrication Approaches to Minimize or Prevent Electrocatalyst Loss

Based on the data presented thus far the loss of platinum in the FCATT PEM Fuel Cell is attributed to acetic acid increasing the electric conductivity of the water, which in turn diffuses the platinum into or onto the quartz, increasing lattice strain to break the quartz and platinum free.

This section will take a closer look into the effects of changing different processing variables such as: 1. Stack operating approach (such as applying voltage in a continuous manner instead of cycling the voltage), 2. Substrate material, 3. Electrocatalyst material, and 4. Thickness of electrocatalyst material.

The results in this section will not be analyzed to determine an underlying mechanism as there may be multiple different mechanisms present since different materials are being used. The purpose of this section is to highlight possible different methods of fabricating the fuel cell, assuming the solvent in contact with the polymer and electrocatalyst material remain electronically conductive, to reduce or completely prevent the loss of the electrocatalyst material and improve cell performance.

7.1. Continuous vs. Cycling Voltage Application Characterization

The first approach to be analyzed is whether applying a voltage continuously, instead of cycling the voltage off and on, would help minimize the electrocatalyst loss. Each continuously applied voltage test used the same total amount of time an equivalent cycle duration lasted. For example, 100 cycles lasted 17 minutes, 200 cycles lasted 33 minutes and 400 cycles lasted 67 minutes.

For these experiments voltages of 15.5V and 0.8V were used with a current of 20 mA and 0.7 mA, respectively. A 6nm thick platinum strip with the same dimensions previously used was sputter coated onto each sample and was in contact with 5 vol% acetic acid solvent. Each voltage was tested for 8 minutes (~50 cycles), 17 minutes (~100 cycles), 33 minutes (~200 cycles) and/or 67 minutes (~400 cycles). Changes in the magnitude of electrocatalyst loss were characterized using optical microscopy since platinum loss was dramatic enough to observe using a microscope.

Figure 57 shows optical microscopy images of the 6nm of platinum sputter coated onto the PEM material after application of an 15.5V electrical bias using cycles (left column) and using a continuous application (right column). 50 cycles/8 minutes (top row), 100 cycles/17 minutes (middle row) and 200 cycles/33 minutes (bottom row) were tested.

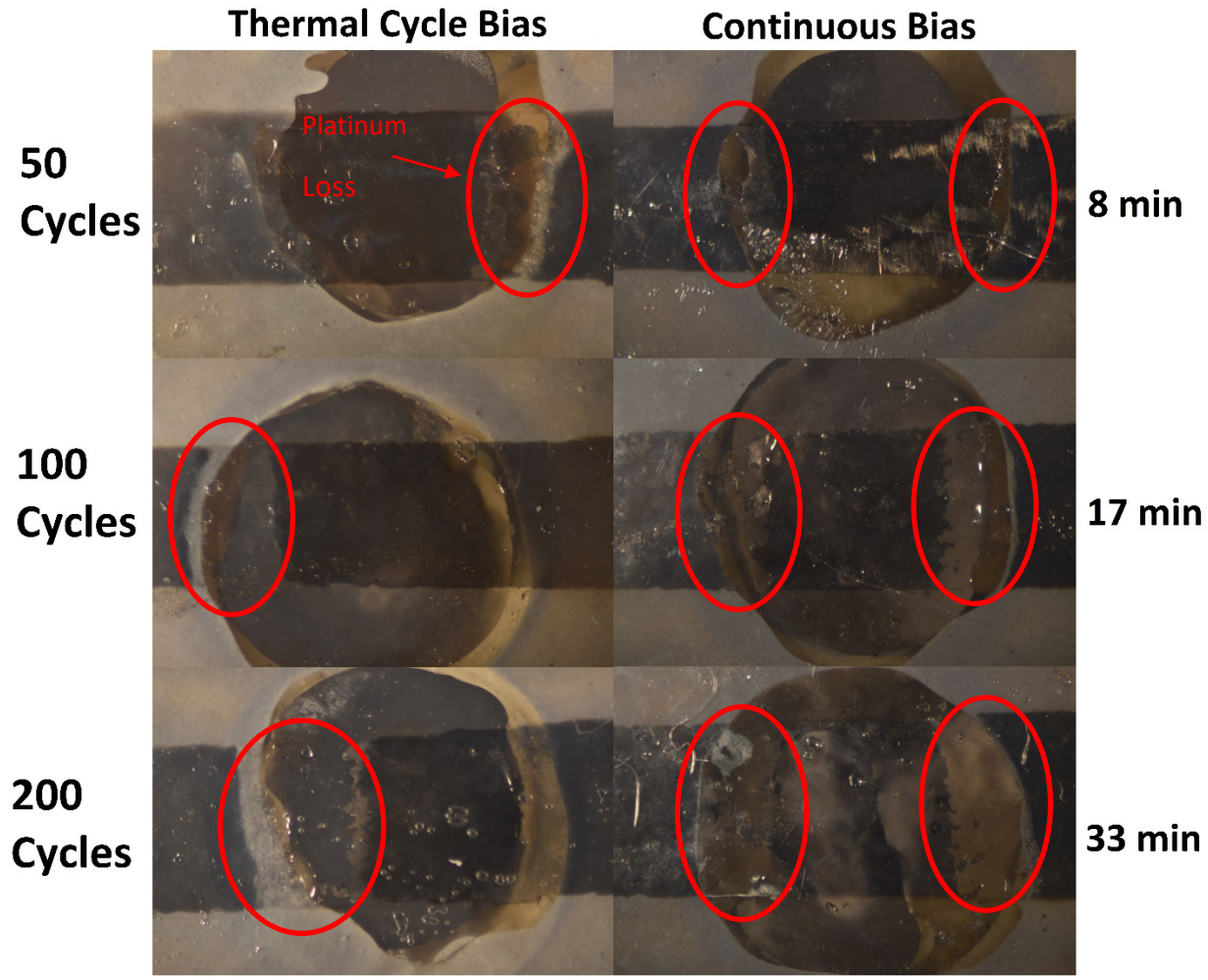

Figure 57: Electrical Bias Cycling Optical Microscopy Results (left column) and Continuous Bias Optical Microscopy Results (right column) Applied using 15.5V and 20 mA. 50 Cycles/8 Minutes (top row), 100 Cycles/17 Minutes (middle row) and 200 Cycles/33 Minutes (bottom row) are Shown.

Results from applying a continuous bias of 15.5V, compared to an equivalent amount of time with cycles, showed similar platinum loss. The magnitude in platinum loss for each cycle/continuous duration comparison was nearly identical. The only difference was there was platinum loss in two locations using the continuous bias method, instead of one with the cycle method. As mentioned earlier, the mechanism behind the platinum loss using the continuous method will not be investigated as that is not the focus of this paper.

Figure 58 shows optical microscopy images of the 6nm of platinum sputter coated onto the PEM material after application of an 0.8V electrical bias using cycles (left column) and using a continuous application (right column). 100 cycles/17 minutes (top row), 200 cycles/33 minutes (middle row) and 400 cycles/67 minutes (bottom row) were tested.

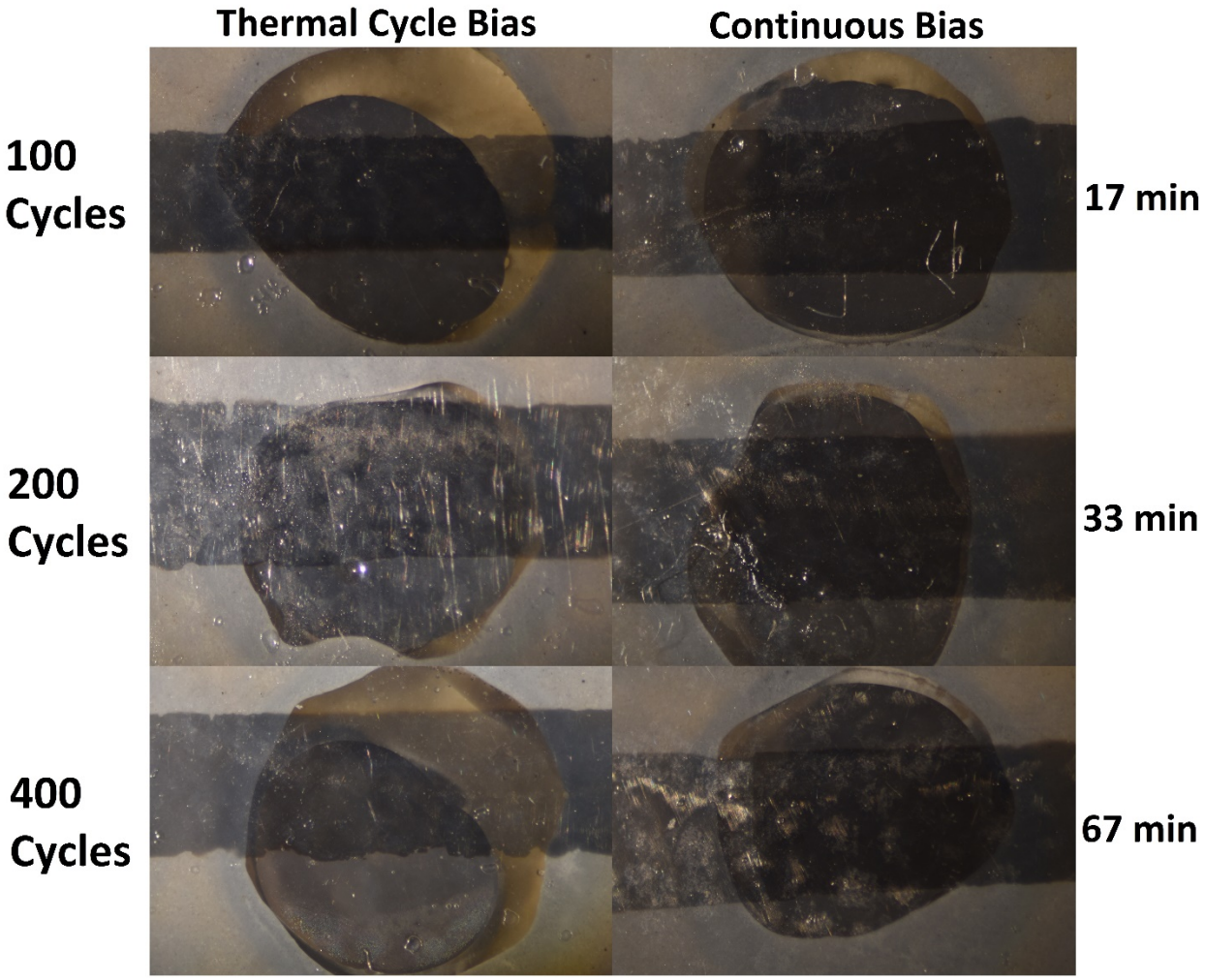

Figure 58: Electrical Bias Cycling Optical Microscopy Results (left column) and Continuous Bias Optical Microscopy Results (right column) Applied using 0.8V and 0.7 mA. 100 Cycles/17 Minutes (top row), 200 Cycles/33 Minutes (middle row) and 400 Cycles/67 Minutes (bottom row) are Shown.

Results were, again, very similar between the cycle and continuous bias tests in that no visible platinum loss was observed using optical microscopy. Since the cycle EDS results did show platinum loss, simply relying on optical microscopy in this scenario will not be sufficient to determine if the continuous bias removed less platinum. Simply assuming that since the continuous bias approach would be the same here as with the 15.5V characterization is incorrect as the underlying mechanism for the continuous bias may not be the same as the cycle mechanism

Figure 59 shows the EDS data for the platinum peak from the platinum sputter coated PEM material samples before (yellow data) and after (red data) a 0.8V electrical bias was applied using either cycles (left column) or continuously (right column). Samples had the electrical bias applied for 100 cycles/17 minutes (top row), 200 cycles/33 minutes (middle row) and 400 cycles/67 minutes (bottom row).

Figure 60 shows the EDS data for the silicon peak from the platinum sputter coated PEM material samples before (yellow data) and after (red data) a 0.8V electrical bias was applied using either cycles (left column) or continuously (right column). Samples had the electrical bias applied for 100 cycles/17 minutes (top row), 200 cycles/33 minutes (middle row) and 400 cycles/67 minutes (bottom row).

Results from the EDS data show that platinum loss was observed when the electrical bias was applied continuous. The amount of platinum loss was similar in magnitude to the cycle results as well for all durations of time. The silicon data showed that silicon levels remained mostly constant for the cycle and continuous bias samples.

Clearly platinum loss was observed when continuously applying the bias, so simply operating the stack for longer periods of time will not reduce the performance degradation. Since the manner in which the stack is operated did not alter the degradation, maybe the materials used in the cell construction would minimize the electrocatalyst loss. The next section will characterize the effect the substrate material had on the amount of electrocatalyst material removed.

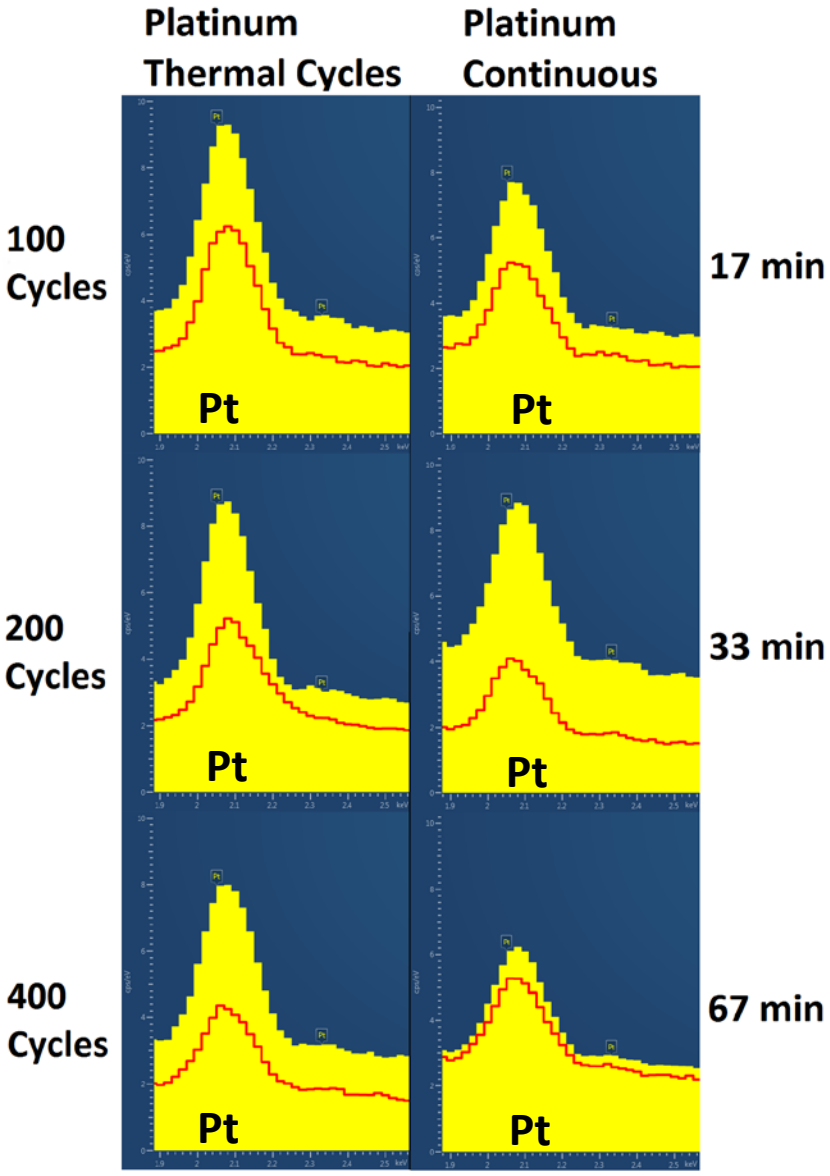

Figure 59: EDS Data for Platinum Sputter Coated PEM Material Samples Applied with a 0.8V Electrical Bias Applied using Cycles (left column) and Applied Continuously (right column). Electrical Bias Cycles were Applied for 100 (top left), 200 (middle left) and 400 (bottom left) Times, while the Continuously Applied Bias was Applied for 17 min (top right), 33 min (middle right) and 67 min (bottom right). All Samples were in Contact with 5 vol% Acetic Acid Solvent at Room Temperature.

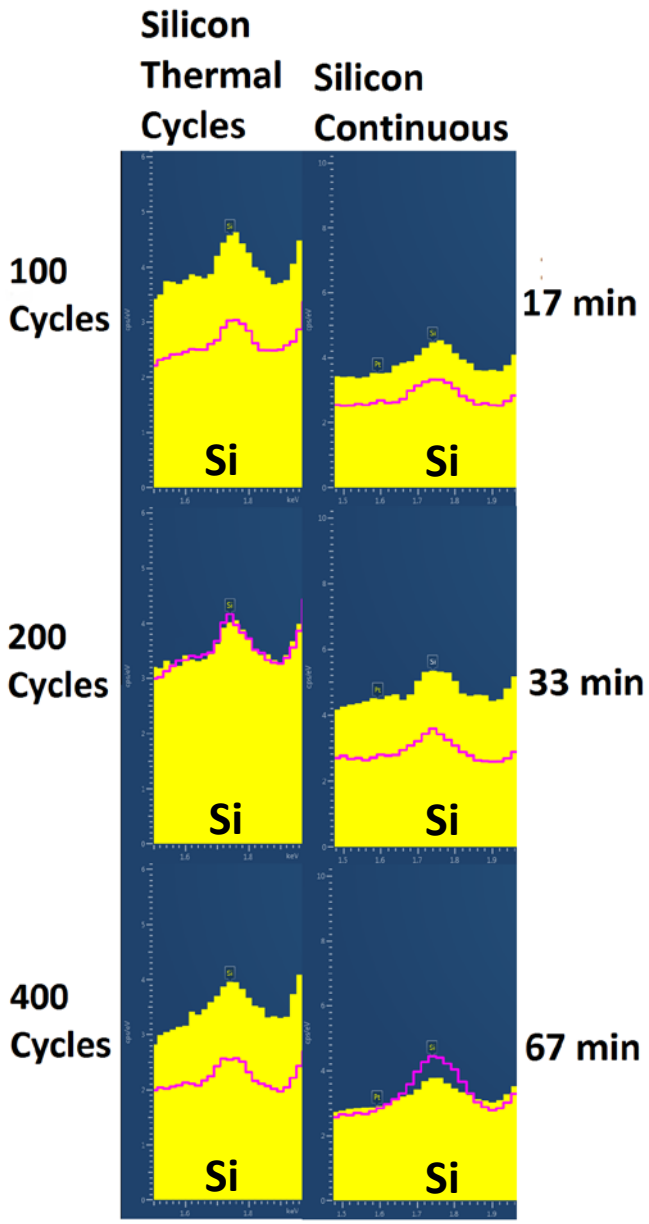

Figure 60: EDS Data for Silicon Peaks Located on the Platinum Sputter Coated PEM Material Samples Applied with a 0.8V Electrical Bias Applied using Cycles (left column) and Applied Continuously (right column). Electrical Bias Cycles were Applied for 100 (top left), 200 (middle left) and 400 (bottom left) Time, while the Continuous Applied Bias was Applied for 17 min (top right), 33 min (middle right) and 67 min (bottom right). All Samples were in Contact with 5 vol% Acetic Acid Solvent at Room Temperature.

7.2. Substrate Material Characterization

Since the quartz, which is partly responsible for causing the platinum loss, is located in the PEM material substrate it makes sense to try and find an alternate substrate material that does not contain quartz or elements which are as mobile. 5 vol% acetic acid was still applied to each platinum sputter coated sample below since the compound that thermally decomposed originally to form acetic acid may still be required for stack operation. Simply removing the quartz from the cell may limit the electrocatalyst loss.

EDS scans were taken of all substrate materials used to certify that each material did not obtain unknown elements that may influence experimental results. Results from these material scans showed no unexpected elements present. Exterior and Interior scans of the zinc and cadmium plated steel to show steel was present underneath the zinc and cadmium coating. The EDS scans can be found in Appendix A at the end of this report.

Figure 61 shows optical microscopy images of 6nm of platinum sputter coating onto different polymer substrate materials which had a 15.5V 20 mA electrical bias applied in contact with 5 vol% acetic acid. Optical microscopy images were taken before (left column) and after (middle column) the electrical bias was applied for 100 cycles. Two substrate materials required the interior section (which was in contact with the 5 vol% acetic acid) to be cut out to better document platinum loss results, which are shown in the right column. The polymer materials are arranged to show decreasing platinum loss from top (PEM material) to bottom (Polystyrene).

Results from experiments using different polymer substrates showed overall mixed results. All polymers tested showed some degree of visible platinum loss with polystyrene having the best results. All the polymer materials have different chemical structures and different elements used in their formulation. The mechanism for platinum loss may be different for every polymer based on their chemical formulation and atomic interactions with the platinum, so determination as to why each polymer had different results is beyond the scope of this paper. A general recommendation is that polymer substrates promote platinum loss when in contact with an electronically conductive solvent.

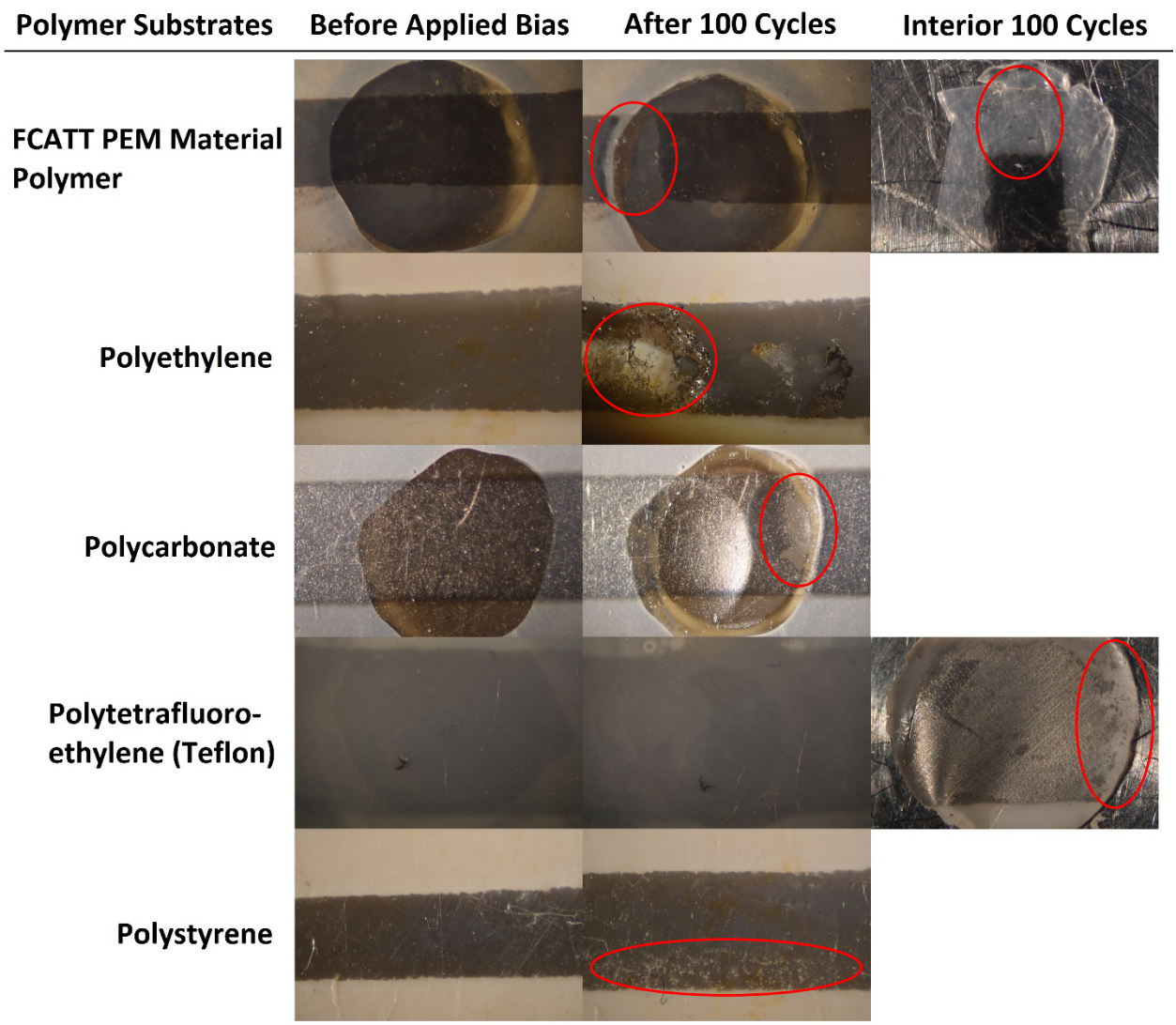

Figure 61: Optical Microscopy Images of Platinum Sputter Coated onto Various Polymer Substrate Materials. Images of the Platinum Coating are Shown before (left column) and after (middle column) the Electrical Bias was Applied. Interior Cutouts (right column) after the Electrical Bias was Applied are also Shown. Polymer Materials used were: PEM Material (top row), Polyethylene (2nd from top), Polycarbonate (3rd from top), Polytetrafluoroethylene (4th from top), Polystyrene (bottom row). Electrical Bias was Applied for 100 Cycles using 15.5V and 20 mA in Contact with 5 vol% Acetic Acid.

Figure 62 shows optical microscopy images of 6nm of platinum sputter coating onto different glass/ceramic substrate materials which had a 15.5V 20 mA electrical bias applied in contact with 5 vol% acetic acid. Optical microscopy images were taken before (left column) and after (right column) the electrical bias was applied for 100 cycles. The substrate materials are arranged to show decreasing platinum loss from top (amorphous glass) to bottom (aluminum oxide).

Results from experiments using glass and ceramic substrates showed positive results. The amorphous glass showed significant platinum loss, which could be contributed to the high silicon concentrations and/or other trace elements used in its formulation. The aluminum oxide (alumina) showed no visible platinum loss at all. The markings on the bottom right image are just discoloration marking from the 5 vol% acetic acid solution after it dried. The alumina sample shows that changing the substrate to which the platinum is adhered to can influence it loss from the cell.

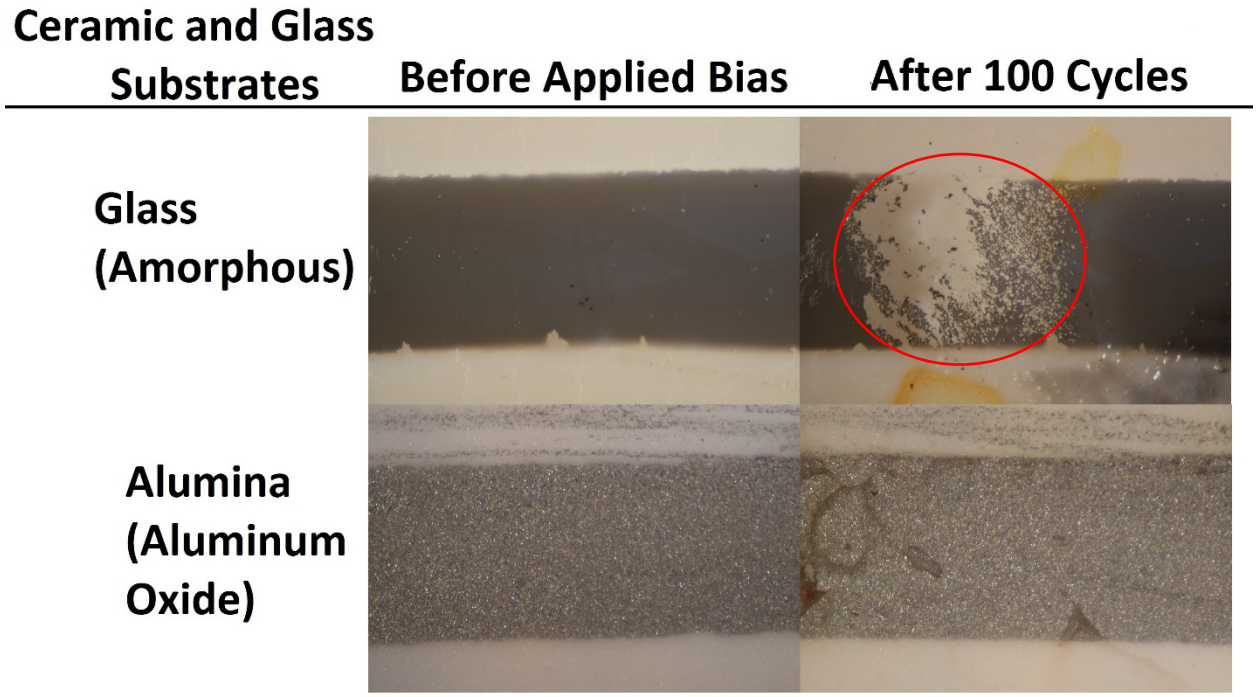

Figure 62: Optical Microscopy Images of Platinum Sputter Coated onto Various Glass/Ceramic Substrate Materials. Images of the Platinum Coating are Shown Before (left column) and After (right column) the Electrical Bias was Applied. Materials used were: Amorphous Glass (top row) and Aluminum Oxide (bottom row). Electrical Bias was Applied for 100 Cycles using 15.5V and 20 mA in Contact with 5 vol% Acetic Acid.

Figure 63 shows optical microscopy images of 6nm of platinum sputter coating onto different bulk metal substrate materials which had a 15.5V 20 mA electrical bias applied in contact with 5 vol% acetic acid. Optical microscopy images were taken before (left column) and after (right column) the electrical bias was applied for 100 cycles. An optical microscope image of the cadmium plated steel substrate (right column), before platinum was coated was also included to provide a reference for what the sample looked like to help identify platinum loss. The substrate materials are arranged to show decreasing platinum loss from top (zinc plated steel) to bottom (aluminum).

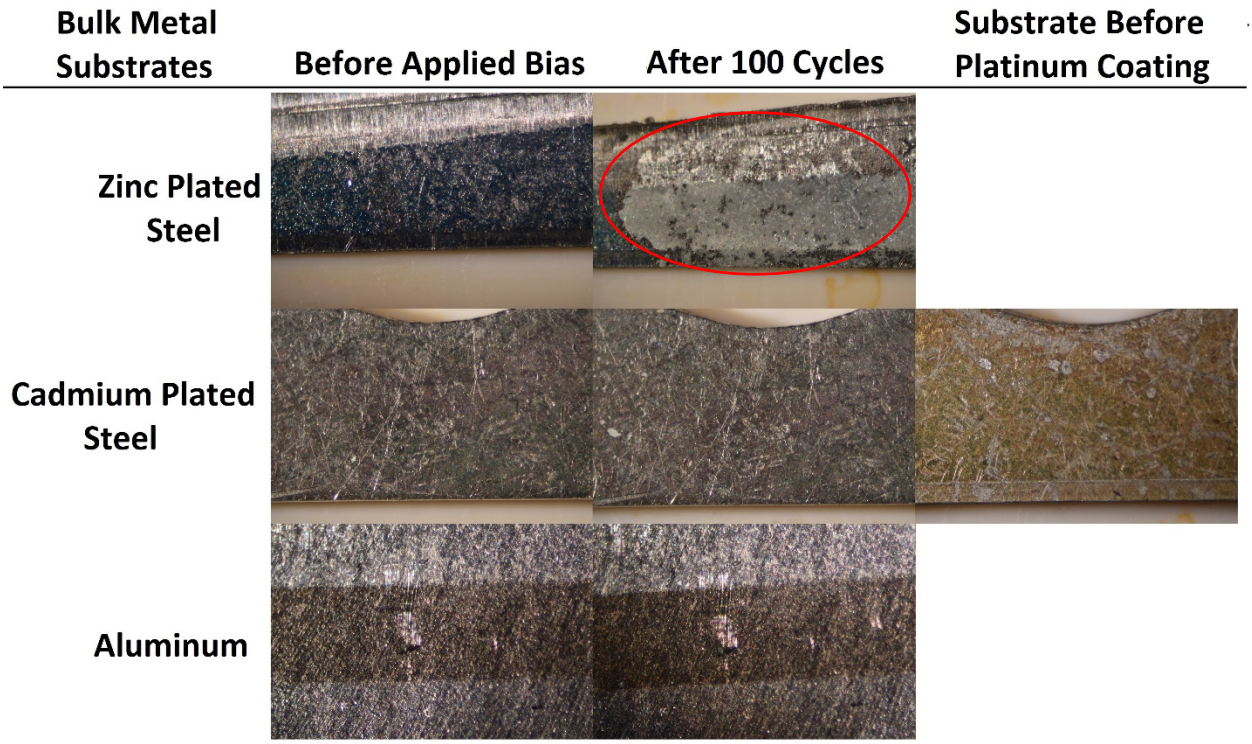

Figure 63: Optical Microscopy Images of Platinum Sputter Coated onto Various Bulk Metal Substrate Materials. Images of the Platinum Coating are Shown Before (left column) and After (middle column) the Electrical Bias was Applied. Images of Substrate Materials before the Platinum Sputter Coating was Applied are Shown in the Right Column. Materials used were: Zinc Plated Steel (top row), Cadmium Plated Steel (middle row) and Aluminum (bottom row). Electrical Bias was Applied for 100 Cycles using 15.5V and 20 mA in Contact with 5 vol% Acetic Acid.

Results from experiments using different bulk metal substrates also showed positive results. As with the glass and ceramic substrates some of the bulk metal demonstrated no visible platinum loss. The zinc plated steel showed significant loss and some of the zinc coating may have been removed as well as the platinum coating. This is not a surprise as zinc is used in many applications as a sacrificial corrosion layer. Both the cadmium plated steel and the aluminum showed no visible platinum loss similar to the alumina sample above. Again, bulk metal substrates could be used to minimize platinum loss as with the ceramic substrate.

7.3. Electrocatalyst/Coating Material Characterization

Alternate substrate materials were identified that did not promote platinum loss. The next approach to take is to characterize the interaction between different electrocatalyst/coating materials and the PEM material substrate. Just as platinum appeared to interact differently with different polymer substrates, different electrocatalyst materials may interact differently with the PEM material substrate too. This approach is important to try for two reasons, which are: 1. platinum could be replaced by other elements which are also catalytically active and 2. If a non-catalytically active element is found to remain on the PEM material substrate then that element possibly may be placed underneath the platinum to prevent its removal.

Figure 64 shows optical microscopy images of 6nm of various coating materials Sputtered onto the PEM material substrate. Each coating material had a 15.5V 20 mA electrical bias applied while in contact with 5 vol% acetic acid. Optical microscopy images were taken before (left column) and after (right column) the electrical bias was applied for 100 cycles. Coating materials used were platinum (top row), gold (2nd from top), copper (3rd from top) and carbon (bottom row).

Results show that most of the coating materials used were removed after 100 cycles, except for the carbon, which showed no visible indications of being removed from the substrate material. These results are important because they show that a non-electrically conductive coating (carbon) was not affected while coatings with high electrical conductivity were readily removed.

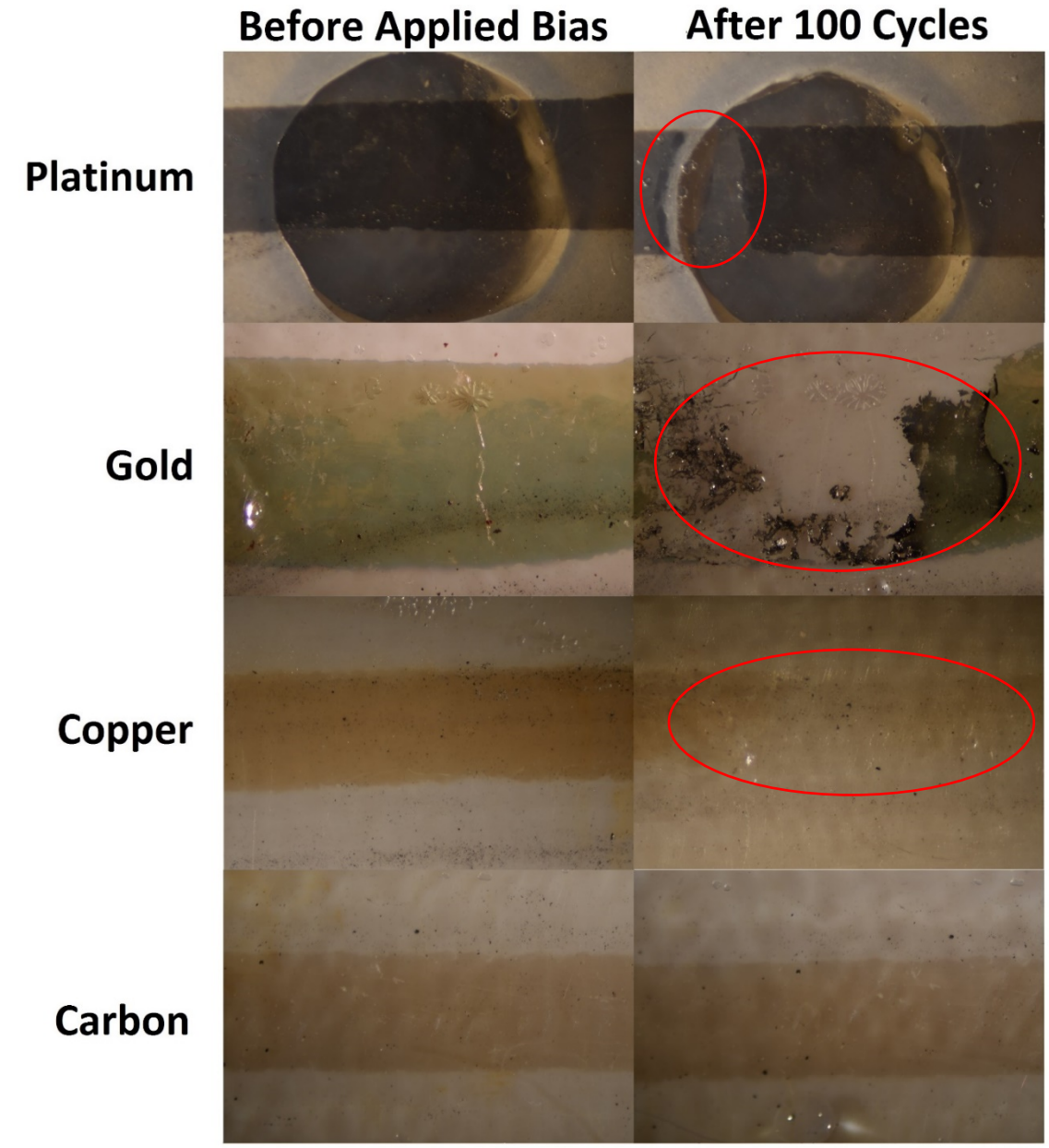

Figure 64: Optical Microscopy Images of Various Electrocatalyst/Coatings Sputter Coated onto the PEM Material Substrate. Images of each Coating are Shown Before (left column) and After (right column) the Electrical Bias was Applied. Coating Materials used were: Platinum (top row), Gold (2nd row), Copper (3rd row) and Carbon (bottom row). Electrical Bias was Applied for 100 Cycles using 15.5V and 20 mA in Contact with 5 vol% Acetic Acid.

7.4. Electrocatalyst/Coating Deposition Thickness Characterization

The thickness of the sputter coating material deposited on the PEM material was next characterized. The same coating materials were used as previously shown. Coating material thicknesses were increased in all cases to 50nm, except for the carbon coating, which was increased only to 20nm. The reason for a thinner coating thickness with carbon will be explained.

Figure 65 shows optical microscopy images of 6nm and 50nm of various coating materials sputtered onto the PEM material substrate. Each coating material had a 15.5V 20 mA electrical bias applied while in contact with 5 vol% acetic acid. Optical microscopy images were taken before (left column) and after (right column) the electrical bias was applied for 100 cycles. Coating materials used were platinum (top two rows) and gold (bottom two rows).

Results show both platinum and gold have similar responses depending on the thickness of the coating layer. Both coatings are removed when 6nm in thickness, but show no visible indications of being removed or starting to be removed, such as stress cracks starting to form, at 50nm in thickness. It is still possible that both these materials are being removed when the coatings are 50nm and possibly only prolongs the coatings life instead of preventing loss completely.

Figure 66 shows similar optical microscopy images as Figure 65 but using copper and carbon instead. The copper was deposited using 6nm and 50nm, while the carbon was deposited 8nm and 20nm. The carbon was deposited using slightly different thicknesses because the carbon deposition process was not as accurate (for the 8nm) and the carbon rope burned up after 20nm of continuous deposition.

Results for these final two materials show different results than with the platinum and gold coatings. The copper was removed using both coating thicknesses and no carbon was removed with either coating thicknesses. The fact carbon was not removed in either experiment was attributed to carbon having an electrical conductivity which ~10,000 times lower than platinum or gold, which prevented loss of the coating. Copper, however, has a similar conductivity to that of platinum or gold, so what is different?

Copper, unlike platinum or gold, reacts with acetic acid to form copper acetate [31]. To test whether copper acetate would form when copper was in contact with acetic acid at room temperature the mass loss of pure copper placed in glacial acetic acid was recorded after 69 hrs to determine the approximate rate copper reacts with the acetic acid. Overall a bright blue powder was formed and XRD analysis showed it to be mostly copper acetate. The mass lost was 3.1% and the average rate of mass loss was 0.05%/hr.

Platinum metal is known not to react with acetic acid at room temperature, but the same experiment was performed using platinum for comparison purposes. Overall, after 91 hrs there was no platinum mass

loss and no precipitates that formed. Experimental results between copper in acetic acid and platinum in acetic acid are shown in Appendix B.

This reaction between copper and acetic acid would possibly be magnified when nano-scale copper particles were exposed to the acetic acid due to their increased surface area. This reaction between the acetic acid and copper nano-particles is hypothesized to be the reason copper was removed while platinum and gold were unaffected using thicker coating thicknesses.

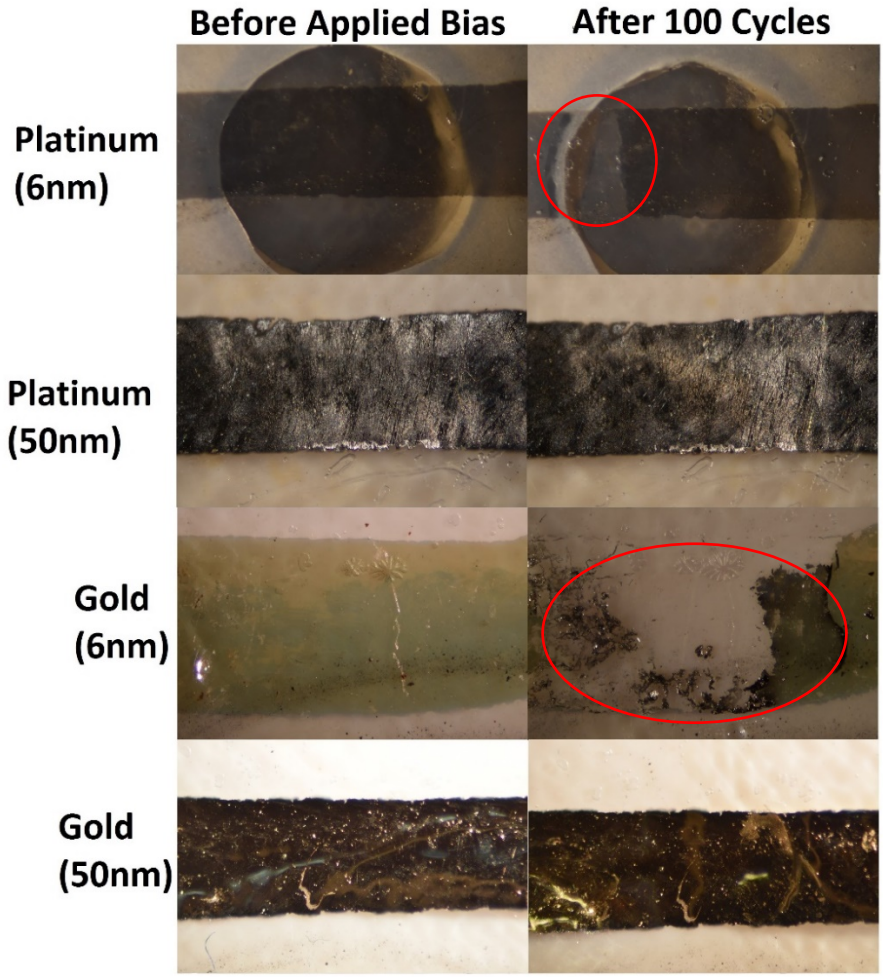

Figure 65: Optical Microscopy Images of Various Electrocatalyst/Coatings Sputter Coated onto the PEM Material Substrate with Coating Thicknesses of 6nm and 50nm. Images of each Coating are Shown Before (left column) and After (right column) the Electrical Bias was Applied. Coating Materials used were: Platinum (top two rows) and Gold (bottom two rows). Electrical Bias was Applied for 100 Cycles using 15.5V and 20 mA in Contact with 5 vol% Acetic Acid.

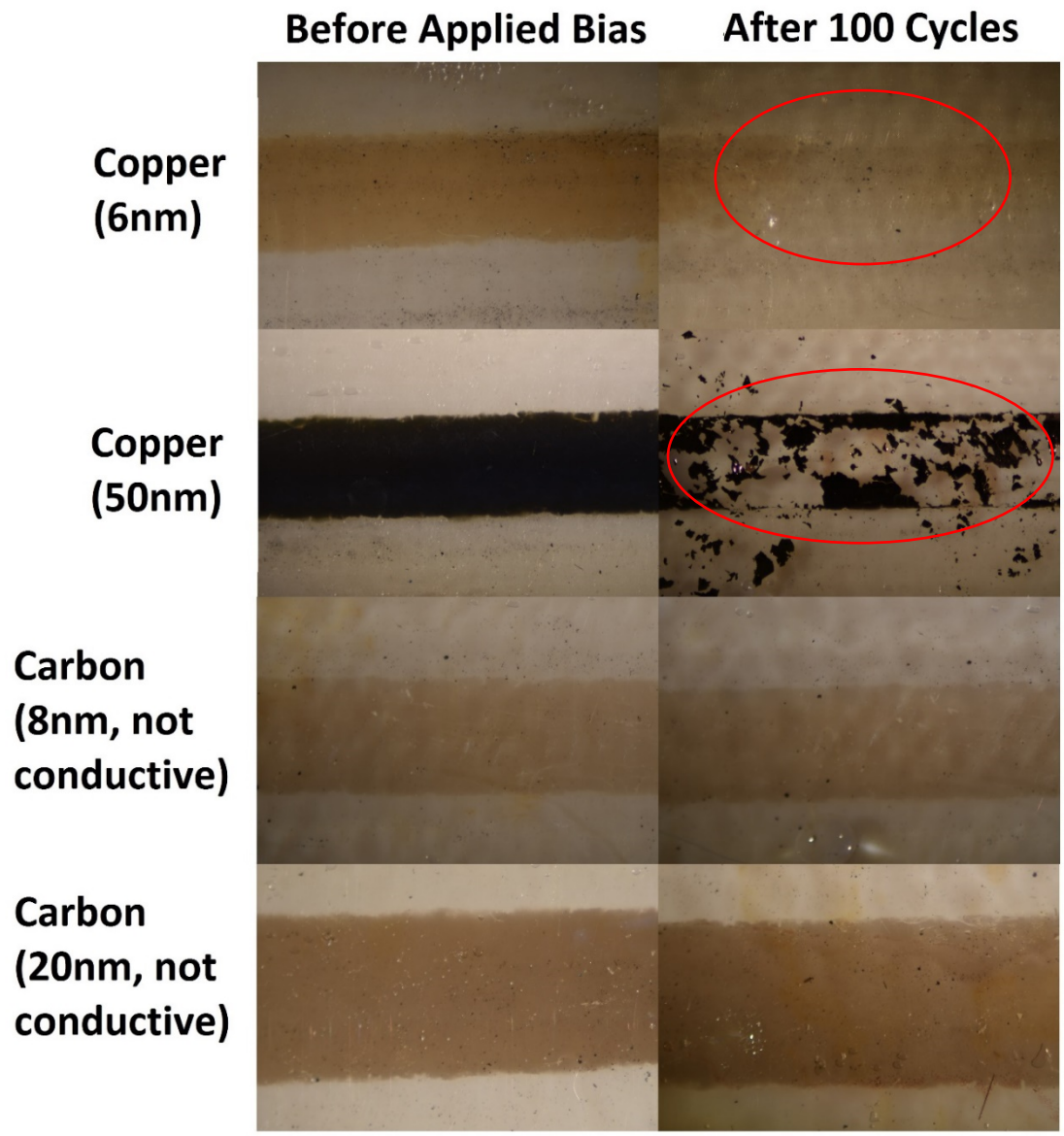

Figure 66: Optical Microscopy Images of Various Electrocatalyst/Coatings Sputter Coated onto the PEM Material Substrate with Coating Thicknesses of 6nm, 8nm, 20nm and 50nm. Images of each Coating are Shown Before (left column) and After (right column) the Electrical Bias was Applied. Coating Materials used were: Copper (top two rows) and Carbon (bottom two rows). Electrical Bias was Applied for 100 Cycles using 15.5V and 20 mA in Contact with 5 vol% Acetic Acid.

After analyzing these results the following trends can be observed. First, overall a thicker deposit of electrocatalyst/coating material minimized the loss of that material. Electrocatalyst/coating material may still be lost over time at further evaluation would be needed. Second, the copper deposited material was removed even with a coating thickness of 50 nm, which was due to the copper reacting with the acetic acid. Coating materials that react with the solvent should be avoided to minimize complications in stack operation. Finally, nonconductive coating materials, such carbon, worked equally as well with a thick or thin deposit thickness.

After characterizing the effects of changing the substrate material, electrocatlyst/coating material and electrocatalyst/coating deposit thickness one additional characterization will be performed to try and combine the findings from these tests. Changing the substrate to a ceramic or metal material may not be as practical but increasing the overall deposit thickness and using non-electronically conductive coatings are possibilities. The following section will investigate whether platinum can be elevated using a less-expensive coating to save on costs and prevent overall coating loss using 5 vol% acetic acid solution.

7.5. Combined Electrocatalyst/Coating Deposit Material Thickness Characterization

The following experiments first attempt to sputter gold onto the PEM material substrate, using different coating thicknesses, and then apply a 6nm of layer of platinum on top. Since both gold and platinum were shown, when sufficiently thick enough, to resist be removed when an electrical bias was applied in contact with 5 vol% acetic acid. Both of these materials is non-reactive in this scenario and gold is also less expensive compared to platinum.

Carbon will also be used in place of gold as it also resisted being removed from the substrate material. Carbon has an even lower cost than gold and due to its lower electrical conductivity it may allow for thinner coatings between the platinum and substrate.

Figure 67 shows the results of coating different materials between platinum and the PEM material substrate. The top two rows use gold at 5nm (top row) and 15nm (2nd from top), while carbon was applied with 5nm (bottom row). Platinum was sputter coated on top of all samples with a thickness of 6nm. All experiments placed a 15.5V electrical bias across the sample while in contact with 5 vol% acetic acid solvent for 100 cycles.

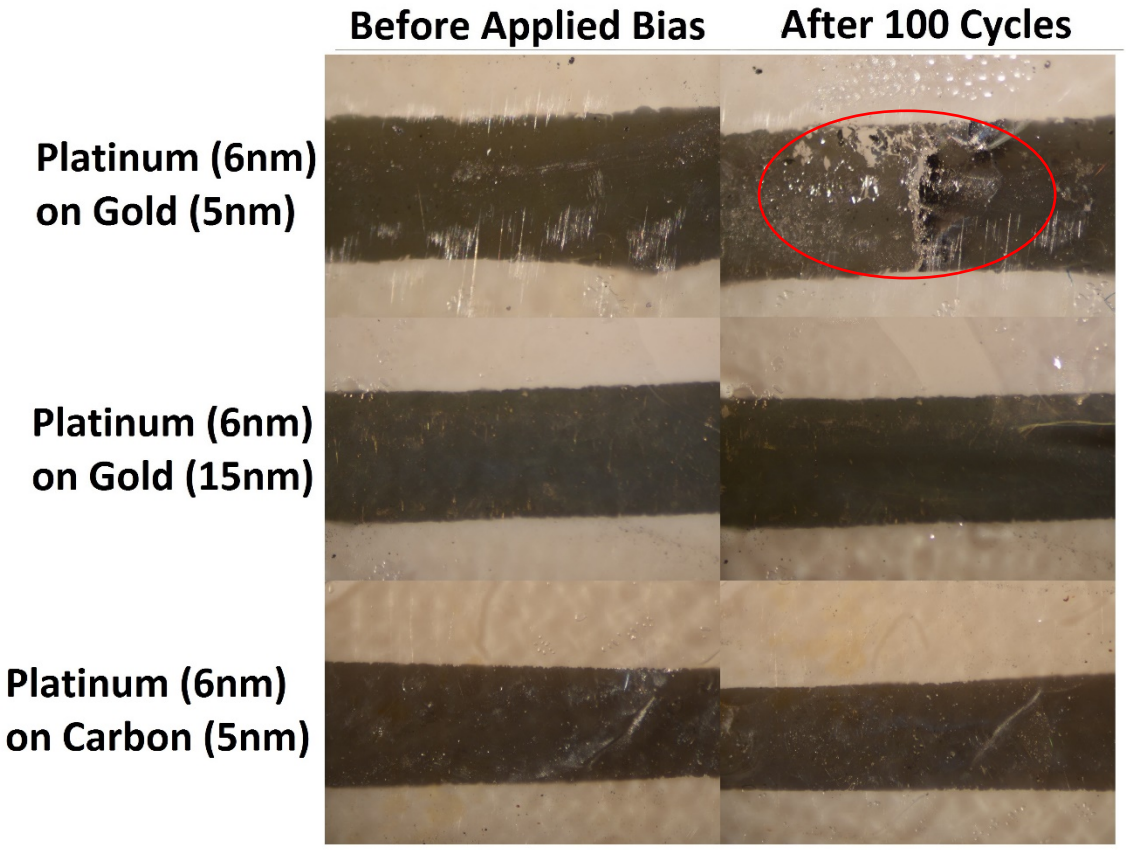

Figure 67: Optical Microscopy Images of Platinum/Gold and Platinum/Carbon Sputtered Coated on to PEM Material Substrates Before (left column) and After (right column) a 15.5V Electrical Bias was Applied for 100 Cycles in Contact with 5 vol% Acetic Acid. Gold was Applied at 5nm (top row) and 15nm (middle row) Thicknesses. Carbon was Applied at 5nm (bottom row) Thickness. Platinum was Applied at 6nm for all Experiments.

Results, for gold, show coating loss can occur and a sufficient amount of gold must be placed underneath the platinum to prevent coating loss. The amount of gold necessary is still minimal with 15nm being sufficient. The carbon, when coated underneath the platinum, showed no loss of either material after 100 cycles. The carbon has a significantly lower cost than gold or platinum and was able to prevent platinum loss from the substrate with a very thin layer of 6nm.

7.6. Operating Techniques and Cell Fabrication Approaches Summary

Many different alternate approaches were attempted and discussed in the pursuit of reducing or preventing electrocatalyst/coating loss from the substrate material. The following is a summary of the findings of those tests:

1. Applying the electrical bias continuously, instead of cycling the bias on-and-off, did not show any positive results. The degradation behavior between electrical bias applied through cycling and applied continuously was nearly identical.
2. Using different substrate materials, instead of the starting PEM material, showed mixed results. All polymer substrates used demonstrated some level of visible electrocatalyst/coating loss using optical microscopy. Alumina (aluminum oxide), a ceramic substrate material, resulted in no electrocatlyst/coating loss. Cadmium plated steel and aluminum metal substrate materials also resulted in no loss either.
3. Deposit thickness of the electrocatalyst/coating impacted whether the coating would be removed, as long as the coating did not react with the solvent. Platinum, gold and carbon all showed no coating loss when they reached a specific coating thickness. Platinum and gold showed no loss around 50nm and carbon showed no loss at 8nm. Those deposit thickness value may be lowered to achieve an optimal coating thickness. Copper was removed up to a coating thickness of 50nm because copper reacts with acetic acid and it was hypothesized the reaction promoted additional coating loss.
4. Electrical conductivity of coating material appeared to impact degradation behavior. Platinum, gold and copper all have similar electrical conductivity values and all are removed from the PEM material substrate when their coatings are 6nm thick. Carbon, which has an electrical conductivity which is 10,000 times lower, was not removed when 6nm was applied to the same substrate material.
5. The addition of a coating material placed underneath platinum can help minimize degradation. When 15nm of gold was placed underneath 6nm of platinum both materials were not removed. Similar results were observed when 6nm of carbon was placed underneath 6nm of platinum. The addition of a second, non-reactive coating material, allowed for cost savings by not requiring as much expensive platinum be used plus prevents overall degradation of the electrocatalyst/coating material.

8. Overall Project Conclusions

The following summary highlights the findings for: 1. Acetic acid production in the PEM material, 2. Platinum loss from the PEM fuel cell and 3. Alterative operating techniques and fabrication approaches that may be used to reduce or prevent electrocatalyst/coating loss from the cell substrate material.

8.1. PEM Material Acetic Acid Production Mechanism Characterization Summary

1. The PEM material in both Cell 1 and 31, when characterized by TGA-FTIR, showed one major component of the off-gas was acetaldehyde.
2. The MEA samples most likely produced acetic acid by the acetaldehyde oxidation reaction.
3. The PEM material samples most likely produced acetic acid by the oxidative fermentation reaction.

8.2. Platinum Electrocatalyst Loss Degradation Mechanism Characterization Summary

1. The loss of platinum from the PEM material was found to be associated with the solvent having electronic conductivity. Solvents that did not conduct electrons did not show statistically significant losses in platinum levels.
2. The mechanism behind the loss of platinum was determined to not be a reaction between the solvent and the platinum, as three different electronically conductive acid solvents were used (which contained different chemistries) and resulted in similar levels of platinum loss.
3. An electric field, generated by current flowing through the platinum, improved the diffusion of quartz to the PEM material surface. The solvent electronic conductivity promoted increased interaction between the quartz and platinum at the PEM material surface.
4. Platinum is either agglomerating onto the quartz surface or diffusing into the quartz lattice structure resulting in increased quartz particle size and strain. The quartz attempts to reduce the strain by detaching itself and the platinum from the PEM material and enters the solvent. A strain value of 1.00% or greater appears to be where platinum loss is noticed.

8.3. Operating Techniques and Cell Fabrication Approaches

1. Applying the electrical bias continuously, instead of cycling the bias on-and-off, did not show any positive results. The degradation behavior between electrical bias applied through cycling and applied continuously was nearly identical.
2. Using different substrate materials, instead of the starting PEM material, showed mixed results. All polymer substrates used demonstrated some level of visible electrocatalyst/coating loss using

optical microscopy. Alumina (aluminum oxide), a ceramic substrate material, resulted in no electrocatlyst/coating loss. Cadmium plated steel and aluminum metal substrate materials also resulted in no loss either.

3. Deposit thickness of the electrocatalyst/coating impacted whether the coating would be removed, as long as the coating did not react with the solvent. Platinum, gold and carbon all showed no coating loss when they reached a specific coating thickness. Platinum and gold showed no loss around 50nm and carbon showed no loss at 8nm. Those deposit thickness value may be lowered to achieve an optimal coating thickness. Copper was removed up to a coating thickness of 50nm because copper reacts with acetic acid and it was hypothesized the reaction promoted additional coating loss.
4. Electrical conductivity of coating material appeared to impact degradation behavior. Platinum, gold and copper all have similar electrical conductivity values and all are removed from the PEM material substrate when their coatings are 6nm thick. Carbon, which has an electrical conductivity which is 10,000 times lower, was not removed when 6nm was applied to the same substrate material.
5. The addition of a coating material placed underneath platinum can help minimize degradation. When 15nm of gold was placed underneath 6nm of platinum both materials were not removed. Similar results were observed when 6nm of carbon was placed underneath 6nm of platinum. The addition of a second, non-reactive coating material, allowed for cost savings by not requiring as much expensive platinum be used plus prevents overall degradation of the electrocatalyst/coating material.

8.4. Overall Recommendations to Reduce and/or Prevent Electrocatalyst/Coating Loss in FCATT PEM Fuel Cell

The different, alternate, techniques described above that possibly could be employed to reduce or prevent the electrocatalyst/coating material loss from the substrate are all viable options. They provide avenues that could be investigated further, or used as secondary methods of prevention, if absolutely required but they all add complexity to the overall system. The data provided so far has been preliminary and while results appear promising additional work is still required to determine the impact these alternative approaches would have on the stack and system.

There is, however, one fabrication technique that is not as complex and has been shown to eliminate the electrocatalyst/coating loss completely. The PEM material was shown to produce the acetic acid from an additive located, which formed acetaldehyde, in the polymer structure during thermal decomposition. The elimination of that additive or the use of a different polymer, so the water does not become electrically conductive (acetic acid caused the water to become electrically conductive), would be the first recommended course of action to prevent electrocatalyst/coating loss from the fuel cell. Results clearly

showed that when the solution in contact with electrocatalyst material was non-conductive then no degradation was observed.

If a substitute polymer formulation, which does not produce an electronically conductive solution, cannot be developed and/or implemented then alternative approaches should be considered and implemented to minimize the electrocatalyst loss in the fuel cell stack. Based results shown in this paper a combination of carbon, or some other electronically insulating coating, placed between the platinum and substrate material. Increasing the thickness of the electrocatalyst material also proved to be effective, but is more costly.

9. References

[1] T. Burye, "FCATT PEM Fuel Cell Failure Analysis Report," 2017.

[2] M. Sadeghi, M. Semsarzadeh and H. Moadel, "Enhancement of the Gas Separation Properties of Polybenzimidazole (PBI) Membrane by Incorporation of Silica Nano Particles," *J. Membr. Sci.,* vol. 331, pp. 21-30, 2009.

[3] B. Sadeghalvad, A. Azadmehr and A. Hezarkhani, "Assessment of Iron Ore Mineral Wastes for Sulfate Removal from Groundwater Wells: A Case Study," *RSC Adv.,* pp. 1-39, 2015.

[4] A. Rajib, S. Horita, A. Rahman and A. Bakar, "Study of the Influence of Temperature on the Deposition of SiO2 Films from Reaction of Silicone Oil Vapor and Ozone Gas," *J. Sci. & Eng.,* vol. 44, pp. 1-8, 2016.

[5] P. Chu, F. Guenther, G. Rhoderick and W. Lafferty, "NIST Chemistry Webbook for Acetic Acid Ethenyl Ester," 2018. [Online]. Available: http://webbook.nist.gov/cgi/cbook.cgi?ID=108-05-4&Type=IR-SPEC&Index=QUANT-IR,10.

[6] C. S. Inc., "NIST Chemistry Webbook Acetic Acid," 2018. [Online]. Available: NIST Webbook, http://webbook.nist.gov/cgi/cbook.cgi?ID=C64197&Type=IR-SPEC&Index=2.

[7] S. S. NIST Mass Spec Data Center, "NIST Chemistry Webbook for Acetic Acid, 1-Methylethyl Ester," 2018. [Online]. Available: http://webbook.nist.gov/cgi/cbook.cgi?ID=C108214&Type=IR-SPEC&Index=0.

[8] C. S. Inc., "NIST Chemistry Webbook for Acetic Acid, Methyl Ester," 2018. [Online]. Available: https://webbook.nist.gov/cgi/cbook.cgi?ID=C79209&Type=IR-SPEC&Index=3.

[9] C. S. Inc., "NIST Chemistry Webbook for Acetic Acid, n-Pentyl Ester," 2018. [Online]. Available: https://webbook.nist.gov/cgi/cbook.cgi?ID=C628637&Type=IR-SPEC&Index=2.

[10] S. S. NIST Mass Spec Data Center, "NIST Chemistry Webbook for Acetic Acid Benzyl Ester," 2018. [Online]. Available: https://webbook.nist.gov/cgi/cbook.cgi?ID=C140114&Units=CAL&Type=IR-SPEC.

[11] C. S. Inc., "NIST Chemistry Webbook for Acetic Acid Propyl Ester," 2018. [Online]. Available: https://webbook.nist.gov/cgi/cbook.cgi?ID=C109604&Type=IR-SPEC&Index=1.

[12] C. S. Inc., "NIST Chemistry Webbook for Acetic Acid Cyclohexyl Ester," 2018. [Online]. Available: https://webbook.nist.gov/cgi/cbook.cgi?ID=C622457&Type=IR-SPEC&Index=2.

[13] P. Chu, F. Guenther, G. Rhoderick and W. Lafferty, "NIST Chemistry Webbook for Ethyl Acetate," 2018. [Online]. Available: https://webbook.nist.gov/cgi/cbook.cgi?ID=141-78-6&Type=IR-SPEC&Index=QUANT-IR,1.

[14] C. S. Inc., "NIST Chemistry Webbook for Geraniol Acetate," 2018. [Online]. Available: https://webbook.nist.gov/cgi/cbook.cgi?ID=C105873&Mask=80#IR-Spec.

[15] N. Yoneda, S. Kusano, M. Yasui, P. Pujado and S. Wilcher, "Recent Advances in Processes and Catalysts for the Production of Acetic Acid," *Appl. Catal. A: Gen.,* vol. 221, no. 1-2, pp. 253-265, 2001.

[16] M. Lancaster, Green Chemistry, An Introductory Text, 2002.

[17] J. Zoeller, V. Agreda, S. Cook, N. Lafferty, S. Polichnowski and D. Pond, "Eastman Chemical Company Acetic Anhydride Process," *Catal. Today,* vol. 13, no. 1, pp. 73-91, 1992.

[18] P. Chenier, Survey of Indusrtial Chemistry, 2002.

[19] G. Chotani, A. Gaertner, M. Arbige and T. Dodge, Industrial Biotechnology: Discovery to Delivery, Springer, 2007.

[20] T. A. W. R. Institute, "The Austrailian Wine Research Institute Wine Failts," 2018. [Online]. Available: https://www.awri.com.au/industry_support/winemaking_resources/sensory_assessment/recognition-of-wine-faults-and-taints/wine_faults/#oxidationfaults.

[21] F. Hemming, in *Glycolipids*, Elsevier Science Publishers, 1985.

[22] W. Lee, "High Resistivity of dc-Sputtered Metal Films," *J. Appl. Phys.,* vol. 42, p. 4366, 1971.

[23] J. Nagano, "Electrical Resistivity of Sputtered Molybdenum Films," *Thin Solid Films,* vol. 67, no. 1, pp. 1-8, 1980.

[24] D. Hofman, "Metallurgical and Protective Coatings Stress and Property Control in Sputtered Metal Films Without Substrate Bias," *Thin Solid Films,* vol. 107, no. 4, pp. 353-358, 1983.

[25] R. Serway, Principles of Physics, Fort Worth, 1998.

[26] C. H. Jr. and W. Pawlewicz, "Thermal Conductivities of Thin, Sputtered Optical Films," *Applied Optics,* vol. 32, no. 1, pp. 91-101, 1993.

[27] J. Verhoogen, "Ionic Diffusion and Electrical Conductivity in Quartz," *American Mineralogist,* vol. 37, no. 7-8, pp. 637-655, 1952.

[28] R. Deshpande, Y.-T. Cheng, M. Verbrugge and A. Timmons, "Diffusion Induced Stresses and Strain Energy in a Phase-Transforming Spherical Electrode Particle," *J. Electrochem. Soc.,* vol. 158, no. 6, pp. A718-A724, 2011.

[29] S. Matsumoto, Y. Akao, K. Kohiyama and T. Niimi, "Effects of Diffusion-Induced Strain and Dislocation on Phosphorus Diffusion into Silicon," *J. Electrochem. Soc.,* vol. 125, no. 11, pp. 1840-1845, 1978.

[30] J. Lawrence, "Diffusion-Induced Stress and Lattic Disorders in Silicon," *J. Electrochem. Soc.,* vol. 113, no. 8, pp. 819-824, 1966.

[31] S. DeMeo, "Does Copper Metal React with Acetic Acid?," *J. Chem. Educ.,* vol. 74, no. 7, pp. 844-846, 1997.

10. Appendix A: Supplementary Information

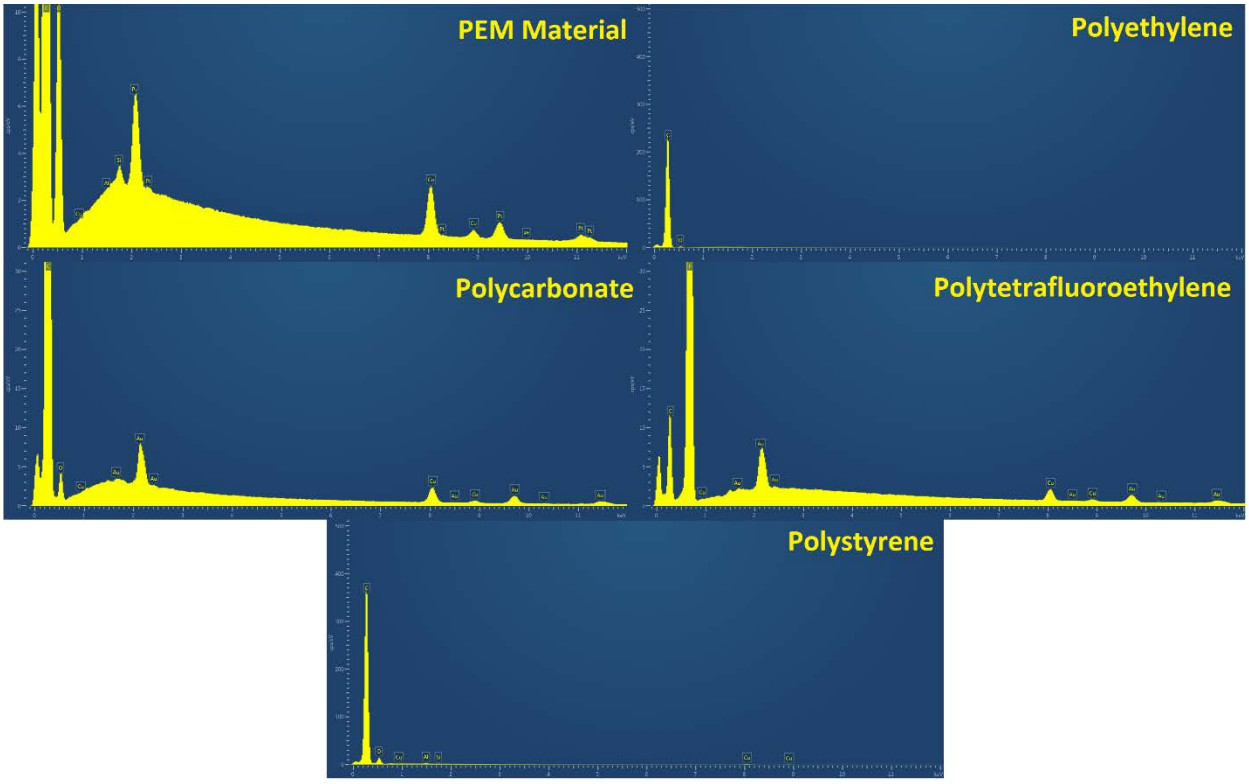

Figure 68: EDS Scan Results from Polymer Substrate Materials

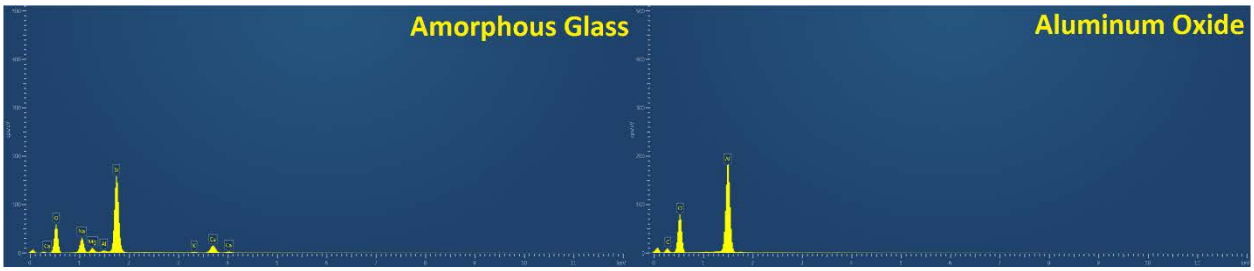

Figure 69: EDS Scan Results from Glass/Ceramic Substrate Materials

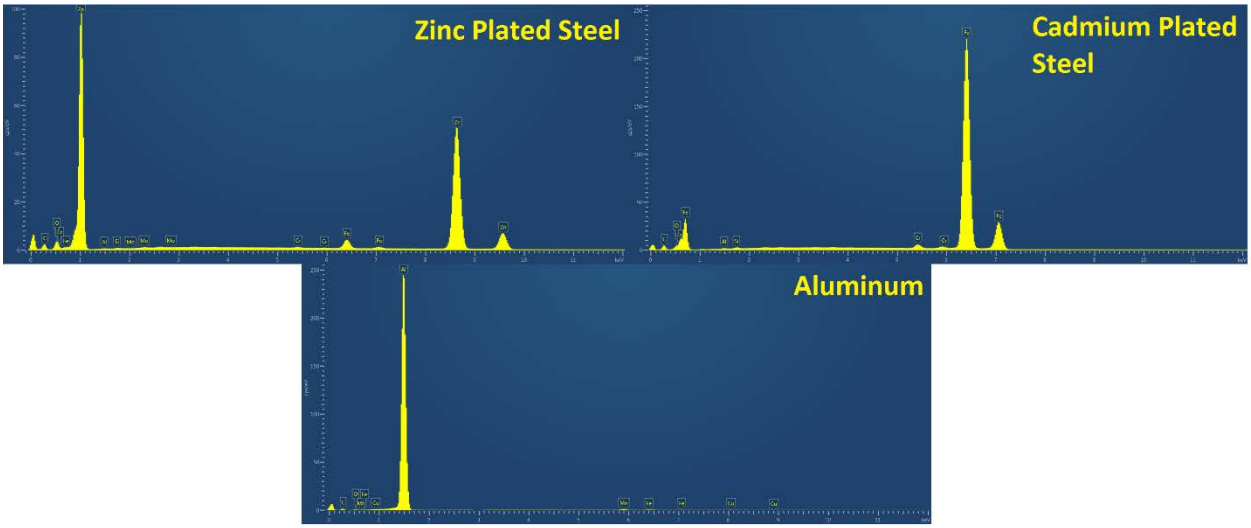

Figure 70: External EDS Scan Results from Bulk Metal Substrate Materials

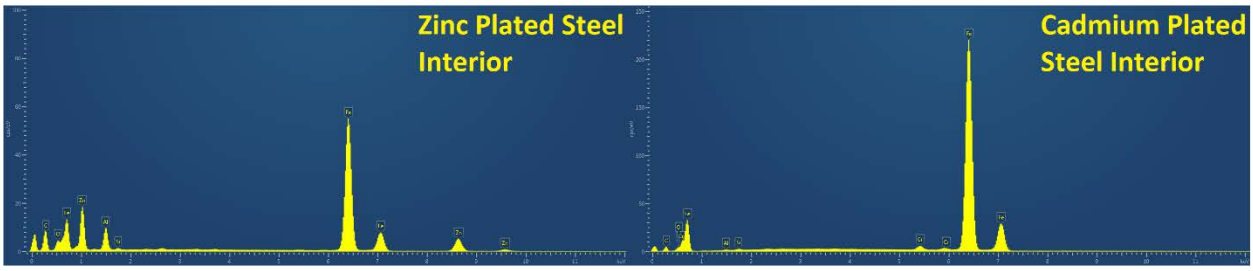

Figure 71: Interior EDS Scan Results from Zinc and Cadmium Plated Steel Substrate Materials

11. Appendix B: Platinum and Copper in Glacial Acetic Acid

11.1. Copper in Glacial Acetic Acid

Table 8: Copper Mass Loss in Glacial Acetic Acid

Time Passed (hrs)	Recorded Mass (g)	% Mass Lost	% Mass Lost/hr (%/hr)
0	0.2003	0	0
5	0.1996	0.349	0.070
22	0.1982	1.048	0.047
23.5	0.1975	1.397	0.059
43.5	0.1964	1.947	0.045
69	0.1941	3.095	0.045

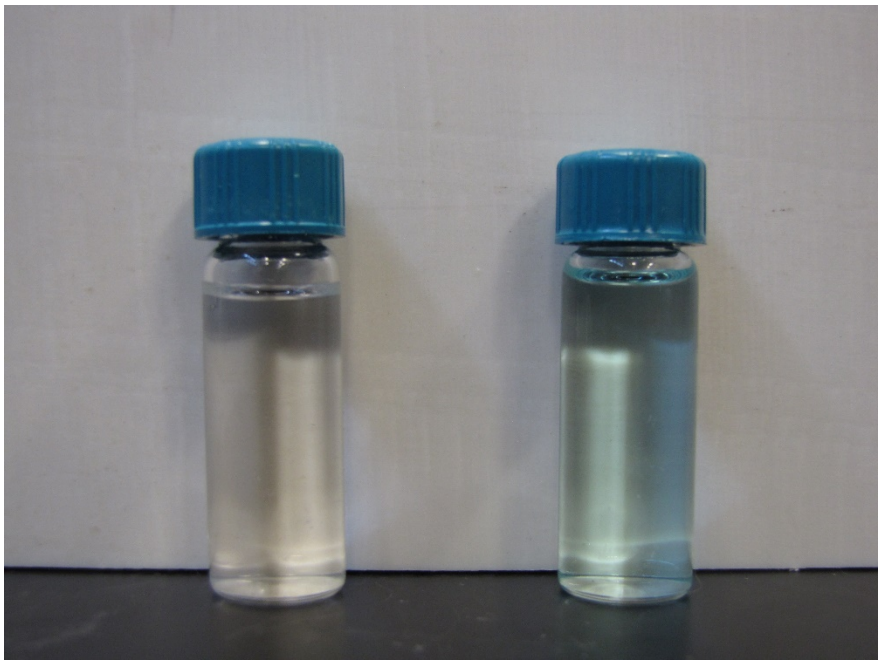

Figure 72: Copper in Glacial Acetic Acid for 69hrs (right) and Pure Glacial Acetic Acid (left)

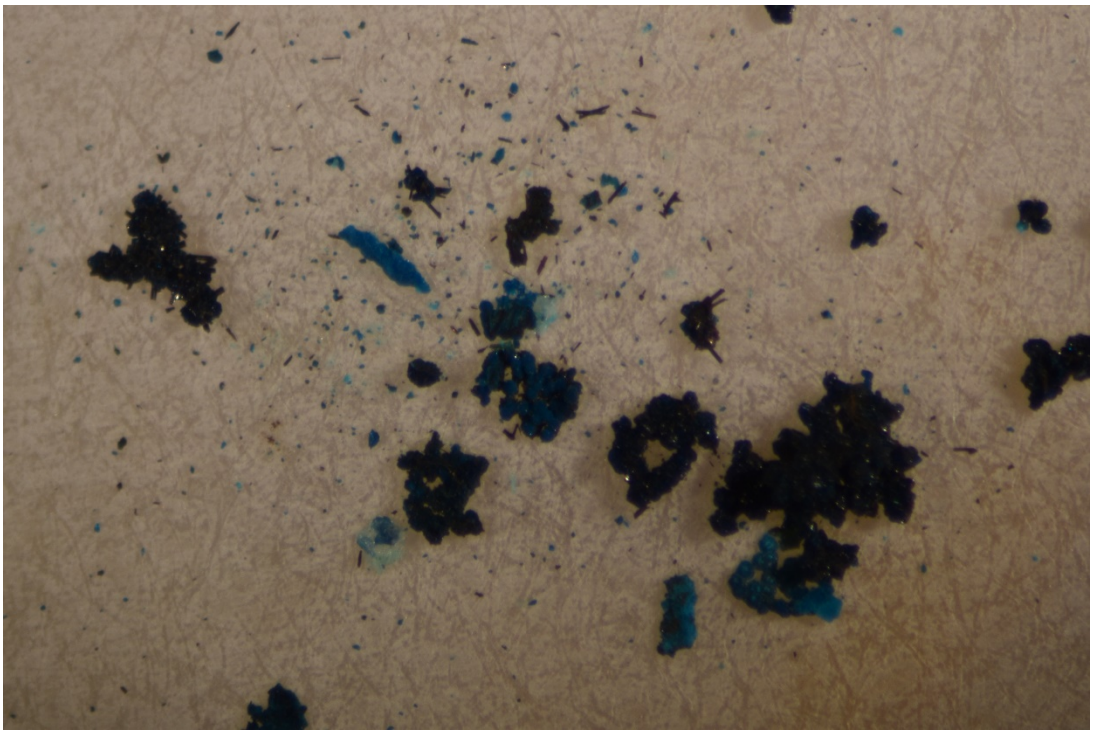

Figure 73: Optical Microscopy Image of Precipitate Power from Copper in Glacial Acetic Acid

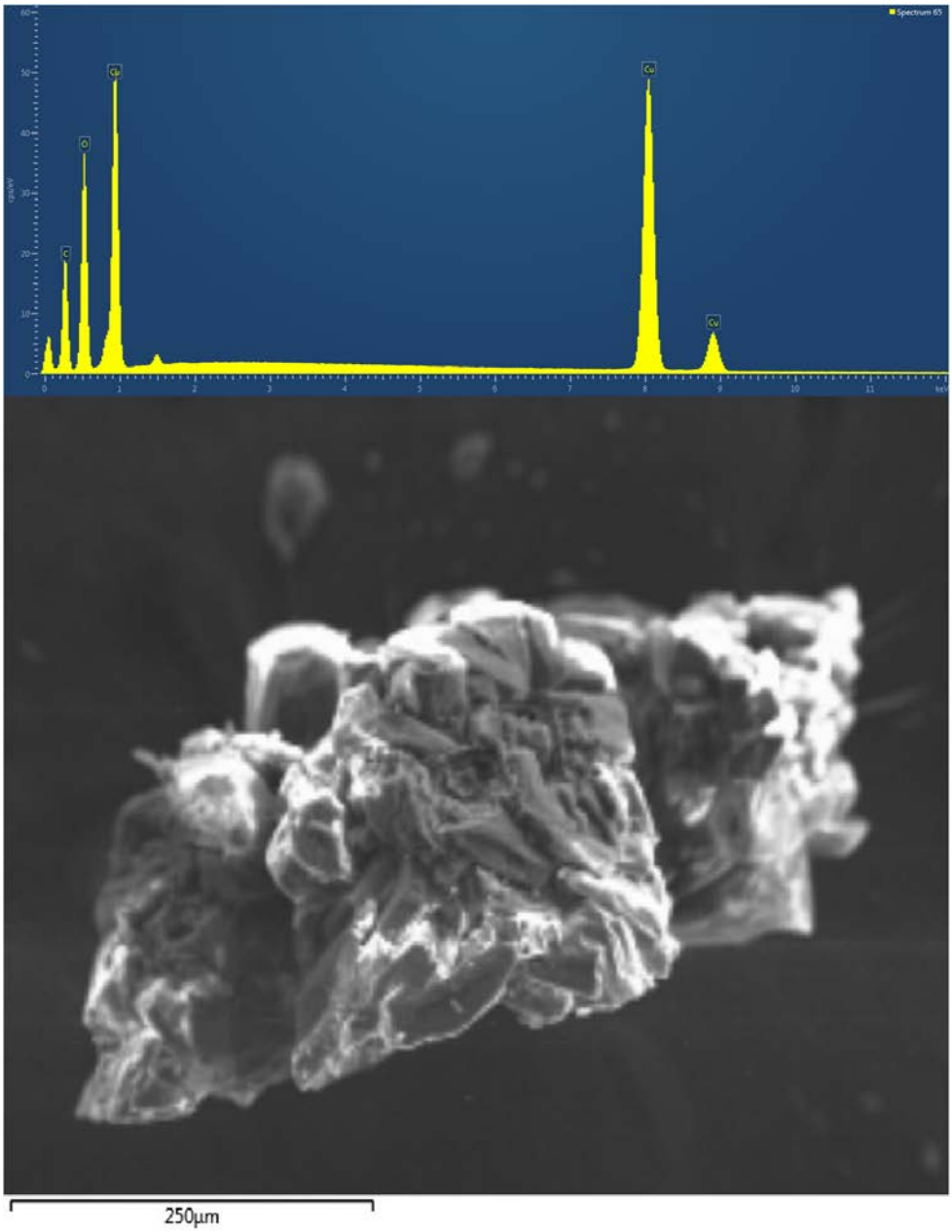

Figure 74: EDS Scan Results (top) and Scanning Electron Microscopy Image (bottom) of Precipitate from Copper in Glacial Acetic Acid.

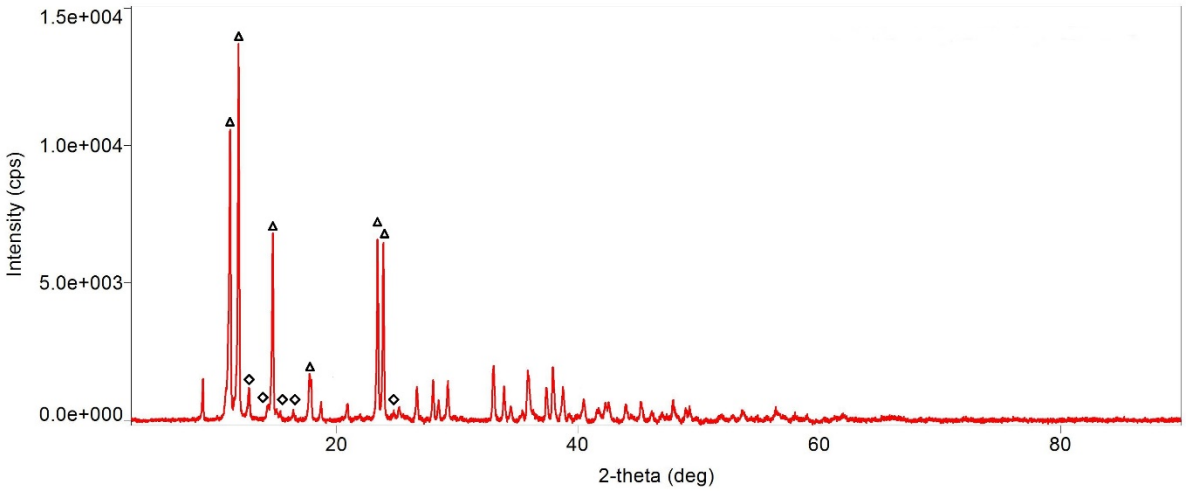

Figure 75: XRD Scan of Precipitate Powder from Copper in Glacial Acetic Acid. △= Copper (II) Acetate and ◊ =Copper (II) Acetate Monohydrate

11.2. Platinum in Glacial Acetic Acid

Table 9: Platinum Mass Loss in Glacial Acetic Acid

Time Passed (hrs)	Recorded Mass (g)	% Mass Lost	% Mass Lost/Hr (%/hr)
0	0.3903	0	0
2.25	0.3902	0.026	0.011
91	0.3904	-0.026	0.000